

Thermoresponsive Starch Nanoparticles for Use in the Extraction of Oil from Oil Sands

by

Qian Zhang

A thesis

presented to the University of Waterloo

in fulfillment of the

thesis requirement for the degree of

Master of Science

in

Chemistry

Waterloo, Ontario, Canada, 2018

© Qian Zhang 2018

Author's Declaration

I hereby declare that I am the sole author of this thesis. This is a true copy of the thesis, including any required final revisions, as accepted by my examiners.

I understand that my thesis may be made electronically available to the public.

Abstract

Oil sands represent the most abundant reserves of oil in the world. Nearly 97% of the oil reserves of Canada are found in the form of oil sands. Despite continued research, the extraction of oil from oil sands is costly and remains challenging. Thermoresponsive polymeric surfactants have been introduced as shuttling agents to improve the oil extraction efficiency, but they are costly and their synthesis cannot be easily scaled up. This project is to study the potential of thermoresponsive starch nanoparticles (tSNPs) as shuttling agents to improve the extraction of oil from oil sands. The use of starch, an abundant biopolymer obtained directly from plants, to prepare the tSNPs should be a cost-effective alternative to reduce the production cost of thermoresponsive polymeric shuttling agents. Two types of tSNPs were investigated. The first type was an SNP modified with poly(2-(2-methoxyethoxy)ethyl methacrylate) (tP(x)-SNP with x representing the weight percentage (wt%) of thermoresponsive polymer (tP)). A second type of tSNP was prepared by covalently attaching x mol% of styrene oxide and y mol% of butene oxide to an SNP to yield SO(x)-BO(y)-SNP. The efficiency of the tSNPs to shuttle the oil from oil sands to the surface of an aqueous tSNP dispersion was characterized in the presence of minute quantities of different co-solvents (toluene, octanol, and cumene).

After numerous trials, the sample tP(15)-SNP with a degree of substitution around 0.02 was the best sample tried so far, with an oil extraction yield around 32 wt% when using a small amount of toluene. This yield was much higher than the yields of around 9 wt% obtained with pure water or aqueous dispersions of most other tSNPs employing a similar amount of organic co-solvent.

Pyrene fluorescence was also applied to assess the relative hydrophobicity of different tSNPs in an attempt to relate the hydrophobicity of tSNPs to their efficiency for oil extraction. The results obtained by steady-state and time-resolved fluorescence indicate differences in the hydrophobicity of the tSNPs which can be used to improve the results from oil extraction yields.

Acknowledgements

I would like to thank my dear supervisor, Prof. Jean Duhamel, for providing me with the opportunity to work on this project. Starting from my undergraduate studies until now, he has guided, supervised, and encouraged me for the past three years. As an international student for whom English is not my mother tongue, he had to spend time and be patient to allow me to improve my study, language, and life. He helped me adapt to the Canadian life style and become a better person. He and his wife, Mary Ann, have treated me as their own daughter, making me never feel alone in this foreign country.

I would like to express my appreciation of Prof. Mario Gauthier and Prof. Scott Taylor for guiding me through my experiments and taking the time to attend my presentations.

I would like to thank my colleagues Natun Dasgupta and Bowei Zheng for providing the samples that were used for the entire project. Both of them are excellent researchers, who kept on making useful suggestions during the two years of my MSc thesis.

I would like to acknowledge the contribution from Austin Richard, a co-op student who joined the Duhamel group in Fall 2017. Austin carried out numerous oil extraction experiments and evaluated the effectiveness of various co-solvents during oil extraction.

Lu Li, a graduate student of the Duhamel group, made also many valuable suggestions for this project.

I would like to express my gratitude to all current and former lab members of the Duhamel and Gauthier groups for their contributions to my study, especially Lu Li, Damin Kim, Janine Thoma, Bethsy Aguilar, Remi Casier, Kiarash Gholami, Sanjay Patel, and Abdullah Ba Salem.

Finally, I am indebted to EcoSynthetix and NSERC for financial support, and to Drs. Niels Smeets, Julien Mesnager, and Steven Bloembergen from EcoSynthetix for their time and valuable suggestions.

Dedication

To my loving parents Wenbin Zhang and Hongyan Sun.

And to all my dear friends who made my life happy and memorable.

Table of Contents



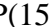
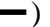










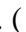

Author's Declaration.....	ii
Abstract.....	iii
Acknowledgements.....	v
Dedication.....	vii
Table of Contents	viii
List of Figures.....	x
List of Tables.....	xvi
List of Abbreviations.....	xix
Chapter 1.....	1
1.1 Oil Sands.....	2
1.2 Reserves and Mining of Oil Sands.....	3
1.3 Hot Water Separation of Bitumen.....	5
1.3.1 The separation plant.....	5
1.3.2 Factors that influence the oil extraction by hot water separation.	7
1.4 Oil Extraction from Oil Sands with Thermoresponsive Polymeric Surfactants .	11
1.4.1 Thermoresponsive polymeric surfactants	11
1.4.2 Role of PEG- <i>b</i> -PMeEO ₂ MA in the oil extraction process.....	11
1.5 Thermoresponsive Starch Nanoparticles for Extraction of Oil from Oil Sands .	13
1.6. Thesis Outline	15
Chapter 2.....	17
2.1 Characterization and Comparison of Different Oil Sands	18
2.1.1 Soxhlet Extraction.....	19
2.2 Oil Extraction Protocols.....	20
2.2.1 Primary oil extraction protocols.....	20
2.2.2 Determination of the oil extraction yields	24
2.2.3 Adjustment of vial cap	25
2.4 Characterization of the tSNPs.....	29
2.4.1. Lower critical solution temperature (LCST) determination	29
2.4.2 Characterization of the tSNPs by pyrene fluorescence.....	31
Chapter 3.....	37
3.1 LCST Determination of the tSNPs by Turbidimetry	38

3.1.1 SO-BO-SNP samples	38
3.1.2 tP-sP-SNP Samples	41
3.2 Results from Oil Extraction Experiments	46
3.3 Characterization of tSNPs by Pyrene Fluorescence.....	57
3.3.1 SNPs modified with styrene and butene oxide	57
3.3.2 SNPs modified with PMeEO ₂ MA and PHEA	62
Chapter 4.....	68
4.2 Future Work	73
References.....	74
Appendices.....	81

List of Figures

Figure 1.1. A) Physical make up of oil sand particles ³ and B) picture of the Sample Bank oil sands used in this study.	3
Figure 1.2. Open mining technology used for oil extraction from oil sands.	4
Figure 1.3. In-situ technology used for oil extraction of oil sands.	5
Figure 1.4. Diagram for a hot water separation plant to extract bitumen from oil sands. .	7
Figure 1.5. Oil extraction from oil sands with a thermoresponsive block copolymer (PEG-b-PMEO ₂ MA) as proposed by Yang and Duhamel. ³¹	13
Figure 1.6. Chemical Structure of A) tP(x)-sP(y)-SNP prepared by Dasgupta and B) SO(x)-BO(y)-SNP prepared by Zheng. ³³	14
Figure 2.1. Pictures of (A) Imperial Oil oil sands (IOos), (B) Sample Bank oil sands (SBos), (C) solid phase of IOos, and (D) solid phase of SBos.....	18
Figure 2.2. Apparatus for Soxhlet extraction. ³⁷	19
Figure 2.3. Oil extraction protocol applied to determine the yield of oil extraction.....	21
Figure 2.4. Extraction yield as a function of toluene amount for oil extractions conducted with 1 g of SBos and 15 mL of water (■) or 15 mL of 1 g/L PMeEO ₂ MA-b-PEG aqueous dispersion (bars) shaken at 45 °C for 24 hrs.	23
Figure 2.5. The oil droplets are present in the aqueous phase.	25
Figure 2.6. Oil extraction yields for the extraction conducted at 45 °C with 1 g of OIos,	

15 mL of 1 g/L PEG-b-PMeEO ₂ MA aqueous dispersion, and 60 mg of toluene and with (right) or without (left) a proper seal.....	27
Figure 2.7. Plot of (—) T% and (·····) dT%/dT as a function of temperature for a 1 g/L aqueous dispersion of tP(15)-sP(15)-SNP(0.06).....	31
Figure 2.8. Fluorescence spectrum of a 0.5 μM pyrene solution in milli-Q water. The fluorescence intensities I ₁ and I ₃ at the first and third peaks have been indicated. λ _{ex} = 336 nm.....	33
Figure 2.9. Time-resolved fluorescence decay of 0.5 μM pyrene in 1 g/L SNP aqueous dispersion.....	35
Figure 3.1. Plot of transmittance at 500 nm as a function of temperature for 10 g/L aqueous dispersions of SO-BO-SNP: Sample #4 (———), Sample #5 (———) and Sample #6 (- - - -).....	39
Figure 3.2. Plot of transmittance at 500 nm as a function of temperature for a 3 and 5 g/L aqueous dispersion prepared with two PEG-SO-BO-SNPs.	40
Figure 3.3. Oil extractions carried out with 4 g of BSos at 45 °C, 200 mg of toluene, and 60 mL of 1 g/L of SO-BO-SNP aqueous dispersions.....	41
Figure 3.4. A) Plot of transmittance at 500 nm as a function of temperature for 1 g/L aqueous dispersions of SNPs modified with (———) 5.9, (- - - -) 15, and (———) 27 wt% PMeEO ₂ MA. B) Plot of LCST as a function of the PMeEO ₂ MA	

content used to modify the SNP.....	42
Figure 3.5. A) Plot of transmittance at 500 nm as a function of temperature for 1 g/L aqueous dispersions of tP(15)-SNPs modified with () 0, () 15, and () 30 wt% PHEA. B) Plot of LCST as a function of the content of PHEA grafted onto the tP(15)-SNP substrate.	43
Figure 3.6. A) Plot of transmittance at 500 nm as a function of temperature for 1 g/L aqueous dispersions of all tP-sP-SNP samples. B) Selected profiles of tP-sP-SNP exhibiting a shallow drop in T% above the LCST as observed for PEG-b-PMeEO ₂ MA.	44
Figure 3.7. Plots of T% as a function of temperature for a series of tP(15)-SNPs with DS equal to () 0.016, () 0.020, () 0.022, () 0.038, and () 0.060.....	45
Figure 3.8. Plot of the yield for the oil extraction from 1 g of SBos as a function of toluene mass added to ( , ) 15 mL of 1 g/L tP(15)-SNP(0.06) aqueous dispersion and ( , ) 15 mL of water. ( , ) Method #1, ( , ) Method #2.....	47
Figure 3.9. Yields obtained for oil extractions conducted at 45 °C with 4 g of SBos, 60 mL of 1 g/L aqueous dispersions of tP(15)-SNP(0.06), tP(27)-SNP(uk), and tP(15)-sP(15)-SNP(0.06) or 60 mL of water and 200 mg toluene/octanol.....	48
Figure 3.10. Yields for extractions conducted at 45 °C with 1 g of SBos, 15 mL of 1 g/L	

aqueous dispersions of tP(15)-SNP(0.016), tP(15)-sP(7.5)-SNP(0.016), and tP(15)-SNP(0.06) or 15 mL of water and 60 mg toluene.	49
Figure 3.11. Extraction yields obtained for different organic solvents without (top) and with (bottom) tP(15)-SNP(0.02). ⁶⁰	51
Figure 3.12. Oil extraction yield as a function of the mass of (A) 1-octanol and (B) cumene used in extractions conducted with 1 g of SBos and 15 mL of 1 g/L tP(15)-SNP(0.016), tP(15)-SNP(0.020), and tP(30)-SNP(0.022) at 45 °C. ⁶⁰	53
Figure 3.13. Plot of the yield for the extraction of 1 g of SBos as a function of toluene mass added to (■, ▲) 15 mL of 1 g/L tP(15)-SNP(0.02) aqueous dispersion, (■, ▲) 15 mL of water, and (■, ▲) 15 mL of 1 g/L tP(15)-SNP(0.06) aqueous dispersion. (■, ■, ■) Method #1, (▲, ▲, ▲) Method #2.....	54
Figure 3.14. Pictures of (A) the clear three layers obtained for an ideal oil extraction and (B) the most common outcome from extractions showing large oil droplets stuck at the sand-water interface.....	56
Figure 3.15. Yields for oil extractions conducted at 45 °C with 1 g of SBos, 15 mL of 1 g/L aqueous dispersions of tP(15)-SNP(0.06), and 60 mg toluene. The black portion represent the amount of oil collected after a normal oil extraction and the white bars refer to the oil portion that was collected in the second step of the oil extraction (see text for further explanations).	57

Figure 3.16. I_1/I_3 ratio as a function of [tSNP] determined by steady-state fluorescence for aqueous dispersions of tSNPs with [Py]=0.5 μ M. (Sample #1 (\blacklozenge), Sample #2 (\blacksquare), Sample #3 (\blacktriangle), and Sample #3c (\times))..... 59

Figure 3.17. Ratio $[Py_b]/[Py_w]$ plotted as a function of [tSNP] obtained from the analysis of the time-resolved decays acquired with [Py]=0.5 μ M in aqueous dispersion of tSNPs. (Sample #1 (\blacklozenge), #2 (\blacksquare), #3 (\blacktriangle), and #3c (\times))..... 61

Figure 3.18. I_1/I_3 ratio plotted as a function of polymer concentration obtained from the analysis of the fluorescence spectra of 0.5 μ M pyrene in a 1 g/L aqueous solution of (A) PEG-b-PMeEO₂MA and 1 g/L aqueous dispersions of (B) tP(15)-SNP(0.02), (C) SO(0.26)-BO(0.82)-SNP (Sample #4), and (D) naked SNP. Empty and filled symbols acquired at 25 and 50 $^{\circ}$ C, respectively. 63

Figure 3.19. Ratio $[Py_b]/[Py_w]$ as a function of polymer concentration obtained from the analysis of the time-resolved fluorescence decays acquired for 0.5 μ M pyrene in a 1 g/L aqueous solution of (\bigcirc) PEG-b-PMeEO₂MA and 1 g/L aqueous dispersions of (\blacklozenge , \blacklozenge) tP(15)-SNP(0.02), (\blacktriangle , \blacktriangle) SO(0.26)-BO(0.82)-SNP (sample 4), and (\blacksquare , \square) naked SNP. Empty and filled symbols acquired at 25 and 50 $^{\circ}$ C, respectively. 644

Figure 3.20. $[Py_b]/[Py_w]$ ratio as a function of the PMeEO₂MA massic concentration obtained from the analysis of the time-resolved fluorescence decays of 0.5 μ M

pyrene in aqueous dispersions of (○) PEG-b-PMeEO₂MA and (◇) tP(15)-
SNP(0.02) at 25 °C. 677

List of Tables

Table 2.1. Weight percentages of the PMeEO ₂ MA and PHEA blocks and degree of substitution of the tP(<i>x</i>)-sP(<i>y</i>)-SNP samples prepared by RAFT.	28
Table 2.2. Molar substitution of styrene and butene oxide and weight percentage of PEG for the PEG(<i>z</i>)-SO(<i>x</i>)-BO(<i>y</i>)-SNP samples.	29
Table 3.1. Binding Constant <i>K</i> in L.g ⁻¹ for Sample 1, 2, 3 and 3c of So-Bo-SNP at 25 °C.....	61
Table 3.2. Binding Constant <i>K</i> in L.g ⁻¹ for PEG- <i>b</i> -PMeEO ₂ MA, two Modified SNPs, and the Naked SNPs at 25 °C and 50 °C.....	65
Table S.1. Parameters retrieved from the analysis of the fluorescence spectra and decays with Equation 6 acquired with 0.5 μM pyrene in aqueous dispersions of SoBoSNP(Sample 1) at 25 °C.....	82
Table S.2. Parameters retrieved from the analysis of the fluorescence spectra and decays with Equation 6 acquired with 0.5 μM pyrene in aqueous dispersions of SoBoSNP(Sample 2) at 25 °C.....	84
Table S.3. Parameters retrieved from the analysis of the fluorescence spectra and decays with Equation 6 acquired with 0.5 μM pyrene in aqueous dispersions of SoBoSNP(Sample 3) at 25 °C.....	85
Table S.4. Parameters retrieved from the analysis of the fluorescence spectra and decays with Equation 6 acquired with 0.5 μM pyrene in aqueous dispersions of	

SoBoSNP(Sample 3c) at 25 °C.....	86
Table S.5. Parameters retrieved from the analysis of the fluorescence spectra and decays with Equation 6 acquired with 0.5 μM pyrene in aqueous dispersions of NSNP at 25 °C.....	87
Table S.6. Parameters retrieved from the analysis of the fluorescence spectra and decays with Equation 6 acquired with 0.5 μM pyrene in aqueous dispersions of NSNP at 50 °C.....	88
Table S.7. Parameters retrieved from the analysis of the fluorescence spectra and decays with Equation 6 acquired with 0.5 μM pyrene in aqueous dispersions of SOBO-SNP at 25 °C.	89
Table S.8. Parameters retrieved from the analysis of the fluorescence spectra and decays with Equation 6 acquired with 0.5 μM pyrene in aqueous dispersions of SOBO-SNP at 50 °C.	90
Table S.9. Parameters retrieved from the analysis of the fluorescence spectra and decays with Equation 6 acquired with 0.5 μM pyrene in aqueous dispersions of tP(15)-SNP(0.016) at 25 °C.	91
Table S.10. Parameters retrieved from the analysis of the fluorescence spectra and decays with Equation 6 acquired with 0.5 μM pyrene in aqueous dispersions of tP(15)-SNP(0.016) at 50 °C.	92

Table S.11. Parameters retrieved from the analysis of the fluorescence spectra and decays with Equation 6 acquired with 0.5 μM pyrene in aqueous dispersions of PEG-PM ₂ EO ₂ MA at 25 °C.	93
Table S.12. The LCST values of tP-sP-SNPs determined by UV-Vis spectrophotometry.	94

List of Abbreviations

A	Absorbance
a	Molar fractions of pyrene species in fluorescence decay analysis
b	Path length
BCP	Block copolymer
BO(y)	SNP-bound butene oxide with a molar substitution equal to y
c	tSNP concentration
CHWP	Clark hot water process
DS	Degree of substitution
DP	Degree of polymerization
FRET	Fluorescence resonance energy transfer
Glycol ether EB	2-butoxyethanol
HMPAM	Hydrophobically modified polyacrylamide
h	Hours
I_1/I_3	Fluorescence intensity ratio of the first to the third peak
IOos	Oil sands supplied by Imperial Oil
K	Binding constant
LCST	Lower critical solution temperature
MIBC	Methylisobutyl carbinol
oil%	Percentage of oil recovered
PEG(z)	SNP-bound poly(ethylene glycol) with a weight percentage equal to z
PEG- <i>b</i> -PMeEO ₂ MA	Poly(ethylene glycol)- <i>b</i> -poly(2-(2-methoxyethoxy)ethyl methacrylate)
PHEA	Poly(hydroxyethyl acrylate)

PMeEO ₂ MA	Poly(2-(2-methoxyethoxy)ethyl methacrylate)
Py	Pyrene
Py _b	Excited pyrene bound to tSNPs
Py _w	Excited pyrene in water
RPM	Revolutions per minute
SBos	Oil sands from the Alberta Innovate Technology Futures Sample Bank
SiO ₂	Silica
SNP	Starch nanoparticle
SO(<i>x</i>)	SNP-bound styrene oxide with a molar substitution equal to <i>x</i>
sP(<i>y</i>)	SNP-bound water-soluble polymer with a weight percentage equal to <i>y</i>
T%	Percentage transmittance
T _c	Cloud point
THF	Tetrahydrofuran
tP(<i>x</i>)	SNP-bound thermoresponsive polymer with a weight percentage equal to <i>x</i>
tPS	Thermoresponsive polymeric surfactant
tSNP	Thermoresponsive starch nanoparticles
VM&P Naptha	Hydrotreated light naphtha
wt%	Weight percentage
ε	Molar extinction coefficient
τ _w	Lifetime of free pyrene in water
τ _b	Lifetime of pyrene bound to tSNPs

Chapter 1
Introduction

1.1 Oil Sands

Oil sands can be described as unconventional bitumen deposits because they cannot be directly extracted from oil wells. Most oil sands contain about 85% solids, 5% water, and 10% bitumen.¹ The main part of the solids are coarse silica particles which contribute 70-90 wt% of the solid content. Fine solids and clay constitute the rest of the solid part of the oil sands. The physical make-up of the oil sands is shown in Figure 1.1. The sand particle is at the core of the oil sands, and it is surrounded by a thin layer of fines, itself embedded in a coat of bitumen. The fines found in the interfacial layer are composed of mineral matter including clay particles that are less than 44 μm in size.³ These fines are generally saturated with water. The bitumen forms a film around the fines layer and that film represents the outer layer of the oil sand particle.³ Since the bitumen is black in color, the oil sands look black. However, if an oil sands particle were cut through the middle as shown in Figure 1.1B, the interior of the oil sands particle would show the same brown color as the sand particle located at its core.

Bitumen is a heavy oil that contains naphthenics with many contaminants that are rich in nitrogen, sulphur, and traces of metals. Compared with conventional and heavy crude oil, bitumen features organic molecules that have a higher molecular weight, lower hydrogen-to-carbon ratio, and higher nitrogen, sulphur, and metal content.⁴ It is a black and sticky semi-solid at room temperature that is highly viscous.² Bitumen extracted from oil sand patches in Athabasca was found to be constituted of two parts, as determined by Boyd and Montgomery through chromatography on fuller's earth and silica gel.⁵ Ten fractions were collected. The first fraction was a colorless saturated oil with an average molecular weight of $360 \text{ g}\cdot\text{mol}^{-1}$. The oil become darker with increasing fraction number as its aromatic content increased.⁵ The last fraction was a black brown solid constituted of molecules with an average molecular weight of

2,500 g.mol⁻¹ containing 23.6 aromatic rings on average per molecule.⁵ The black brown solids contained many aromatic molecules that represented half of the carbon content or 23 wt% of the bitumen extracted from this sample of oil sands.⁵ Since the oil trapped in oil sand is highly dense and viscous, the main usage of bitumen extracted from oil sands is in paving and roofing applications. Other oil fractions such as kerosene, gasoline, diesel, and mazut are refined from bitumen and have found applications in the energy sector.⁶

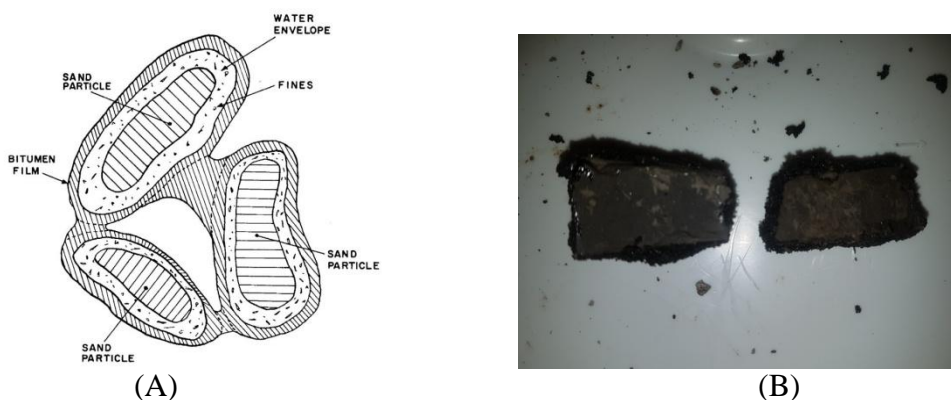


Figure 1.1. A) Physical make up of oil sand particles³ and B) picture of the Sample Bank oil sands used in this study.

1.2 Reserves and Mining of Oil Sands

Canada and Venezuela have the largest oil sands reserves in the world.⁷ The amount of oil trapped in the oil sands of Canada is on the order of 550 to 650 billion cubic meters.² More than 50% of the World's oil sands are found in Alberta.⁸ The Alberta Oil and Gas Conservation Board estimated that the Albertan oil sands deposits are located in Athabasca, Bluesky-Gethin, and Grand Rapids with reserves in place that amount to 626, 51, and 33 billion barrels, respectively.⁹ Together, these areas cover approximately 33,700 square kilometers¹⁰ representing an area equivalent to 5% of the entire province.⁹ The Athabasca oil sands are the world's largest known reserves of oil sands.⁹ The stated oil reserves only account for the oil located in these deposits,

but the amount of oil that can be extracted from these deposits still depends on the oil extraction technology being applied. The classification of oil sand reserves is based on two factors which are the deposit depth and the oil saturation. The deposit depth categories are arbitrarily divided from zero to 100 feet, 100 to 250 feet, and greater than 250 feet.⁹

Different methods have been applied for the recovery of oil from oil sands depending on the depth of burial.⁹ For burial depths of less than 100 feet, oil extraction involves mining and a processing plant. The process is known as open-pit mining technology and is depicted in Figure 1.2. First, the oil sands are dug out and loaded into trucks. The trucks take the oil sands to crushers, where they are prepared for extraction. Hot water is added to the oil sands to generate a mixture that can be transported via hydrotransport to the extraction plant. Finally, the bitumen is extracted from the oil sands in the separation plant. It is at this stage that the thermoresponsive starch nanoparticles described in this thesis would be used to make the oil extraction more efficient and environmentally friendly by reducing waste.

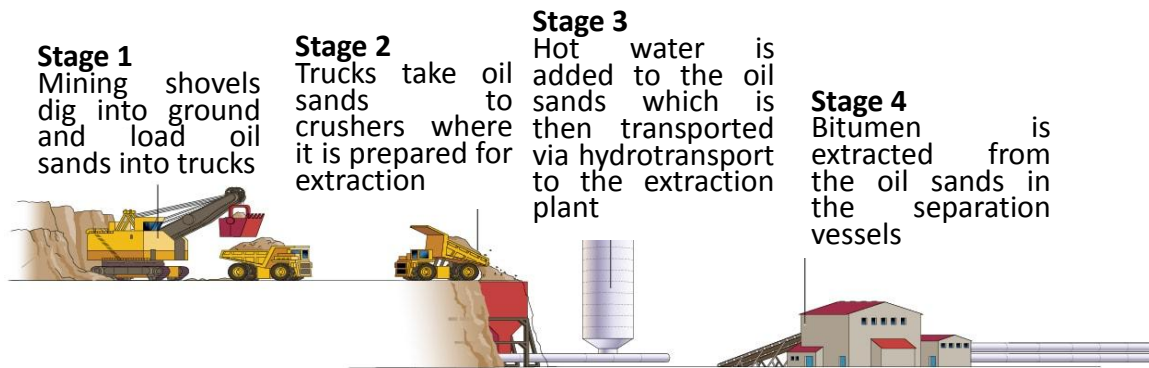


Figure 1.2. Open mining technology used for oil extraction from oil sands.⁶⁴

For oil sands reserves buried below 250 feet, the in-situ technology is applied (Figure 1.3). The oil is extracted by injecting steam or a hot aqueous solution into the ground through a steam injection wellbore where it creates a virtual steam chamber. The oil trapped in the oil sands melt

and it can then be pumped up through a wellbore to the oil production plant. For oil reserves buried between 100 and 250 feet, either in-situ or mining technology can be applied depending on the situation.

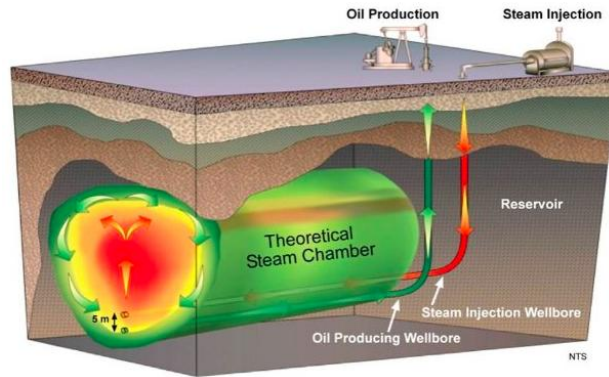


Figure 1.3. In-situ technology used for oil extraction of oil sands.⁶⁵

Oil sands are classified into three categories depending on their oil content. Oil sands with an oil content greater than 10 wt% are defined as oil-rich or simply rich sands.⁹ Oil sands with an oil content between 5 and 10 wt% are described as intermediate. Lean-sands refer to oil sands containing 2 - 5 wt% of oil.⁹ Rich sands usually represent the largest fraction of oil reserves. For example, the Athabasca oil sands deposit has more than 70% of its reserves as rich sand which represents around 440.8 billion barrels of oil.⁹ The oil that can be recovered from raw oil-sands is equivalent to around 260.5 billion barrels.⁹

1.3 Hot Water Separation of Bitumen

1.3.1 The separation plant

In 1944, K. A. Clark came up with a methodology that used hot water to separate bitumen from oil sands.¹¹ This methodology is known as the Clark hot water process (CHWP). It has been widely used to extract oil on an industrial scale. As mentioned earlier, this methodology is applied in the last step of the open-pit mining process when the hot water is added to the oil

sands in the separation plant. Oil extraction from oil sands requires that three tasks be carried out, namely slurry preparation, hydrotransport, and bitumen extraction. The first task is carried out in the slurry preparation plant which has several purposes. First, it vigorously mixes the oil sands with hot water to efficiently aerate the slurry. It also breaks down the solid pieces of oil sands to help separate the oil from the sand. The break-up of the oil sands particles helps the oil bind to air bubbles introduced in the water/oil sands mixture during the oil extraction step. Some oversized debris or material that might damage the equipment used downstream can be removed from the oil sands slurry at that stage. Finally, the dense and semi-homogeneous slurry can be pumped to the bitumen extraction plant through hydrotransport. Slurry preparation plants work with either tumblers, cyclofeeders, mixboxes, rotary beakers, or wet-crushers.² Although their mode of operation varies greatly, they all aim to generate homogeneous and dense aqueous slurries of oil sands. All involve large quantities of water, vigorous mixing, and an extreme environment with high temperature and pH to help create a dense and homogeneous oil sands slurry.¹² After the oil sands slurry is produced in the slurry preparation plant, it is hydrotransported to the gravity separation cell through a feedwell in the bitumen extraction plants.¹² The separation cell is a cone-bottomed vessel with a steep slope. The slurry is evenly distributed in the vessel through the feedwell. The bitumen can bind to air bubbles that help it float to the surface where it forms an intermediate froth product, which contains about 50 to 60 wt% bitumen.¹³ Binding of some fine solids such as clay to bitumen increases the density of bitumen. The denser bitumen/clay mixture lingers in the middle section of the vessel and represents around 2 – 4 wt% of the overall bitumen.¹³ More than 50 wt% of heavy solids such as coarse silica sand particles sink to the bottom of the vessel where they can be removed. All the products in the three layers are sent to downstream treatment. The whole process is schematically

represented in Figure 1.4.

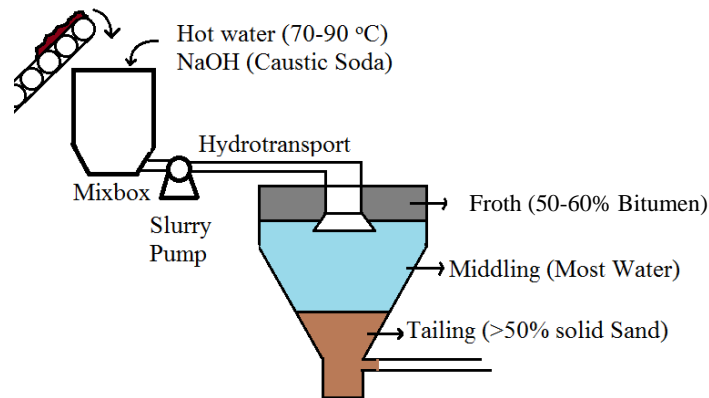


Figure 1.4. Diagram for a hot water separation plant to extract bitumen from oil sands.

1.3.2 Factors that influence the oil extraction by hot water separation.

Temperature, pH, fines, and other factors affect the CHWP.¹¹ They are discussed hereafter.

1.3.2.1 Temperature effects

Temperature is an important factor that directly influences bitumen recovery. The CHWP requires an operating temperature of about 85 °C.¹⁴ Since much of the thermal energy is not recoverable and lost in the discharge of slurry tailings, lowering the extraction temperature is a highly sought-after goal. Achieving this goal would efficiently reduce thermal energy consumption and reduce the cost of oil extraction. In recent years, some industrial extraction processes have been conducted at temperatures as low as 25 °C, but a temperature between 40 and 50 °C is more the norm for these warm water processes.¹⁵ These processes significantly reduce the consumption of thermal energy, but they introduce other problems such as the use of organic solvents that leads to pollution. The effect of pressure on the oil extractions conducted at low temperatures has been also investigated.¹⁵⁻¹⁹ Temperature affects bitumen recovery by lowering the bitumen viscosity. As for any fluid, the viscosity of bitumen decreases sharply with increasing temperature, and the high bitumen viscosity has been found to be the major factor for

the reduced extraction efficiencies obtained at temperatures below 25 °C.¹⁷ Another important physicochemical factor beside viscosity is the adhesion force between bitumen and clays that is also affected by temperature.¹⁵ Atomic force measurements have established that the adhesion force between clay and bitumen decreases with increasing temperature. Above 32-35 °C, the adhesion force was found to completely disappear.^{15,20} Since the adhesion force between clay and bitumen controls how much clay can coat the bitumen surface, which in turn increases the density of bitumen and prevents it from raising to the surface of the aqueous dispersion upon binding to air bubbles, oil recovery increases with increasing temperature as the adhesion force is reduced.

1.3.2.2 pH effects

Clark examined the effect of acidity and alkalinity of the oil sands on the efficiency of separation.¹¹ Sulfuric acid, sodium hydroxide, and sodium carbonate were used to adjust the oil sands slurry to an acid, neutral, or alkaline pH.¹¹ Three types of oil sands were employed in parallel experiments to assess the spread of the error bars when determining the extraction efficiency. The results showed that as enough base was added to the oil sands during the treatment to bring the pH of the oil sands slurry to neutral or alkaline conditions, the amount of oil extracted from oil sands reached a maximum. The amount of oil extracted from an alkaline slurry suggested close to full recovery and that little-to-no bitumen remained in the water phase. Other alkaline reagents such as sodium, ammonium, and potassium hydroxide worked equally well during the neutralization or alkaline treatment of an oil sands slurry.¹¹ In practice, most slurry preparation plants use caustic soda or sodium hydroxide (NaOH).² The addition of caustic soda aims to improve bitumen liberation during the bitumen recovery process.²¹ Increasing addition of NaOH decreases bitumen-water interface tension and increases the wettability of

bitumen.²¹ Both effects enhance bitumen liberation from sand particles. However, an increase in the pH of an oil sands slurry not only results in an increase in the formation of more natural surfactants by the ionization of naphthenic acids, but also causes the surface of air bubbles to become more hydrophilic, which dramatically reduces bitumen-bubble attachment.²¹ Taking into consideration both positive and negative effects of a pH increase on oil extraction experiments, the optimal pH for an oil sands slurry has been found to be around 8.5.²¹ At this pH value, a maximum bitumen extraction yield can be achieved.

1.3.2.3 Effects of fine sand and clay particles on oil extraction

The solid fraction of oil sands contains mostly silica (SiO₂) particles. Solid particles with diameters larger and smaller than 44 μm are defined as coarse and fine, respectively.¹³ Clay particles belong to the fine fraction. The major components of clay are kaolinite and illite.²² Chlorite, smectite, feldspar, and montmorillonite account for a small fraction of clay.²³ Clay is present as platelets in the oil sands. The platelets have two flat surfaces that are negatively charged and a positively charged edge.²⁴ Bitumen surfactants reside at the interface between the bitumen droplets and water, with the bitumen droplets being usually negatively charged. These negative charges help improve bitumen-bubble attachment in the oil extraction process. When clay is present in the oil sands slurry, encounters between the negatively charged surfaces of the bitumen droplets with the positively charged edge of the clay platelets results in the coating of the bitumen droplets with clay slime to the point where the bitumen droplets can no longer bind to the air bubbles. Because of the clay contamination, the bitumen droplets density increases, becoming greater than 1.0 g.mL⁻¹, making it harder for the oil droplets to raise to the water surface. Consequently, these droplets remain in the middle region of the separation vessel instead of floating to the surface of the dispersion. Oil sands with a high clay content usually lead to

poor yields in oil extraction. This type of oil sands is referred to as poorly processing ore. Conversely, oil sands containing small amounts of clay are called good processing ores.²⁵ The CHWP performs well when applied to good processing ores resulting in bitumen recovery higher than 93%, while it does not achieve a decent oil recovery for poor processing ores.²⁵ Recovery of the bitumen trapped in the water phase is achieved by adding a downstream treatment. The middling part of the separation vessel can be withdrawn and transferred to a highly aerated floating cell. Further oil extractions will be conducted in this cell to improve the yield of oil recovery.

1.3.2.4 Other factors

The yields for oil extraction can also be affected by the presence of soluble salts,¹¹ the addition of chemicals,^{2,15} and the amount of water used during the extraction process.²¹ Soluble salts containing calcium and magnesium cations result in poor oil extraction yields due to their positive charges which interact with the ionized naphthenic acids.¹¹ Chemical additives such as methylisobutyl carbinol (MIBC)²⁷ and hydrocarbon²⁸ and naphthenic²⁹ solvents are used to improve the oil extraction yield by decreasing the oil viscosity. Increasing the amount of water added in the slurry preparation plant generates an oil sands slurry that can be more easily aerated and results in improved oil extraction efficiency.³⁰

As a summary of the above discussion, extraction of oil from oil sands can be made more efficient by targeting the following three main areas: decreasing the oil viscosity to allow the bitumen to come off easily from the silica particles, reducing the bitumen-clay adhesion force to prevent the clay from sticking to and increasing the density of the oil droplets, and improving the aeration of the oil to promote the rise of the oil droplets to the surface of the aqueous phase. Optimization of these three factors enables the release of the bitumen from the oil sands and the

binding of air bubbles to the released bitumen for transport to the froth layer in the gravity separation cell.

1.4 Oil Extraction from Oil Sands with Thermoresponsive Polymeric Surfactants

1.4.1 Thermoresponsive polymeric surfactants

In 2015, the Duhamel laboratory suggested that thermoresponsive polymeric surfactants (tPSs) could be employed to extract oil from oil sands.³¹ The tPSs that were investigated were block copolymers of poly(ethylene glycol) (PEG) and poly(methoxyethoxyethyl methacrylate) (PMeEO₂MA) which are water-soluble below 98 °C and 26 °C, respectively. The temperature marking the boundary between the soluble and insoluble regimes is referred to as the lower critical solution temperature (LCST). The LCST of the block copolymer PEG-*b*-PMeEO₂MA was increased to 33 °C, higher than that of 26 °C for pure PMeEO₂MA, due to the presence of the water-soluble PEG block. Consequently, the diblock copolymer (PEG-*b*-PMeEO₂MA) was soluble in water below 33 °C but the PMeEO₂MA block turned insoluble at 33 °C, which led to the self-assembly of the tPS into block copolymer micelles. These micelles were constituted of a water-insoluble PMeEO₂MA-rich core and a water-soluble PEG corona.

1.4.2 Role of PEG-*b*-PMeEO₂MA in the oil extraction process

Figure 1.5 provides a schematic representation for the extraction of bitumen from oil sands with PEG-*b*-PMeEO₂MA. The oil sands that were used in these experiments were supplied by Imperial Oil and they belonged to the good processing ores category.³¹ In a typical experiment, a sample of oil sands (1 g) was placed in a vial containing 15 mL of a 1 g/L PEG-*b*-PMeEO₂MA aqueous solution with 60 mg of toluene that was added to the surface of the water phase.³¹ The vial was capped and placed in a thermostated shaker. The mixtures were shaken at 45 °C in a

circular motion in a flat horizontal plane parallel to that of the base of the vials.³¹ After shaking for 12 hours, the vials were taken out and left on the bench to cool down to room temperature overnight.³¹ The separation between the upper layer of oil, the aqueous solution, and the solid sand sediment was clearly observed. The upper layer of bitumen was skimmed off with toluene. The toluene was further evaporated by blowing nitrogen and the extracted oil was dried in a vacuum oven. Within experiment error, Yang successfully recovered 100% of bitumen from the oil sands with 80% of tPS left in the aqueous phase, which could be recycled and re-used in successive oil extractions.³¹ The formation of block copolymer micelles in water enabled the shuttling of the organic solvent (i.e. toluene) between the oil sands particles at the bottom of the vial and the water surface. The organic solvent reduced the oil viscosity and decreased the bitumen-sand adhesion force. The micellar interior provided an inner hydrophobic environment that replaced the air bubbles and enabled the shuttling of the bitumen from the bottom of the vial to the solution surface. The whole process was conducted at temperatures below 50 °C which would save energy compared with the traditional CHWP. The oil extraction yields were also increased from 80% for the CHWP to 100% with block copolymer (BCP) micelles. The aqueous solution could be recycled at least five times³¹ which dramatically reduced water waste. However, the PEG-*b*-PMeEO₂MA sample had its own drawbacks. Its synthesis was expensive and was difficult to scale up. The extraction process took two days and was thus time-consuming. Furthermore, extractions conducted with PEG-*b*-PMeEO₂MA did not work for the poor processing ores supplied by the Alberta Innovate Technology Futures Sample Bank. These drawbacks represent serious limitations for using PEG-*b*-PMeEO₂MA as a tPS in the extraction of oil from oil sands.³¹

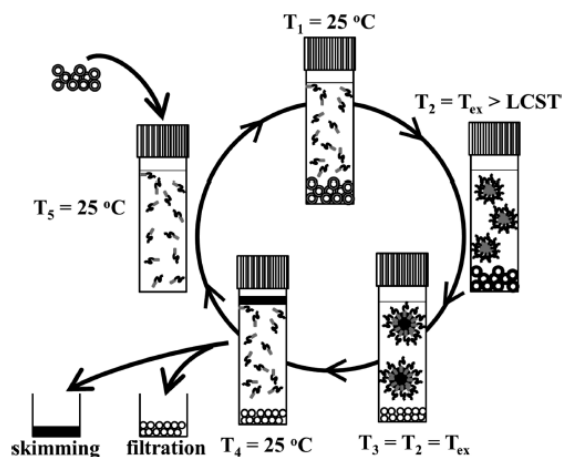


Figure 1.5. Oil extraction from oil sands with a thermoresponsive block copolymer (PEG-*b*-PMeO₂MA) as proposed by Yang and Duhamel.³¹

1.5 Thermoresponsive Starch Nanoparticles for Extraction of Oil from Oil Sands

The discovery by Magda Karski that butene oxide-modified starch nanoparticles (BO(*y*)-SNPs where *y* is the molar substitution in butene oxide) were thermosensitive led to the proposal that BO-SNPs could be used as a tPS, or more precisely, as thermoresponsive SNPs (tSNPs).³² The Taylor group then showed that SNPs modified with both BO and styrene oxide (SO(*x*)-BO(*y*)-SNPs where *x* is the styrene oxide molar substitution) were also tSNPs with the added bonus that the SO moieties would make the tSNP more hydrophobic and more likely to interact with oil sands.³³ Many of the SO-BO-SNPs became insoluble above the LCST so that a poly(ethylene glycol) block was added for stabilization yielding PEG(*z*)-BO(*x*)-BO(*y*)-SNPs. The SO-BO-SNPs studied in this thesis represented one example of tSNPs obtained by small molecule modification of an SNP. By contrast, SNPs were also modified with different combination of poly(methoxyethoxyethyl methacrylate)-*b*-poly(hydroxyethyl methacrylate) (PMeEO₂-MA-*b*-PHEA) by reversible addition fragmentation chain transfer polymerization (RAFT).³⁴ In this case,

the thermoresponsivity of these tSNPs was induced by the P MeEO_2MA block with an LCST of 26 °C in water while water-solubility was enabled by the starch and PHEA components. The SNPs modified with block copolymers were referred to as tP(x)-sP(y)-SNP where tP and sP stand for thermoresponsive (i.e. P MeEO_2MA block) and water-soluble (i.e. PHEA block) polymers present in x and y wt%, respectively. The chemical structures of tP(x)-sP(y)-SNP prepared by Dasgupta and SO(x)-BO(y)-SNP prepared by Zheng are shown in Figure 1.6.

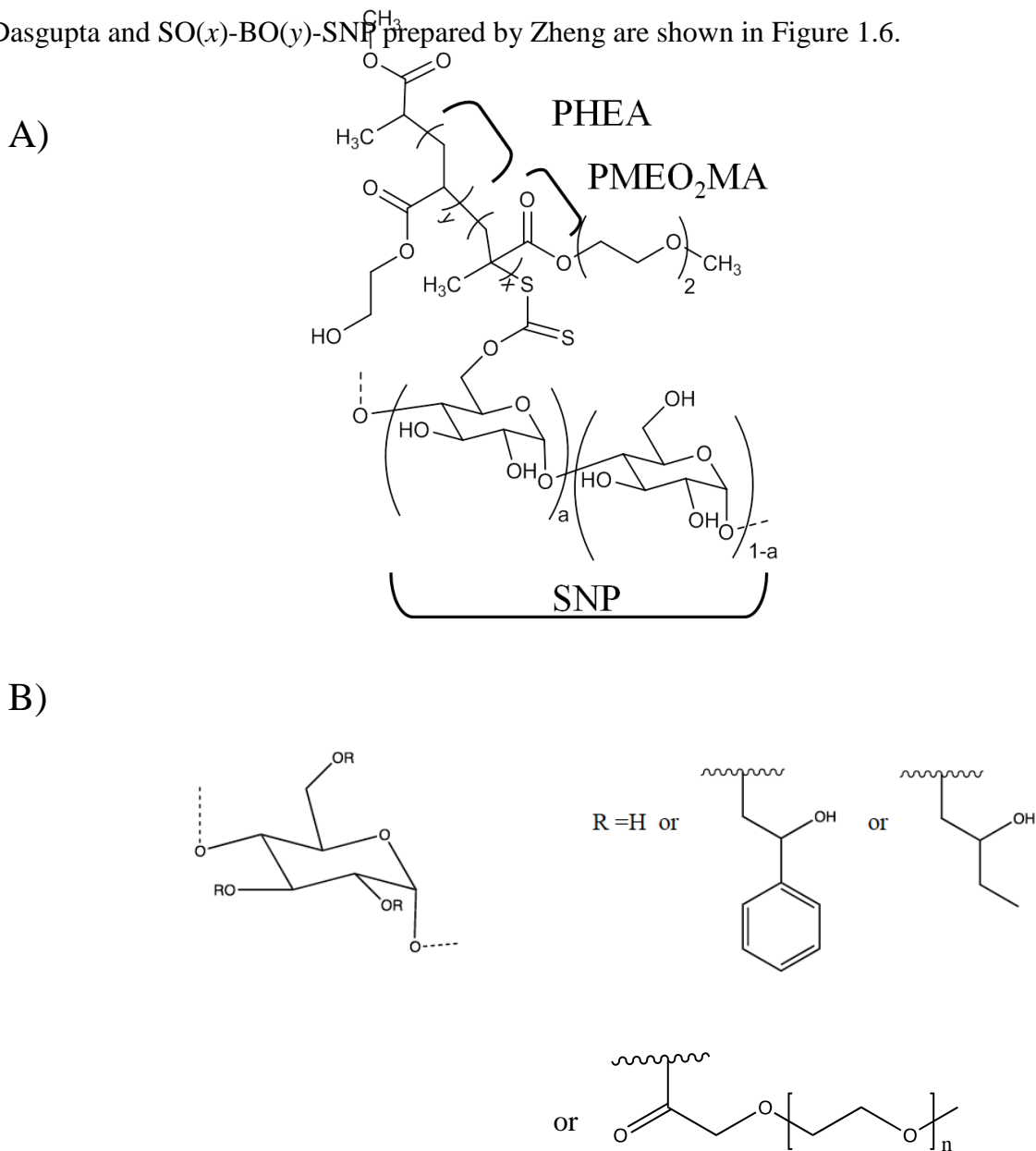


Figure 1.6. Chemical Structure of A) tP(x)-sP(y)-SNP prepared by Dasgupta and B) SO(x)-

BO(y)-SNP prepared by Zheng.³³

1.6. Thesis Outline

tSNP were investigated to assess whether they could be a good replacement for PEG-*b*-PMeEO₂MA which had been found to extract oil from oil sands effectively. Two types of tSNPs were prepared, one by Natun Dasgupta from Prof. Gauthier's group and the other one by Bowei Zheng from Prof. Taylor's group. Dasgupta used PMeEO₂MA as the thermoresponsive polymer block and poly(hydroxyethyl acrylate) (PHEA) as a hydrophilic block to modify starch nanoparticles (SNPs). These tSNPs were referred to as tP(x)-sP(y)-SNP where *x* and *y* represent the weight percentage of thermoresponsive (tP) and water-soluble (sP) polymeric blocks, respectively. Whereas Dasgupta imparted thermoresponsivity to the SNPs by adding a thermoresponsive polymer (tP = PMeEO₂MA), Zheng made the SNPs thermoresponsive by grafting styrene (SO) and butene (BO) oxide onto the SNPs which were referred to as SO(x)-BO(y)-SNP after modification. The objective of this project was to implement a series of oil extractions to determine how the tSNPs would perform at extracting oil from oil sands. Various factors that could affect the oil extractions, such as the type and amount of organic solvent added to the extraction mixture, the presence of salt, the vial and sample size, the amount of water, and how the vials were shaken needed to be optimized. The effect that the amount and length of the block copolymer attached onto the SNPs had on the oil extraction yield were investigated. The LCST of the tSNPs was determined by measuring the turbidimetry of a tSNP aqueous dispersion as a function of temperature with a UV-Vis spectrophotometer. Pyrene binding experiments were conducted by monitoring the fluorescence signal of pyrene as a function of tSNP concentration by steady-state and time-resolved fluorescence to characterize the relative hydrophobicity of the tSNPs as a function of the extent of chemical modification. In turn, the relative hydrophobicity

of a given tSNP could be used as a guide to predict its efficiency at extracting oil from oil sands.

This thesis is divided into four chapters. The first chapter provided an introduction about the methods that are currently applied industrially to extract oil from oil sands. It also described how SNPs were chemically modified to generate tSNPs whose efficiency at extracting oil from oil sands was determined. The second chapter presents the experimental methods that were employed in this thesis to characterize the solution behavior of the tSNPs in terms of their colloidal stability determined by turbidimetry and their relative hydrophobicity by pyrene fluorescence. The procedure implemented to determine the oil extraction yields with the tSNPs are also described in this chapter. The experimental results are discussed in Chapter 3. Chapter 4 reviews the conclusions that were drawn from the studies conducted in this thesis and describes future experiments that could be conducted to further improve the oil extraction yields that could be achieved with the tSNPs.

Chapter 2
Experimental

2.1 Characterization and Comparison of Different Oil Sands

Two types of oil sands were used to conduct the oil extraction experiments. One of the oil sands was supplied by Imperial Oil and was referred to as IOOs. It was the same sample that was used in an earlier study,³¹ but was available in small quantity. The other sample from the Alberta Innovate Technology Futures Sample Bank was referred to as SBos. It was available in a larger quantity. Almost all experiments conducted for this project used the SBos sample. Pictures of both oil sands are presented in Figure 2.1. The IOOs appeared oilier and stickier compared to the SBos. The difference in appearance might be related to the different clay contents between the IOOs and SBos which were found to be good and poor processing ores, respectively.³⁵ The first task in the characterization of these oil sands was to determine their oil content.

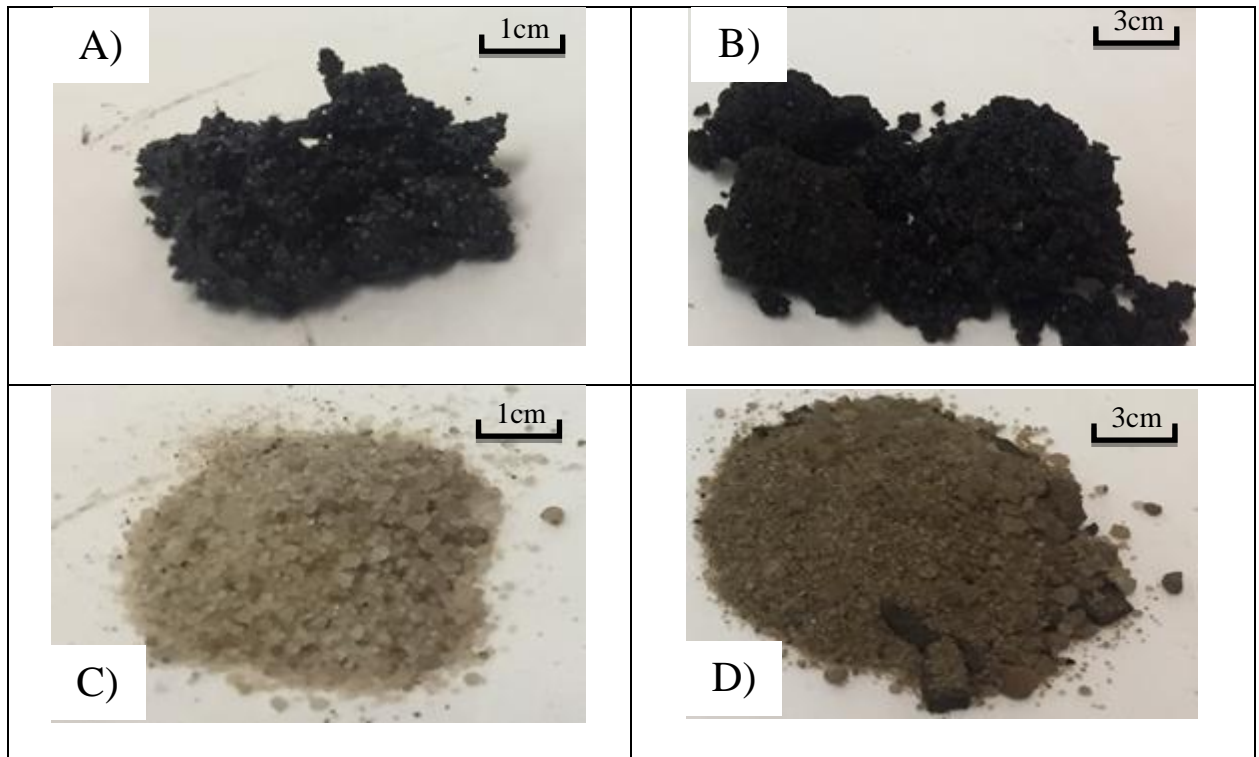


Figure 2.2. Pictures of (A) Imperial Oil oil sands (IOOs), (B) Sample Bank oil sands (SBos), (C) solid phase of IOOs, and (D) solid phase of SBos.

2.1.1 Soxhlet Extraction

Soxhlet extraction was applied to determine the oil content of the oil sands by separating the oil phase from the solid phase after Soxhlet extraction with the apparatus described in Figure 2.2. The oil sands sample was wrapped in filter paper which was placed inside the Soxhlet chamber. The Soxhlet apparatus was fit to a round bottom flask filled with tetrahydrofuran (THF).³⁶ The round bottom flask was immersed into a water bath which was maintained at 66 °C to reflux the THF. During the operation of the Soxhlet, the oil-in-THF solution accumulated in the round bottom flask. After the extraction was complete, the THF was evaporated under a gentle flow of nitrogen leaving behind a film of oil. The oil was further dried in a vacuum oven at 70 °C. The weight percentage of oil trapped in the oil sands sample was determined by taking the mass of oil recovered divided by the mass of the original oil sands sample. The experiments were repeated three times and the oil content of each type of oil sands was determined. The IOOs and SBos samples were found to contain 11.1 (± 0.1) and 10.5 (± 0.2) wt% of oil, respectively. Although the oil contents of the two types of oil sands were similar, the appearance of the solid parts left in the filter paper was different as shown in Figures 2.1C and D.

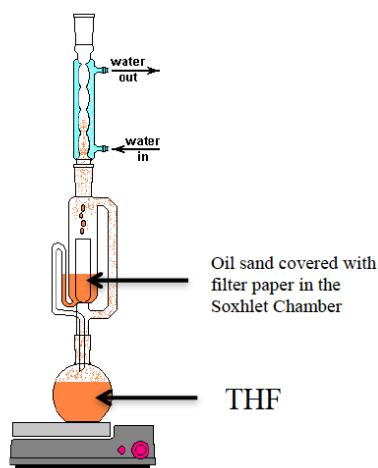


Figure 2.2. Apparatus for Soxhlet extraction.³⁷

The sand particles left in the filter paper after Soxhlet extraction were passed through a sieve with a mesh size of 44 μm to separate the fine from the coarse sand particles.³ Sand particles with a size lower than 44 μm are referred to as fines and are likelier to contain clay particles.³ The results showed that the solids in the SBos sample contained 2 wt% of fines while the IOos contained none. Further experiments were conducted to assess whether the presence of 2 wt% clay particles in the SBos could affect the oil extraction yields.

2.2 Oil Extraction Protocols

2.2.1 Primary oil extraction protocols

The protocol applied for the oil extraction followed closely that developed by Yang.³¹ A 1 g sample of oil sands was placed in a small 20 mL vial. It was covered by 15 mL of a 1 g/L polymer aqueous dispersion and 60 mg of toluene was added to the solution surface. The vial was placed in a shaker (Innova 4000, New Brunswick Scientific Co., Inc., Nijmegen, Netherlands) where it was left to stir at 250 RPM at 45 °C.³¹ After 24 hrs shaking, the vial was taken out and placed on the bench. After the vial had cooled and the aqueous mixture had stabilized, toluene was added to the upper layer of the mixture to solubilize the bitumen located at the surface of the aqueous phase, and the bitumen-in-toluene solution was collected. The water-rich middle layer was collected as well, and the sand particles at the bottom of the vial were washed with THF to collect any remaining oil. The sand fraction was also collected. The toluene or THF solvents were evaporated under nitrogen and the recovered oil and sand were further dried in a vacuum oven. The mass of the three components, namely the oil found at the surface of the aqueous mixture, the oil remaining at the bottom of the vial, and the sand particles,

was determined to calculate the yield of oil extraction. Figure 2.3 describes the oil extraction protocol. At the end of the procedure, the clean sand, polymer aqueous dispersion, oil left with the sand, and extracted oil were completely separated from each other.

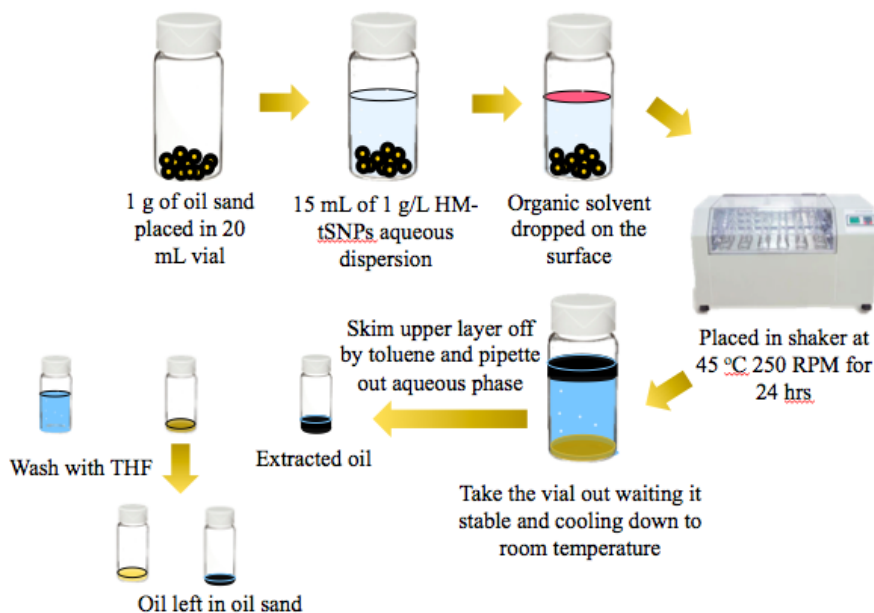


Figure 2.3. Oil extraction protocol applied to determine the yield of oil extraction.

Since the presence of fines in the SBos samples accentuated the heterogeneity of the oil sands, a second extraction protocol was introduced to reduce experimental error associated with the handling of heterogeneous samples. This second extraction protocol consisted in scaling all quantities involved in an extraction by a factor of 4. As a result, the amount of oil sands used for oil extraction was increased from 1 to 4 g. Larger size jars were employed in lieu of the 20 mL vials to accommodate 60 mL of 1 g/L of aqueous tSNP dispersion used to extract the oil instead of the 15 mL volumes used in Figure 2.3. The amount of organic solvents used to assist the oil extraction was also increased four-fold.

Since a limited supply of tSNP was available, and the scaled up procedure consumed four

times more tSNP per trial, the scaled up extraction procedure was not always implemented. Furthermore, it was determined that pre-selecting oil sands samples that did not contain obvious large chunks of rock considerably reduced the level of scatter in the calculation of the extraction yield. Consequently, the small scale extractions were conducted more often and were deemed to provide relevant information about the effectiveness of a given tSNP at extracting oil from oil sands. The effectiveness of a given tSNP sample at extracting oil from oil sands was assessed by conducting the extractions in the presence or absence of tSNP. When the yield of oil extraction without tSNP was substantially lower than that with tSNP, such a tSNP was considered to be a good candidate to further optimize the experimental conditions for oil extraction.

Since the water-insoluble organic solvents used to improve the oil extraction yields could solubilize the oil from the oil sands on their own, conditions needed to be established where addition of organic solvents to the extraction mixture would not induce complete oil extraction without tSNP. Consequently, the extraction efficiency obtained for a given mixture composition without tSNP needed to be determined to establish a baseline against which the effectiveness of the same mixture with tSNP could be compared. Taking toluene as an example, Figure 2.4 shows the extraction yield obtained by placing 1 g of SBos in 15 mL of water or 15 mL of 1 g/L aqueous PMeEO₂MA-*b*-PEG solution as a function of the amount of toluene added to the surface of the water phase. As more toluene was added to the solution, more oil was extracted even if no polymer was present in the solution. Since the improvement in the oil extraction yield obtained by adding more toluene to the solution was the same whether the polymer was present or not, the experiment shown in Figure 2.4 established that PMeEO₂MA-*b*-PEG did not improve the oil extraction yield for the SBos. The result shown in Figure 2.4 was different from that obtained for the oil extractions of IOos with PMeEO₂MA-*b*-PEG that showed full extraction in the presence

of 60 mg of toluene. The difference in extraction yield observed for the SBos sample might be due to the presence of fines that was established in Section 2.1.1. As mentioned earlier, fines are known to inhibit oil extraction by binding onto oil droplets, increasing the oil density, and preventing the rise of the oil droplet to the surface of the aqueous phase where it could otherwise be skimmed off.

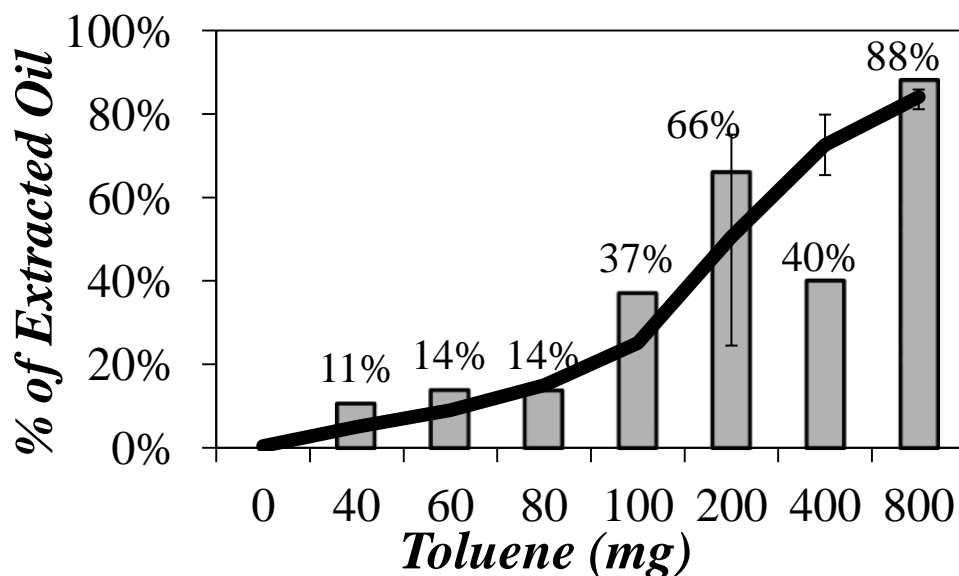


Figure 2.4. Extraction yield as a function of toluene amount for oil extractions conducted with 1 g of SBos and 15 mL of water (—) or 15 mL of 1 g/L PMeEO₂MA-*b*-PEG aqueous dispersion (bars) shaken at 45 °C for 24 hrs.

The effect of the water-insoluble organic solvent used to assist the oil extraction was also investigated. These screening experiments were conducted by Austin Richard, a coop student who worked in the laboratory during Fall 2017. The solvents had boiling points ranging from 100 to 200 °C.^{10,37} High boiling point organic solvents were required in the extraction experiments as their low vapor pressure reduced their evaporation during the extraction experiments conducted at 45 °C. Octanol, 2-ethyl-1-hexanol, isopropylbenzene, *o*-xylene, 1-

decanol, 1-hexanol, 1,3-diisopropylbenzene, hexylbenzene and two industrial solvents, namely Glycol Ether EB³⁸ and VM&P Napthan,³⁹ were used to conduct the oil extraction experiments. Five extraction experiments were usually carried out with these solvents to ensure consistency of the results.

2.2.2 Determination of the oil extraction yield

Two procedures were developed to calculate the oil extraction yield expressed as the weight percentage of oil (Oil%) recovered from the oil sands samples. The first procedure was based on Equation 1. As explained in Section 2.2.1, the mass of oil found at the surface of the aqueous mixture and left at the bottom of the vial in the sand was determined and was used in Equation 1. The Oil% was calculated by multiplying by 100 the ratio of the mass of the extracted oil over the sum of the mass of the extracted oil and the mass of the oil left in the sand.

$$Oil \%^{M1} = \frac{\text{extracted oil (g)}}{\text{extracted oil (g)} + \text{oil left in oil sand (g)}} \times 100\% \quad (1)$$

This method, referred to as Method #1, was implemented to account for heterogeneities in the oil sands that would result in oil extraction yields that would deviate substantially from the average value of about 11 wt%. However, Method #1 did not account for the residual presence of oil in the aqueous phase after completion of the oil extraction as illustrated in Figure 2.5, where some oil droplets remained in the aqueous phase. Since the amount of oil found in the aqueous phase was too low to isolate, Method #1 simply ignored its contribution. However, in some situations, more oil was left in the aqueous phase and Method #2 was introduced to minimize this error.

Method #2 used the average oil content of the oil sands determined by Soxhlet extraction.

Taking SBos as an example, the expected oil content of the SBos was determined to equal 10.5 (± 0.2) wt%. Consequently, the Oil% determined by Method #2 was obtained by multiplying by 100 the ratio of the mass of the extracted oil over the mass of oil expected to be present in the oil sands, determined to equal the total mass of oil sands sample multiplied by 0.105. Equation 2 was applied to yield Oil% according to Method #2.



Figure 2.5. The oil droplets are present in the aqueous phase.

$$Oil \%^{M2} = \frac{\text{extracted oil (g)}}{\text{oil\% from Soxhlet} \times \text{total amount of oil sand}} \times 100\% \quad (2)$$

Method #2 also had its own shortcomings. For instance, it does not account for the presence of large rocks in the oil sands samples that would lower the actual oil content of the sample, and thus result in apparently lower extraction yields.

Methods #1 and #2 were applied to calculate the percentage of oil recovered from the oil sands extractions. In most cases, the Oil% values retrieved from both procedures were fairly close, suggesting that the approximations made in each procedure were acceptable.

2.2.3 Adjustment of vial cap

The cap of the vials used in the extraction experiments had a disk of cardboard coated on one side with aluminum foil and glued on the other side to the bottom of the cap. Cap adjustment was

required to ensure that the glue would not be dissolved by the organic solvent used in the extractions, as this would otherwise add to the oil component, thus affecting the oil extraction yields. Consequently, the cardboard disk was removed from the plastic cap with a pair of tweezers. The glue used to stick the cardboard disk to the bottom of the cap was removed. The layer of aluminum foil was peeled off the cardboard disk. The gel left on the plastic cap was washed off with THF. Then, the cardboard disk was wrapped in aluminum foil and was placed back into the cap of the vial. The layer of aluminum foil was necessary to ensure a good seal between the vial and its cap and minimize the loss of volatile organic compounds escaping the vial during extractions conducted at 45 °C.

The importance of insuring a good seal between the cap and the vial is illustrated in Figure 2.6, which shows the oil recovery yields obtained for 1 g of IOos sample extracted with 15 mL of 1 g/L PEG-*b*-PMeEO₂MA aqueous dispersion and 60 mg of toluene. The results on the left represent the oil extraction yield obtained with an unsealed vial (i.e. without aluminum foil coated cardboard disk), and the results on the right give the oil extraction yield obtained with a vial capped with a properly adjusted cap. The oil extraction yield showed a dramatic increase from 5 to 100 wt% after adjusting the seal of the vial caps. A well-sealed vial minimized the loss of the organic solvent used in the extraction through evaporation and is an important requirement that must be closely adhered to in order to conduct these extraction experiments.

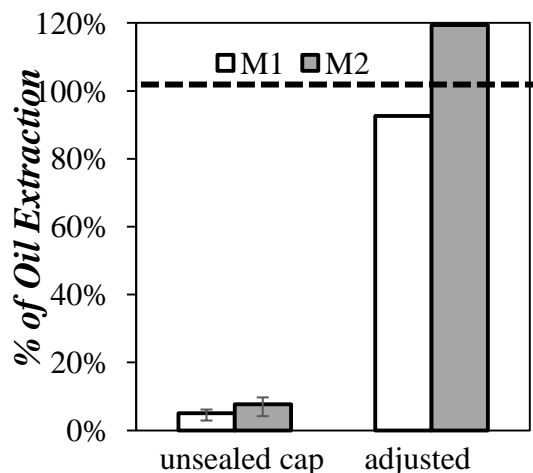


Figure 2.6. Oil extraction yields for extractions conducted at 45 °C with 1 g of IOos, 15 mL of 1 g/L PEG-*b*-PMeEO₂MA aqueous dispersion, and 60 mg of toluene and with (right) or without (left) a proper seal.

2.3 Description of the tSNPs used in this project

The tSNPs presented in Figure 1.6 were employed in oil extraction experiments to screen the most efficient tSNPs and establish conditions to optimize the bitumen extraction from oil sands. Experimental grade SNPs were provided by EcoSynthetix (Burlington, Ontario). The preparation of the SO(x)-BO(y)-SNPs has already been described^{32,33} and that of the tP(x)-sP(y)-SNPs will be presented in the near future. Compared with PEG-*b*-PMeEO₂MA, the preparation of the tSNPs was expected to be more easily scalable. Tables 2.1 and 2.2 list the tP(x)-sP(y)-SNP and SO(x)-BO(y)-SNP samples that were provided by Dasgupta and Zheng, respectively. In many instances, the SNPs modified with polymers were referred to as tP(x)-sP(y)-SNP(DS), where DS represented the degree of substitution for the xanthate moieties that were covalently attached onto the SNPs to initiate RAFT polymerization.

Table 2.1. Weight percentages of the PMeO₂MA and PHEA blocks and degree of substitution of the tP(x)-sP(y)-SNP samples prepared by RAFT.

	PMeO₂MA tP(x)	PHEA sP(y)	DS = Degree of Substitution
tP(5.9)-SNP	5.9	0	0.020
tP(7.5)-SNP	7.5	0	0.016, 0.068
tP(15)-SNP	15	0	0.016, 0.020, 0.022, 0.038, 0.060
tP(27)-SNP	27	0	0.020
tP(30)-SNP	30	0	0.016, 0.022, 0.031, 0.038
tP(15)-sP(15)-SNP	15	15	0.060
tP(15)-sP(27)-SNP	15	27	0.020
tP(27)-sP(27)-SNP	27	27	0.020
tP(15)-sP(7.5)-SNP	15	7.5	0.016, 0.038
tP(15)-sP(30)-SNP	15	30	0.038
tP(30)-sP(15)-SNP	15	7.5	0.031, 0.022, 0.060

Table 1.2. Molar substitution of styrene and butene oxide and weight percentage of PEG for the PEG(z)-SO(x)-BO(y)-SNP samples.

Sample	SO (x)	BO (y)	PEG (z)	Order of chemical modification	Solubility in water (25°C)
1	0.28	0.34	0	1 st Styrene Oxide 2 nd Butene Oxide	Soluble
2	0.24	0.38	0	Styrene Oxide and Butene Oxide together	Soluble
3	0.24	0.40	0	1 st Butene Oxide 2 nd Styrene Oxide	Precipitate observed
4	0.26	0.82	0	1 st Styrene Oxide 2 nd Butene Oxide	Soluble
5	0.25	0.66	0	Styrene Oxide and Butene Oxide together	Soluble
6	0.24	0.82	0	1 st Butene Oxide 2 nd Styrene Oxide	Soluble
7	0.32	0.39	0.5	-	Soluble
8	0.32	0.39	1	-	Soluble

2.4 Characterization of the tSNPs

2.4.1. Lower critical solution temperature (LCST) determination

All tSNPs samples showed a cloud point (T_c).⁴⁰ The cloud point represents the temperature where a polymer solution turns turbid. It is related to the lower critical solution temperature (LCST) of a polymer, which represents the temperature above which the polymer becomes insoluble and precipitates out of the solution.⁴¹ The LCST is usually close to T_c .⁴² As the solution temperature was increased past T_c , the tSNPs dehydrated, became insoluble, and aggregated. At this temperature, the tSNPs were more likely to interact with apolar chemicals such as the organic solvent located at the surface of the aqueous phase. The tSNPs could then transport the organic solvent from the surface of the aqueous phase down to the bottom of the vial, where the organic solvent could then interact with the oil sands and proceed with the extraction of the oil. The tSNPs would then shuttle the extracted oil back to the surface of the aqueous dispersion. The

shuttling of oil from the bottom of the vial to the surface of the dispersion was enabled by the dehydrated tSNPs that could stabilize the oil droplets in the aqueous dispersion as they travelled through it. After completion of the oil extraction, the oil should be found as a thick layer at the surface of the aqueous phase and as oil droplets stabilized by the dehydrated tSNPs in the aqueous phase. Lowering the dispersion temperature below T_c would destabilize the dispersion of oil droplets which could raise to the surface, thus finalizing the extraction.

As the above discussion makes clear, the feasibility of the extraction procedure depends on the cloud point of the tSNPs. Since the goal of the project was to conduct oil extractions at temperatures as low as 45 °C, the tSNPs needed to have a cloud point at a temperature that was lower than 45 °C. The cloud point of the tSNP aqueous dispersions was determined by monitoring the percentage transmittance ($T\%$) as a function of the dispersion temperature with a Cary 100 Bio UV-Vis spectrophotometer.

In these experiments, 3 mL of a 1 g/L tSNPs aqueous dispersion was prepared and placed in a 1 cm path length UV-Vis cuvette. It was cooled to 15 °C by placing the cuvette in the UV-Vis spectrophotometer chamber where it was maintained at 15 °C for 10 min. After inserting the cuvette in the UV-Vis spectrophotometer holder, the temperature was increased from 15 to 90 °C at a rate of 1 °C/min, and $T\%$ was recorded at each temperature. In some instances, no cloud point could be detected with a 1 g/L tSNP dispersion. Since solvency worsens with increasing concentration, the concentration of the tSNPs aqueous dispersion was increased from 1 g/L to 3, 5, and 10 g/L and another temperature ramp was conducted. The resulting plot of $T\%$ as a function of dispersion temperature is shown in Figure 2.7 for a 1 g/L tP(15)-sP(15)-SNP(0.06) aqueous dispersion. The temperature corresponding to T_c is found when the derivative of $T\%$ with respect to temperature ($dT\%/dT$) deviates strongly from zero. The expression of $dT\%/dT$ is

given in Equation 3 and a plot of $dT\%/dT$ is shown in Figure 2.7.

$$\frac{dT\%}{dT} = \frac{T\%(T_2) - T\%(T_1)}{T_2 - T_1} \quad (3)$$

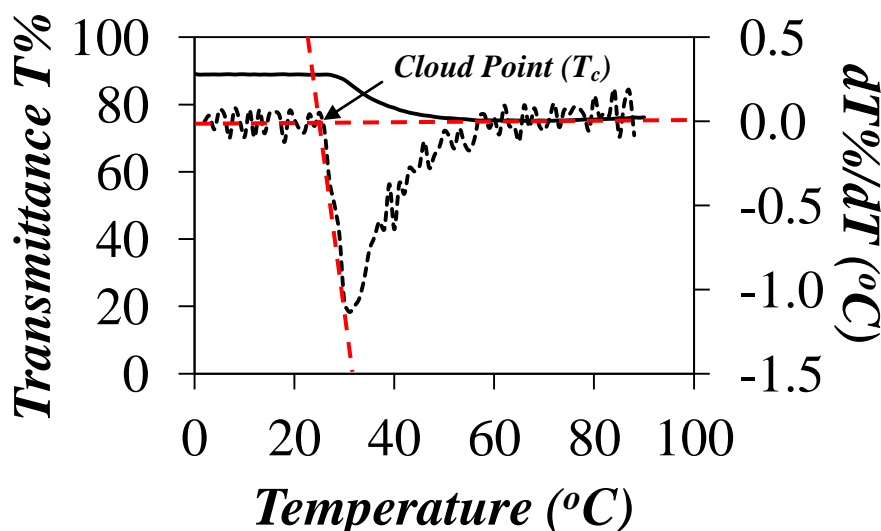


Figure 2.7. Plot of (—) $T\%$ and (·····) $dT\%/dT$ as a function of temperature for a 1 g/L aqueous dispersion of tP(15)-sP(15)-SNP(0.06).

2.4.2 Characterization of the tSNPs by pyrene fluorescence

Aqueous dispersions of tSNPs were prepared with 0.5 μM pyrene. The fluorescence of pyrene was employed to characterize the hydrophobicity of the tSNPs in an effort to establish a hydrophobicity scale for the tSNPs that would enable one to predict the optimal hydrophobicity required to ensure efficient oil extraction from oil sands. The pyrene concentration of 0.5 μM was lower than the saturation limit of 0.7 μM pyrene in water, which ensured that pyrene was fully soluble for these fluorescence experiments. The fluorescence spectra and decays of the tSNPs aqueous dispersions with 0.5 μM pyrene were acquired with a PTI MD-5020 steady-state fluorometer and an IBH time-resolved fluorometer, respectively. More details on these

instruments can be found in earlier publications.⁴³⁻⁴⁸

2.4.2.1 Steady-State Fluorescence

Among the many advantageous photophysical properties of pyrene, one can list its large molar extinction coefficient, good quantum yield, long lifetime, and its ability to form an excimer.^{49,50} These properties make pyrene an ideal chromophore to study macromolecules in solution. Figure 2.8 shows a typical fluorescence spectrum for 0.5 μM pyrene in an aqueous dispersion of tSNPs excited at 336 nm, where the sharp peaks between 360 and 410 nm are characteristic of the monomer fluorescence. The ratio of the fluorescence intensity of the first to the third peak, namely the I_1/I_3 ratio, is known to increase with increasing polarity of the local environment experienced by pyrene.⁵¹ This feature arises from the symmetry-forbidden 0-0 transition of pyrene which corresponds to the I_1 peak. In apolar solvents, the fluorescence intensity of the I_1 peak is suppressed, but it is partially restored in polar solvents, resulting in the dependency of the I_1/I_3 ratio with solvent polarity. In turn, this feature can be harnessed to assess the strength of the binding of pyrene to tSNPs as a function of the level of modification. Pyrene, being sparingly soluble in water, will partition between the aqueous phase and the tSNPs. Stronger binding of pyrene to a more hydrophobic tSNP will be reflected by a lower I_1/I_3 ratio. Thus, the amount of pyrene bound to the tSNPs and the I_1/I_3 ratio of pyrene in an aqueous dispersion of tSNP is related to the hydrophobicity of the chemical modification applied to the SNP, and could help define optimal types and levels of chemical modification to ensure good extraction conditions.⁵²⁻

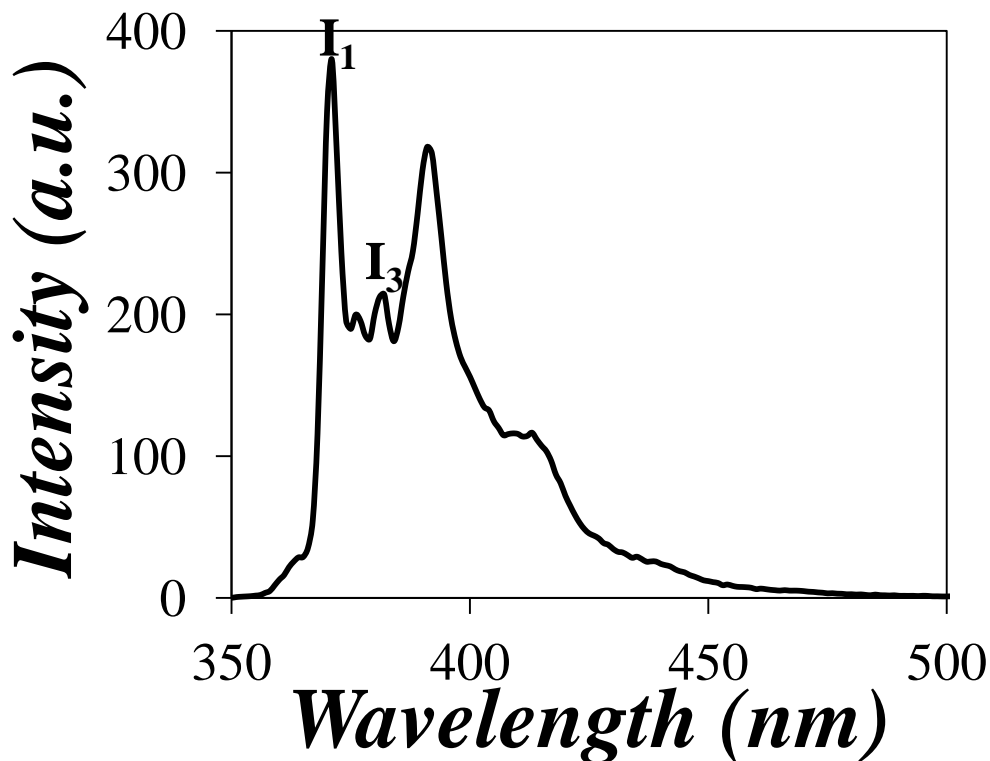


Figure 2.8. Fluorescence spectrum of a 0.5 μM pyrene solution in milli-Q water. The fluorescence intensities I_1 and I_3 at the first and third peaks have been indicated. $\lambda_{\text{ex}} = 336 \text{ nm}$.

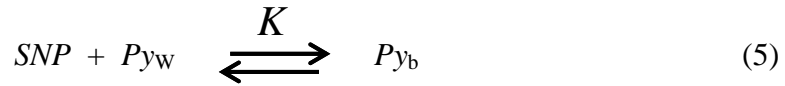
2.4.2.2 Time-resolved fluorescence

Time-resolved fluorescence was applied to characterize the different states that pyrene can occupy in aqueous tSNP dispersions. As it turns out, the lifetime of pyrene is quite sensitive to its local environment. For instance, the lifetime of pyrene in water (τ_w) equals 130 ns,^{55,56} while it takes a much larger value (τ_b) around 280 ns when bound to tSNPs.⁵¹ Consequently, the time-resolved fluorescence decays acquired for pyrene in tSNP aqueous dispersions could be analyzed with a sum of exponentials as shown with Equation 4. In Equation 4, the value of the lifetimes recovered from the analysis could be assigned to a given state of pyrene, and the pre-exponential factors a_w and a_b could be used to calculate the molar fractions of pyrene in a given state,

corresponding to pyrene molecules that were either in water (P_{y_w}) or bound to the tSNPs (P_{y_b}), respectively. The short-lived intrinsic fluorescence of the tSNPs was accounted for by the sum of exponentials $f_{SNP}(t)$ in Equation 4 with a coefficient a_{SNP} . Figure 2.9 shows the time-resolved fluorescence decay of pyrene dissolved in a tSNPs aqueous dispersion. The fluorescence decay could be divided into three temporal regions. The short-lived intrinsic fluorescence of the tSNPs appeared as a spike at the onset of the decay, followed by the longer-lived fluorescence of pyrene in water at intermediate times, and ending with the very long-lived fluorescence of pyrene bound to the tSNP at the end of the decay.

$$[Py^*]_{(t)} = a_{SNP} f_{SNP}(t) + a_{PyW} \exp(-t / \tau_w) + a_{Pyb} \exp(-t / \tau_b) \quad (4)$$

The binding of pyrene to the tSNPs could be represented by the equilibrium shown in Equation 5. The equilibrium constant K in Equation 5 was determined experimentally according to Equation 6 where the parameters a_{PyW} and a_{Pyb} were retrieved from the analysis of the fluorescence decays with Equation 4.



$$K = \frac{[Py_b]}{[Py_w][SNP]} = \frac{a_{Pyb}}{a_{PyW}[SNP]} \quad (6)$$

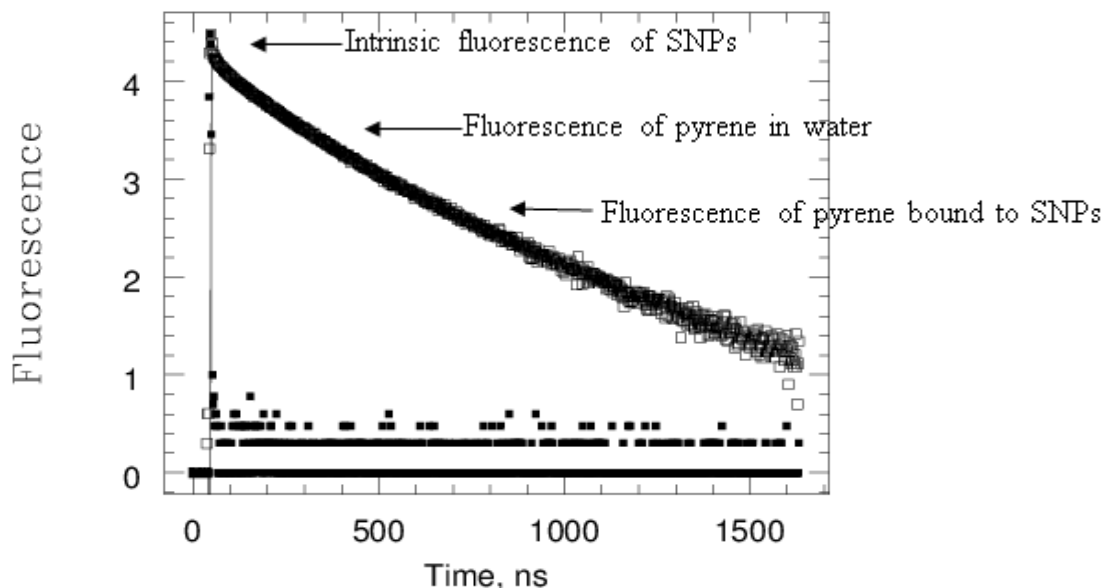


Figure 2.9. Time-resolved fluorescence decay of 0.5 μM pyrene in 1 g/L SNP aqueous dispersion.

2.4.2.3 Sample preparation for the tSNP dispersions with 0.5 μM pyrene

The fluorescence experiments were carried out with a 0.5 μM pyrene concentration in aqueous tSNP dispersions where the tSNP concentration was varied. Since the mass of pyrene required to prepare the dispersions was too small to be measured with an analytical balance, stock solutions of pyrene in water were prepared by first dissolving pyrene in THF. The exact concentration of pyrene was determined by applying the Beer-Lambert law to the absorbance of the pyrene solution in THF using a molar extinction coefficient at 336 nm of $45,000 \text{ M}^{-1}\cdot\text{cm}^{-1}$. The appropriate mass of pyrene solution in THF necessary to prepare 2 mL of a 17 g/L aqueous tSNP dispersion and 20 mL of milli-Q water solution with 0.5 μM pyrene was placed in two vials. Both vials were wrapped with aluminum foil to prevent degradation of pyrene from exposure to light and they were placed in the fumehood, where the THF was evaporated leaving behind a

film of pyrene deposited on the bottom of the vials. The 17 g/L tSNP aqueous dispersion (2 mL) and milli-Q water (20 mL) were separately added to the two vials, that were then agitated in the shaker for 10 mins. The fluorescence spectrum and decay of the 17 g/L tSNP dispersion with 0.5 μM pyrene were acquired. After this task was completed, the 17 g/L tSNP dispersion with 0.5 μM pyrene was diluted with the aqueous solution containing 0.5 μM pyrene and the fluorescence spectrum and decay of the resulting dispersion were acquired. This process was repeated 20 times to obtain the fluorescence spectra and decays of a series of tSNP dispersions where the pyrene concentration was maintained at 0.5 μM and the tSNP concentration was varied from 0 to 17 g/L. The pyrene fluorescence experiments were conducted for all tSNPs at 25 and 50 $^{\circ}\text{C}$, two temperatures that were below and above the cloud point of the selected tSNPs, to assess the effect that the temperature had on the binding of pyrene to the tSNPs.

Chapter 3

Results and Discussion

3.1 LCST Determination of the tSNPs by Turbidimetry

3.1.1 SO-BO-SNP samples

The effect that the order of the addition of styrene- or butene oxide had on the solution properties of the resulting SO-BO-SNPs was investigated by determining their respective LCST. Figure 3.1 shows a plot of transmittance at 500 nm as a function of temperature for a 10 g/L aqueous dispersion of SO-BO-SNP (Samples #4, 5, and 6 in Table 2.2). Since these three samples had comparable DS of SO (0.25 ± 0.01) and BO (0.77 ± 0.09), differences in their LCST could be attributed to differences in the distribution of SO and BO moieties depending on the order in which they were reacted with the SNP substrate. The percentage of transmittance ($T\%$) at low temperature was high, indicating that the SO-BO-SNPs were dispersible in water below 35 °C. As the temperature passed through the LCST, $T\%$ decreased dramatically to less than 10 %. No difference in the LCST of the particles was observed in Figure 3.1, indicating that the order in which SO or BO were reacted with the SNP substrate had no effect on their LCST. The low $T\%$ observed at temperatures above the LCST of the particles was a result of aggregation of the SO-BO-SNPs due to a decrease in their dispersibility above the LCST. Particle aggregates blocked the light beam of the spectrophotometer, which decreased light transmission. Particle aggregation also indicated that the particles were less polar and thus more likely to interact with the oil of the oil sands. However although a decrease in the polarity of the particles was a sought-after feature to induce interactions with oil, a particle that was too hydrophobic would precipitate out of the aqueous phase, preventing it from transporting the oil from the bottom to the surface of the aqueous dispersions, thus achieving low oil extraction of the oil sands. Consequently, the low $T\%$ obtained above the LCST indicated that a combination of degrees of substitution of 0.25 and 0.77 for, respectively, BO and SO, represented a modification that was too hydrophobic for oil

extraction purposes, bound to result in a bad performance in oil extraction experiments for aqueous dispersions of SO(0.77)-BO(0.25)-SNP.

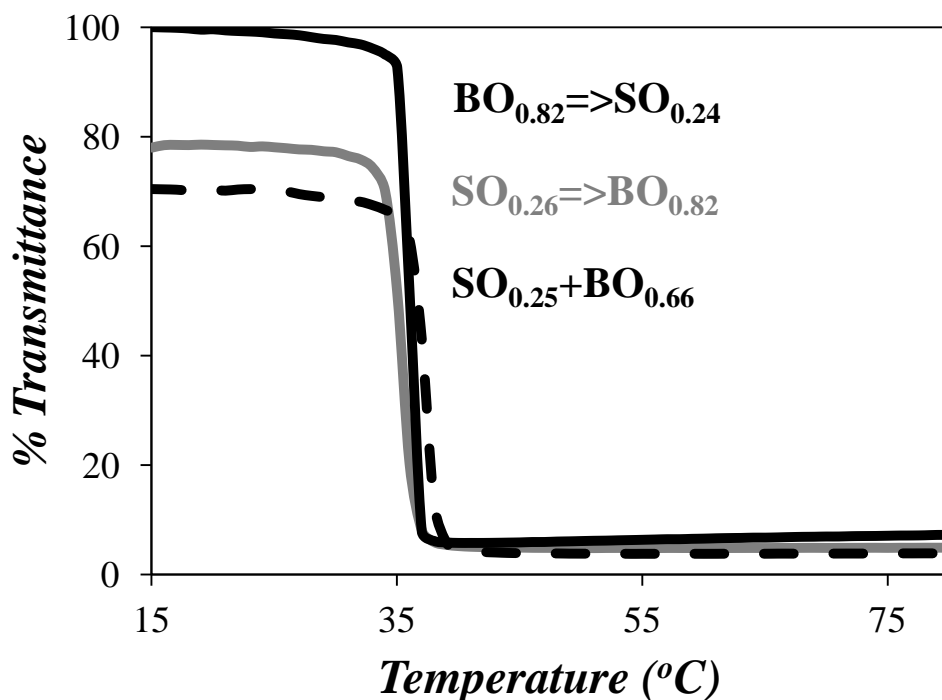


Figure 3.3. Plot of transmittance at 500 nm as a function of temperature for 10 g/L aqueous dispersions of SO-BO-SNP: Sample #4 (—), Sample #5 (—), and Sample #6 (- - -).

A 20K hydrophilic poly(ethylene glycol) (PEG) was grafted onto the SO-BO-SNPs to improve their dispersibility in water. A plot of transmittance at 500 nm as a function of temperature is provided in Figure 3.2 for two aqueous dispersions prepared with two PEG-SO-BO-SNP samples. The traces with dashed and solid lines represent the transmittance for the PEG-SO-BO-SNP where the amount of PEG used for the chemical modification of the SO-BO-SNPs equaled 100 and 50 wt% of the starch. The LCST obtained for the 3 g/L tSNP aqueous dispersions equaled 73 °C. This LCST was too high to conduct oil extractions at 45 °C. However the LCST was found to decrease to 33 °C when the tSNP concentration was increased to 5 g/L.

Unfortunately $T\%$ at temperatures above the LCST was still lower than 20 % indicating poor stability of the particles and thus poor extraction yields. The results shown in Figure 3.2 imply that despite the grafting of PEG20K to the SO-BO-SNPs, their stabilization still requires much improvement.

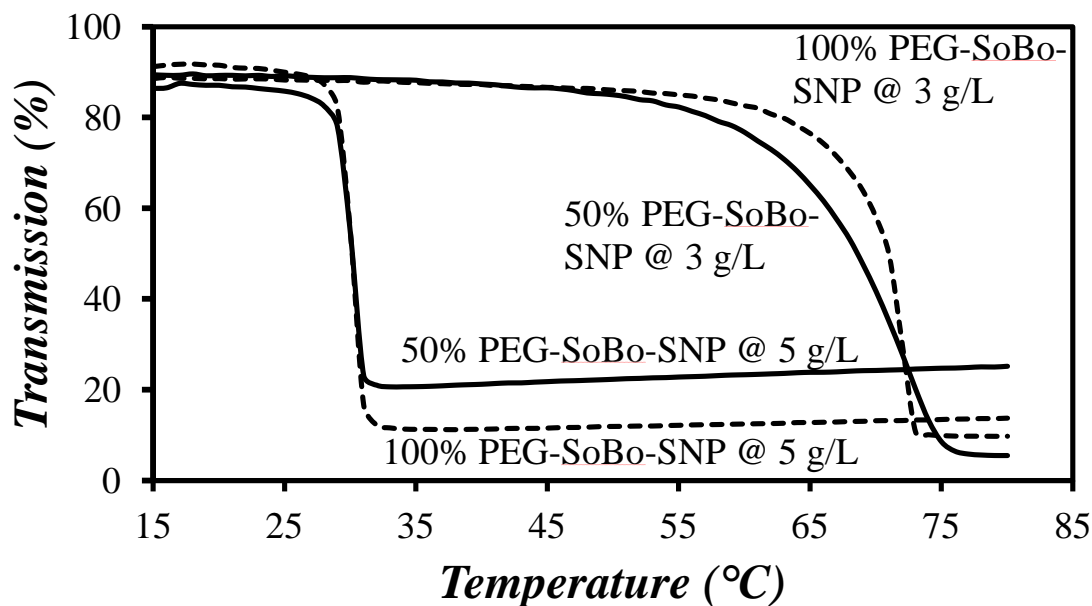


Figure 3.2. Plot of transmittance at 500 nm as a function of temperature for a 3 and 5 g/L aqueous dispersion prepared with two PEG-SO-BO-SNPs.

Oil extractions conducted with Samples #1, 2, and 4 – 6 confirmed the predictions that the poorly stabilized dehydrated PEG-SO-BO-SNPs would perform poorly for oil extractions. As shown in Figure 3.3, barely 10 % of oil was extracted from the oil sands with the SO-BO-SNP aqueous dispersions, probably because the dehydrated particles precipitated out from the aqueous phase as the extraction temperature was kept at 45 °C, above their LCST.

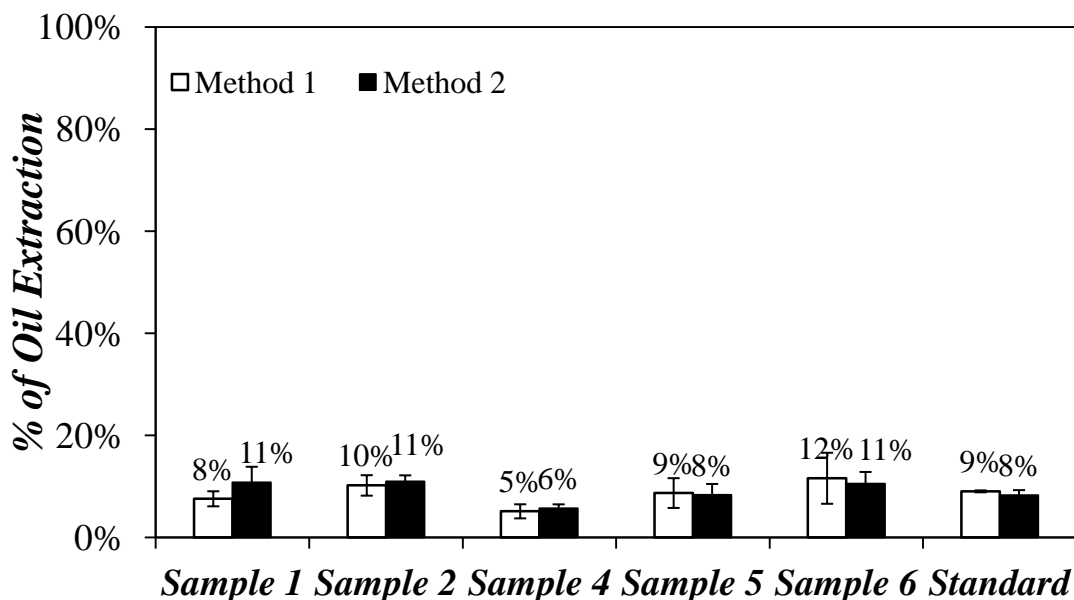


Figure 3.3. Oil extractions carried out with 4 g of SBos at 45 °C, 200 mg of toluene, and 60 mL of 1 g/L of SO-BO-SNP aqueous dispersions.

3.1.2 tP-sP-SNP Samples

The cloud point of 1 g/L tP-sP-SNP aqueous dispersions was determined by monitoring the transmittance at 500 nm as a function of temperature for tSNPs modified with 5.9, 15, and 27 wt% PMeEO₂MA (tP). Rapid inspection of the profiles of $T\%$ as a function of temperature shown in Figure 3.4A suggests that the LCST decreases with increasing amount of tP. The traces shown in Figure 3.4A were analyzed to determine the cloud point of the dispersions which was plotted in Figure 3.4B. T_c was found to decrease with increasing tP content. Decreasing the tP content of the tP-SNP resulted in a higher $T\%$ value at temperatures above T_c , thus reflecting higher solubility of the tP-sP-SNPs at temperatures above their LCST.

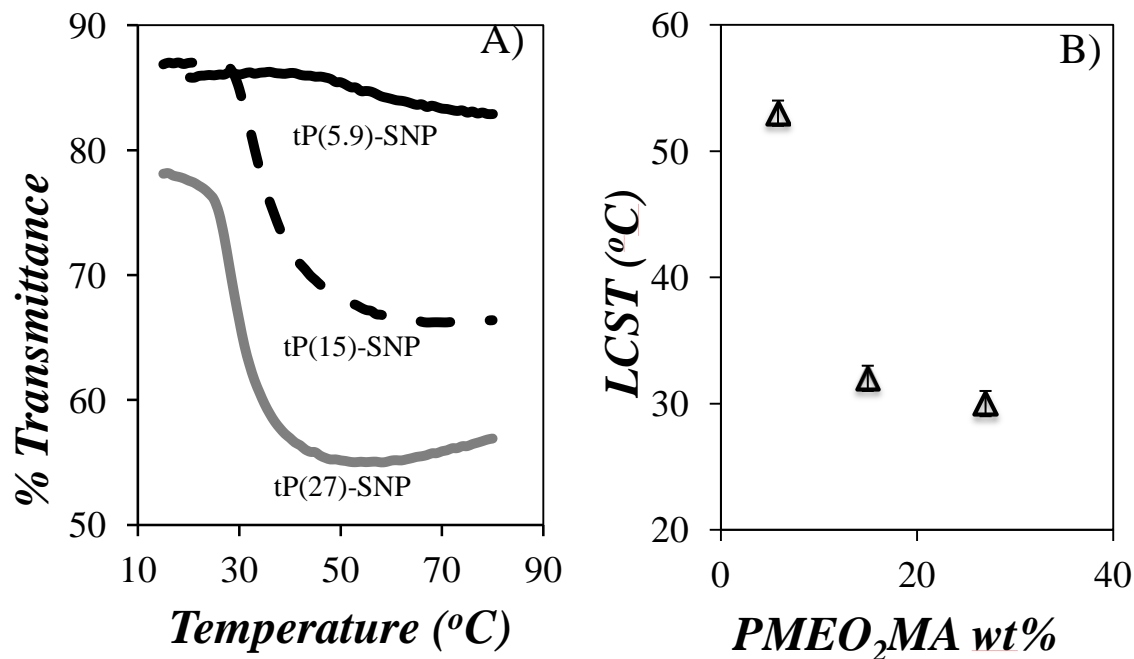


Figure 3.4. A) Plot of transmittance at 500 nm as a function of temperature for 1 g/L aqueous dispersions of SNPs modified with (—) 5.9, (- - -) 15, and (—) 27 wt% PMeO₂MA. B) Plot of LCST as a function of the PMeO₂MA content used to modify the SNPs.

Figure 3.5 illustrates the effect that the amount of water-soluble PHEA (sP) grafted onto the tP(0.15)-SNP sample had on the LCST of the tSNPs. The traces shown in Figure 3.5A are for 1 g/L aqueous dispersions of tP(15)-SNPs modified with 0, 15, and 30 wt% PHEA. The corresponding LCST obtained for a same tP(15)-SNP substrate was plotted as a function of the PHEA content in Figure 3.5B. Figure 3.5A suggests that the addition of the PHEA block to the tP(15)-SNP substrate had a substantial effect on the stability of the resulting tSNPs in water, as $T\%$ increased with increasing amount of grafted PHEA at temperatures above the LCST. The increase in stability observed for the tP(15)-SNPs modified with PHEA represents a desirable feature, as it will minimize precipitation of the particles during oil extraction at temperatures

higher than the LCST. On the other hand, the amount of grafted PHEA had little effect on the LCST, as the drop in $T\%$ occurred at the same temperature in Figure 3.5B, with the LCST decreasing from 31 to 27 °C when the amount of grafted PHEA increased from 0 to 30 wt%.

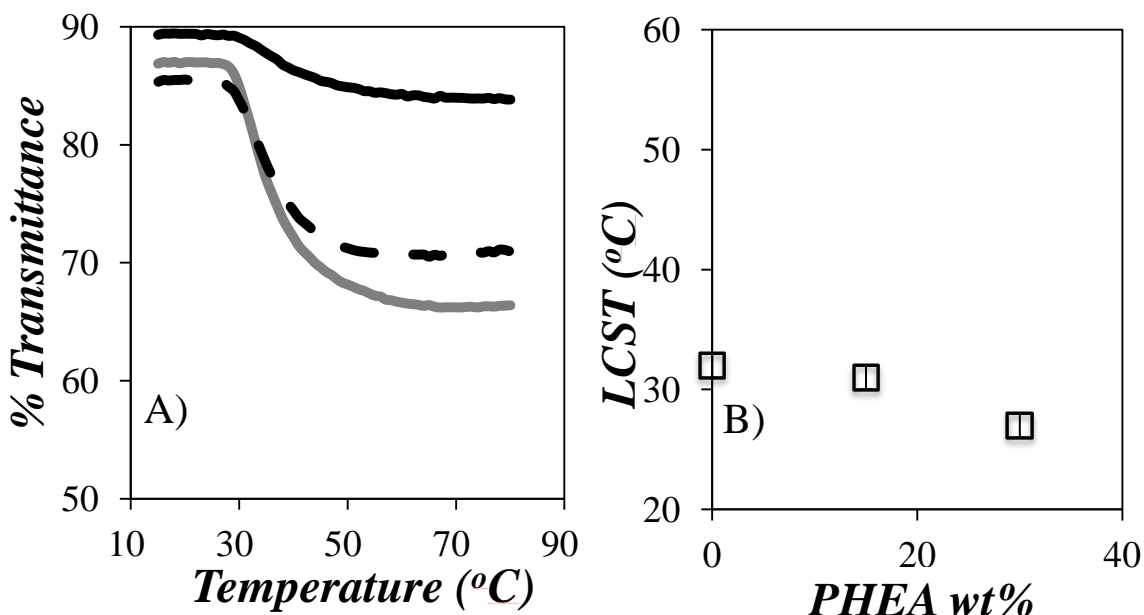


Figure 3.5. A) Plot of transmittance at 500 nm as a function of temperature for 1 g/L aqueous dispersions of tP(15)-SNPs modified with (—) 0, (- - -) 15, and (—) 30 wt% PHEA. B) Plot of LCST as a function of the content of PHEA grafted onto the tP(15)-SNP substrate.

Figure 3.6A represents the plots of transmittance at 500 nm as a function of temperature for 1 g/L aqueous dispersions of all the tP(x)-sP(y)-SNP samples. The corresponding LCSTs have been listed in Table S12. For reference, the trace obtained for a 1 g/L PEG-*b*-PMeEO₂MA aqueous solution is highlighted in black in Figure 3.6A. The drop in $T\%$ at the LCST for the block copolymer was minimal due to the enhanced phase separation of the block copolymers that resulted in the formation of well-defined small and colloidally stable block copolymer micelles.

Since the good extraction yields that had been obtained with PEG-*b*-PMeEO₂MA for the IOos had been attributed to the good colloidal stability of the resulting block copolymer micelles that formed above the LCST of the PMeEO₂MA block, tSNPs with a profile matching the trace obtained for PEG-*b*-PMeEO₂MA were thus selected as candidates of interest for oil extraction experiments.

Out of all the tP-sP-SNPs investigated, those with a PMeEO₂MA content of 15 wt% prepared with a low DS (0.016 or 0.020) showed a shallow drop at the LCST. Consequently, samples tP(15)-SNP(0.016), tP(15)-SNP(0.020), tP(15)-SNP(0.022) and tP(15)-SP(7.5)-SNP(0.016) were selected for further extraction experiments.

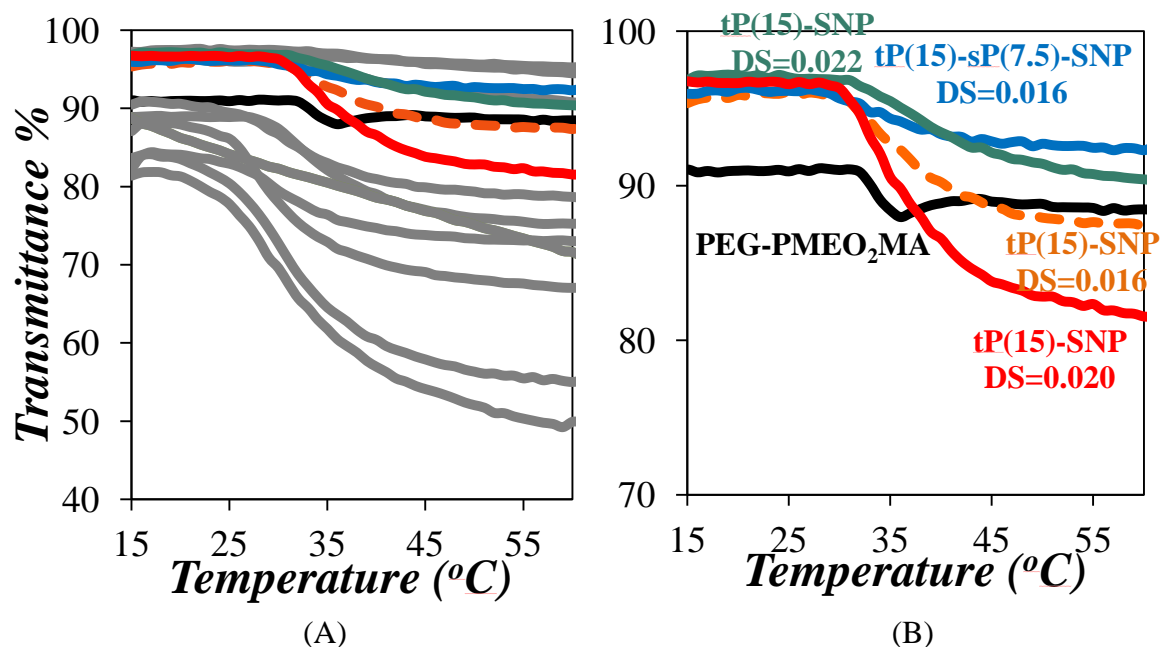


Figure 3.6. A) Plots of transmittance at 500 nm as a function of temperature for 1 g/L aqueous dispersions of all tP-sP-SNP samples. B) Selected profiles of tP-sP-SNP exhibiting a shallow drop in $T\%$ above the LCST as observed for PEG-*b*-PMeEO₂MA.

Both the weight percentage and the degree of polymerization (DP) of PMeEO₂MA

grafted onto the SNP substrate needed to be carefully controlled for the oil extractions. First, a thermoresponsive behavior would be observed only if a large enough quantity of PMeEO₂MA had been attached onto the SNPs. However, too much PMeEO₂MA would jeopardize the stability of the tP-SNPs above their LCST. A poor colloidal stability could be inferred from a low *T*% value at temperatures above the LCST of the tP-SNPs. Based on the trends shown in Figure 3.6, SNPs modified with 15 wt% of PMeEO₂MA contained enough thermoresponsive polymer to exhibit an LCST, but appeared stable since *T*% remained above 80% at temperatures above the LCST. Second, to ensure that PMeEO₂MA would interact with the organic solvent (toluene), the PMeEO₂MA chains needed to be long enough, which could be achieved by maintaining a low DS, since the DS and average DP of each tP-segment of each segment chain are inversely proportional. The *T*%-versus-*T* profiles of a series of tP(15)-SNPs with DS ranging from 0.016 to 0.060 are presented in Figure 3.7. While tP(15)-SNP(0.06) is a clear outlier, showing an LCST lower than 15 °C, the effect of DS on the profiles shown in Figure 3.7 was not obvious since all other tP(15)-SNP samples showed a shallow drop in *T*% above the LCST.

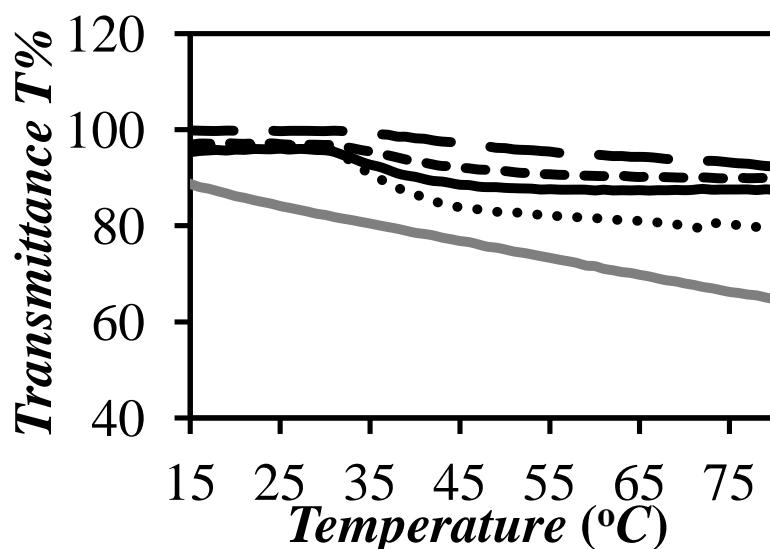


Figure 3.7. Plots of *T*% as a function of temperature for a series of tP(15)-SNPs with DS equal to (—) 0.016, (·····) 0.020, (- - -) 0.022, (— · -) 0.038, and (———) 0.060.

3.2 Results from Oil Extraction Experiments

As the tP(15)-SNP samples with a low DS were only prepared at a later stage of the project, early extractions were conducted with tP(15)-SNP(0.06). The extraction results were compared in Figure 3.8 to those obtained under similar experimental conditions but where the tSNP aqueous dispersion was replaced by pure water as a control. The oil sand used in these experiments was the SBos sample. The extraction yields were determined according to the two methods described in the Experimental section. Within experimental error, both methods resulted in similar extraction yields as shown in Figure 3.8. As the amount of toluene added to the surface of the polymer dispersion increased, so did the extraction yield reaching 80% when more than 400 mg of toluene was added to the extraction mixture. While the oil extraction was the same in the presence and absence of polymer for low toluene amounts, the presence of polymer worsened the oil recovery when larger amounts of toluene were used. Consequently, the tP(15)-SNP(0.06) sample was found, at best, not to affect or, at worst, to reduce the oil extraction yield. These disappointing results were attributed to poor interactions between tP(15)-SNP(0.06) and the organic solvent, as strong interactions between the organic solvent and the thermoresponsive block have been found to be critical to ensure good oil extraction yields.³¹

The poor interactions between tP(15)-SNP(0.06) and toluene could also be inferred from the large error bars obtained for the calculation of the extraction yields in Figure 3.8. Poor interactions would result in metastable dispersions where minute differences in experimental conditions could result in either poor or good extractions. Based on these observations, it was decided that toluene was not a good solvent to generate stable aqueous dispersions with tP(15)-SNP(0.06).

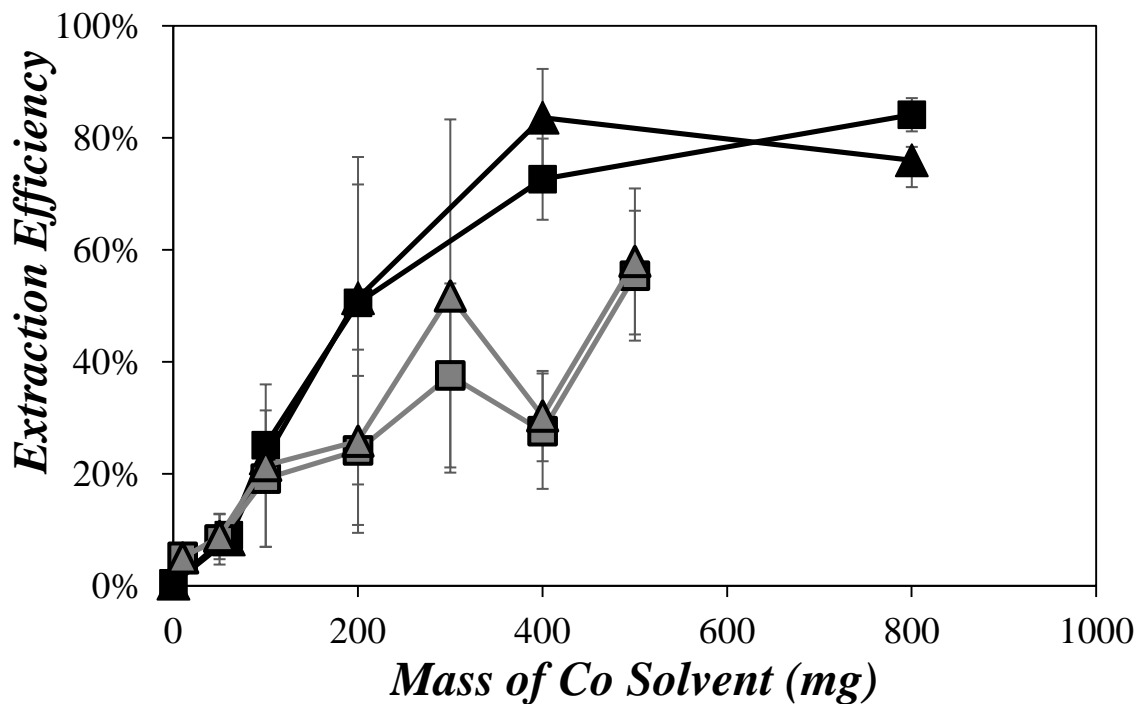


Figure 3.8. Plot of the yield for the oil extraction from 1 g of SBos as a function of toluene mass added to (■,▲) 15 mL of 1 g/L tP(15)-SNP(0.06) aqueous dispersion and (■,▲) 15 mL of water. (■,□) Method #1, (▲,△) Method #2.

Octanol is a hydrophobic solvent that is often used in combination with starch.⁵⁷⁻⁵⁹ Extraction experiments were carried out with octanol to assess whether this solvent would promote better interactions with the tSNPs that would result in better oil extraction yields. The extraction yields achieved with 60 mL of 1g/L aqueous dispersions of tP(15)-SNP(0.06), tP(27)-SNP(0.02), and tP(15)-sP(15)-SNP(0.06) for oil extraction experiments conducted with 4 g of SBos are shown in Figure 3.9 when 200 mg of toluene/octanol was added to the dispersion surface before the vials were placed in the shaker. All tSNP dispersions resulted in a better oil extraction yield when octanol was used instead of toluene. Unfortunately, a similar improvement

was also observed for the extractions conducted with pure water without tSNPs, indicating that octanol extracted oil more efficiently than toluene.

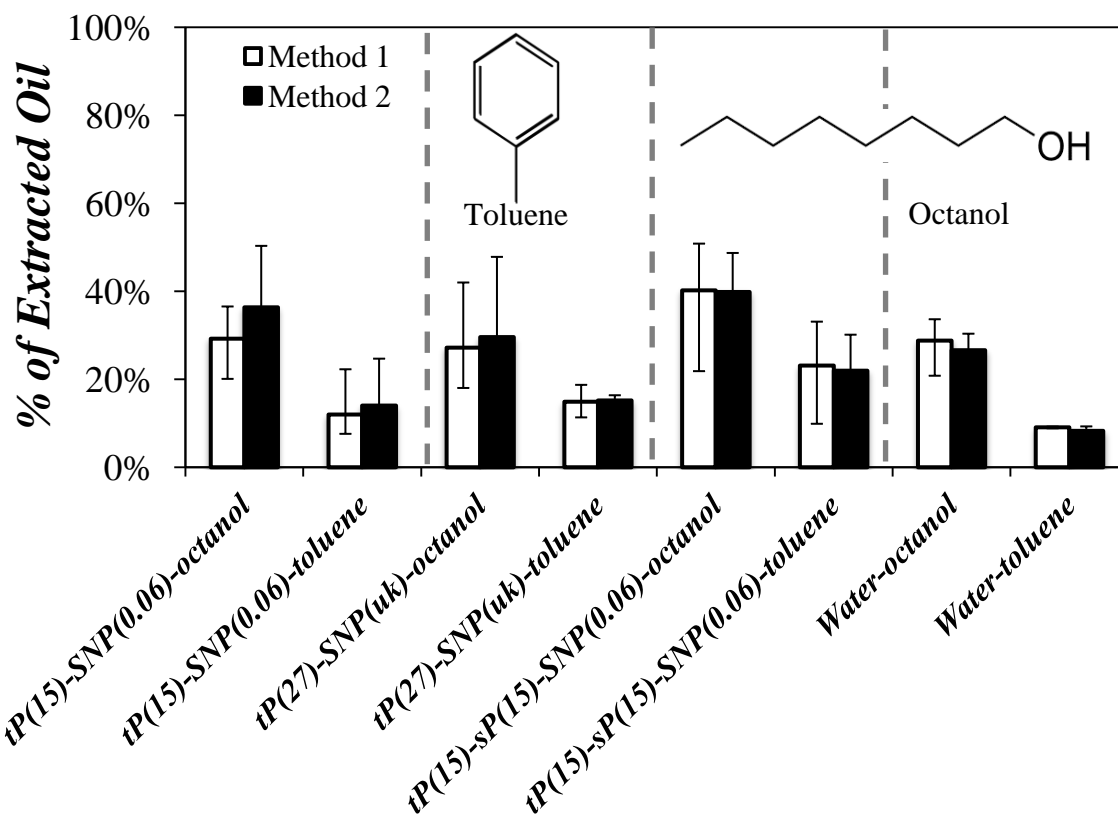


Figure 3.9. Yields obtained for oil extractions conducted at 45 °C with 4 g of SBos, 60 mL of 1 g/L aqueous dispersions of tP(15)-SNP(0.06), tP(27)-SNP(uk), and tP(15)-sP(15)-SNP(0.06) or 60 mL of water and 200 mg toluene/octanol.

Another parameter that was investigated for its effect on the efficiency of oil extraction was the degree of substitution (DS) of the tP-SNPs. As mentioned earlier, strong interactions between the co-solvent and the thermoresponsive polymer are critical for the stability of the aqueous dispersions and the oil extraction yield.³¹ Toluene has been found to be a good solvent for PMeO₂MA. For strong interactions to exist between PMeO₂MA and toluene, the segments of thermoresponsive polymers grafted on the SNPs must reach a critical degree of polymerization.

If the segments are too short, the tP-SNPs will behave like starch and will not interact favorably with toluene. Since the degree of polymerization of the polymers is inversely proportional to the DS of the xanthate fragments attached onto the SNPs, for a same mass of thermoresponsive polymer added onto a SNP substrate, the DS of xanthate becomes an important parameter to monitor for the optimization of tSNPs.

Figure 3.10 shows the yields obtained for oil extractions conducted with 1 g of SBos and 15 mL of 1 g/L aqueous dispersions of tP(15)-SNP(0.016), tP(15)-sP(7.5)-SNP(0.016), and tP(15)-SNP(0.06). The oil extraction yield increased dramatically when tP(15)-SNP(0.016) was used in lieu of tP(15)-SNP(0.06). Furthermore, the 32 (\pm 11) wt% extraction yield obtained for tP(15)-SNP(0.016) was much better than that of 9 (\pm 1) wt% obtained with 15 mL of water, an extraction yield similar to that of 8 (\pm 4) wt% obtained for tP(15)-SNP(0.06). This result demonstrated the importance of the DS, and thus the degree of polymerization of the PMeEO₂MA chains, on the extraction yield.

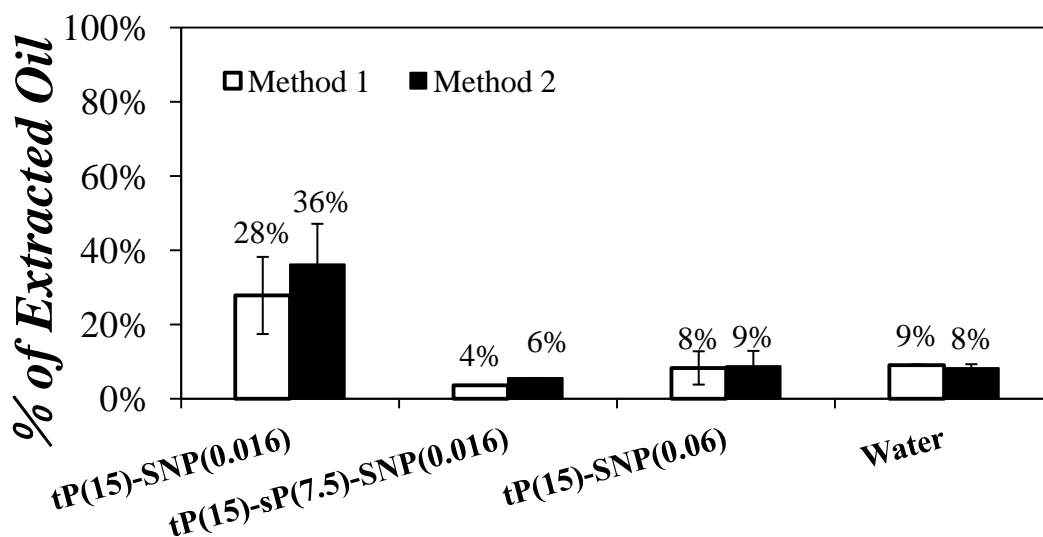


Figure 3.10. Yields for extractions conducted at 45 °C with 1 g of SBos, 15 mL of 1 g/L aqueous dispersions of tP(15)-SNP(0.016), tP(15)-sP(7.5)-SNP(0.016), and tP(15)-SNP(0.06) or 15 mL of water and 60 mg toluene.

No improvement in the extraction yield was obtained after a PHEA block was added to tP(15)-SNP(0.016) to yield tP(15)-sP(7.5)-SNP(0.016). It would seem that the PHEA block made the tSNPs too water-soluble, which resulted in a poor oil extraction yield. Thus, all following extraction experiments were conducted with tP(15)-SNP with a comparable DS equal to 0.016, 0.020, or 0.022.

Since tP(15)-SNP(0.016) resulted in the best extraction yields obtained so far, tP(15)-SNP samples with a DS around 0.02 were selected to conduct further extractions. The DS value varied slightly from batch-to-batch. Since toluene had been the only solvent investigated in the extraction experiments, the influence of the organic co-solvent used for the extractions was investigated by replacing toluene by other common organic solvents. The extraction yields obtained with these other solvents are presented in Figures 3.11 and 3.12. These extractions were conducted by co-op student Austin Richard under my direct supervision.

Toluene was selected as a co-solvent at the beginning of the project because it was found to interact strongly with the oil and PMeEO₂MA at temperatures higher than the LCST. Furthermore toluene has a boiling point of 110 °C, which ensures that the small amount of toluene used in the extractions will not evaporate off when the aqueous dispersions with oil sands are left to shake overnight at 45 °C. Keeping these conditions in mind, several organic solvents were considered to conduct further extractions. These solvents included hexylbenzene, 1,3-diisopropylbenzene, 1-hexanol, 1-decanol, o-xylene, isopropylbenzene, 2-ethyl-1-hexanol, 1-octanol and two industrial solvents involving 2-butoxyethanol (glycol ether EB), and hydrotreated light naphtha (VM&P Naptha). Figure 3.11 shows a plot of the oil extraction yields obtained with the different organic solvents in the presence or absence of tP(15)-SNP(0.02). This series of oil extraction experiments was conducted with 1 g of SBos, 15 mL of 1 g/L tP(15)-

SNP(0.02) aqueous dispersion, and 100 mg of organic solvent. Within experimental error, none of the extractions conducted with tP(15)-SNP(0.02) resulted in an extraction yield that was better than for an extraction conducted without polymer.

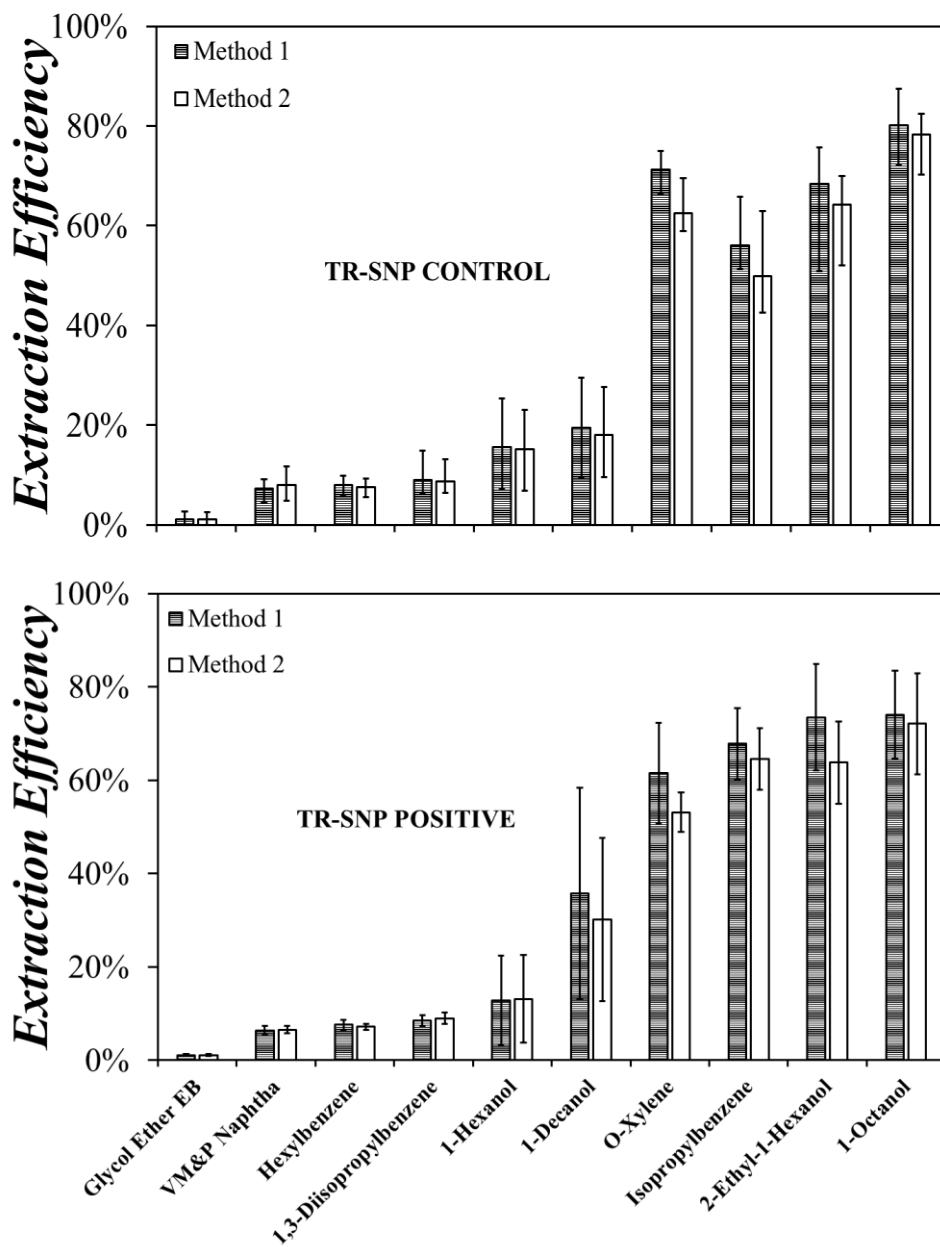


Figure 3.11. Extraction yields obtained for different organic solvents without (top) and with (bottom) tP(15)-SNP(0.02).⁶⁰

Differences in the extraction efficiency could be correlated to the chemical structure of the

organic solvent. For instance, *o*-xylene and isopropylbenzene, with a benzene ring like toluene, all resulted in decent extraction even if no tP(15)-SNP(0.02) was employed. Interestingly 1-octanol and 2-ethyl-1-hexanol also showed good extraction efficiency whereas 1-hexanol and 1-decanol did not. 1-Hexanol and 1-decanol might have been, respectively, too water-soluble and too water-insoluble to interact positively with tP(15)-SNP(0.02).⁶⁰ By contrast, 1-octanol and 2-ethyl-1-hexanol might possess the optimal balance to ensure good oil extraction.

Since Figure 3.11 suggested that 100 mg of isopropylbenzene (cumene) and 1-octanol resulted in good oil extraction even without tP(15)-SNP(0.02), a series of extraction experiments was conducted as a function of the mass of organic solvent, either cumene or 1-octanol, to determine whether conditions could be established where the extractions would be good in the presence of tP(15)-SNP(0.02) but poor in its absence. Figure 3.12A and B show the extraction yields obtained as a function of the mass of, respectively, 1-octanol and cumene in the presence and absence of tP(15)-SNP with DS of 0.016 or 0.020.⁶⁰ The results obtained in Figure 3.12 indicate that within experimental error, similar extraction yields were obtained with and without the tP(15)-SNP aqueous dispersion. The effect of the P(MeO)₂MA content was investigated with tP(30)-SNP(0.022) in Figure 3.12B. Extractions conducted with an aqueous dispersion of tP(30)-SNP(0.022) resulted in even poorer yields than those obtained without polymer. The poorer extraction yield achieved with tP(30)-SNP(0.022) was attributed to its higher hydrophobicity above the LCST imparted by its larger P(MeO)₂MA content.

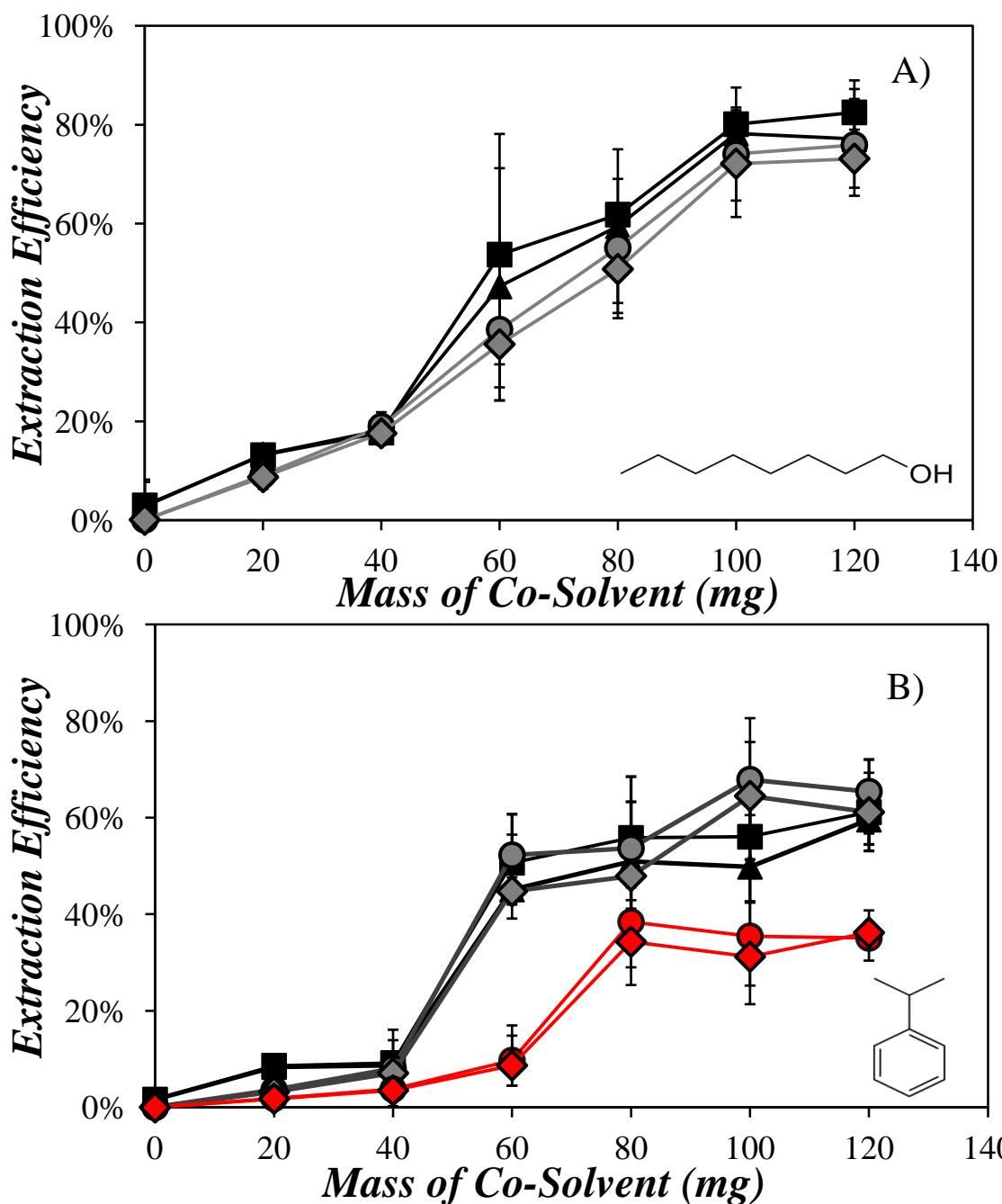


Figure 3.12. Oil extraction yield as a function of the mass of (A) 1-octanol and (B) cumene used in extractions conducted with 1 g of SBos and 15 mL of (■,▲) water, (●,◆) 1 g/L tP(15)-SNP(0.016), and (●,◆) tP(30)-SNP(0.022) at 45 °C.⁶⁰ Method #1 (■,●,●); Method #2 (▲,◆,◆) 15 mL of 1 g/L tP(15)-SNP(0.06) aqueous dispersion and (■,▲) 15 mL of water. (■,■) Method #1, (▲,▲)

So far, the extraction yields were somewhat disappointing. The most promising result was obtained with tP(15)-SNP(0.02) where an oil extraction yield of 32 (± 11) wt% was achieved with 60 mg of toluene whereas only 9 (± 2) wt% extraction yield was achieved without polymer. In all other combinations examined so far, the presence of tP-SNP never managed to improve the oil extraction yield substantially compared to an extraction conducted without tSNP.

Consequently, oil extractions were conducted as a function of the mass of toluene added to the extraction mixture consisting of 1 g of SBOs and 15 mL of 1 g/L tP(15)-SNP(0.02). Contrary to the extractions conducted with tP(15)-SNP(0.06) and toluene in Figure 3.8, much improved oil extraction yields were consistently obtained when the extractions were conducted with tP(15)-SNP(0.02). For all toluene additions, the extraction efficiency was dramatically improved compared to that obtained with 15 mL of pure water.

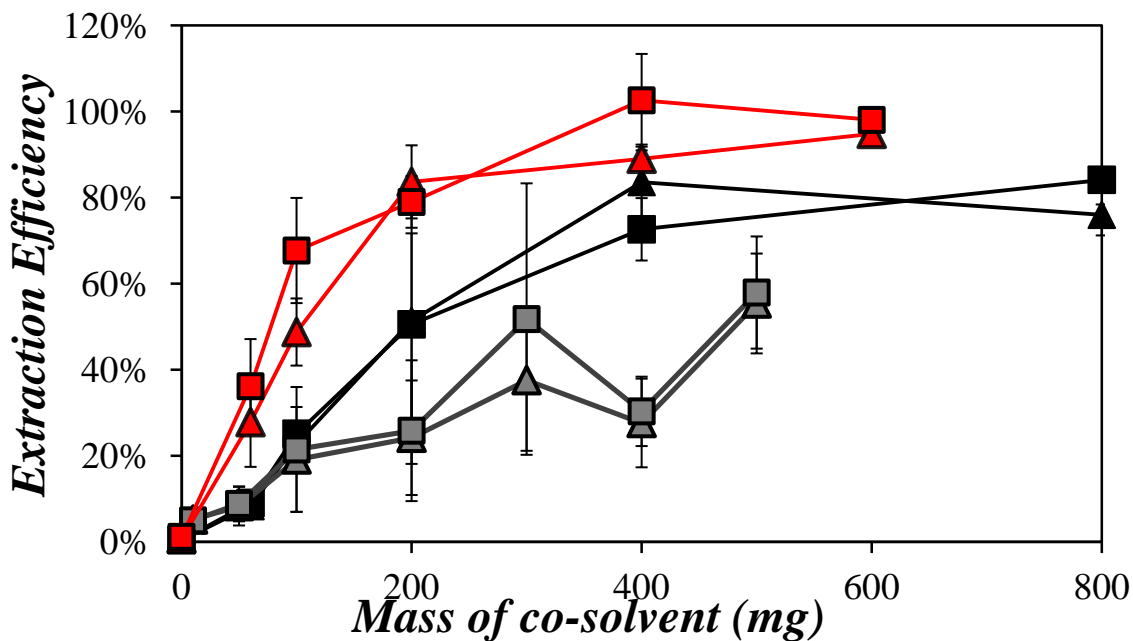


Figure 3.13. Plot of the yield for the extraction of 1 g of SBOs as a function of toluene mass added to 15 mL of (■, ▲) 1 g/L tP(15)-SNP(0.02) aqueous dispersion, (■, ▲) water, and (■, ▲) 1 g/L tP(15)-SNP(0.06) aqueous dispersion. (■, ■, ■) Method #1, (▲, ▲, ▲) Method #2.

While many extraction yields were disappointing, there were many cases however where

poor extraction yields did not mean that the separation of oil from the sand did not happen. The picture shown in Figure 3.14A represents an ideal oil extraction resulting in three separate layers, one with the clean sand at the bottom, the oil at the top, and the aqueous dispersion in the middle. In most oil extractions involving tSNPs, a portion of the oil managed to reach the surface of the aqueous dispersion but the rest remained at the bottom of the vial. Large oil droplets can be seen in Figure 3.14B. In fact, zooming in on the bottom layer would show droplets covered with fine sand particles. The sand particles adsorbed at the surface of the oil droplets increased their density and prevented them from raising to the surface of the aqueous dispersion. The tP-SNP aqueous dispersions appeared to effectively separate the oil from the sand particles, but did not manage to shuttle the oil to the surface. If an external force were introduced to help the buoyancy of the oil droplets, the oil extraction yield could be substantially increased.

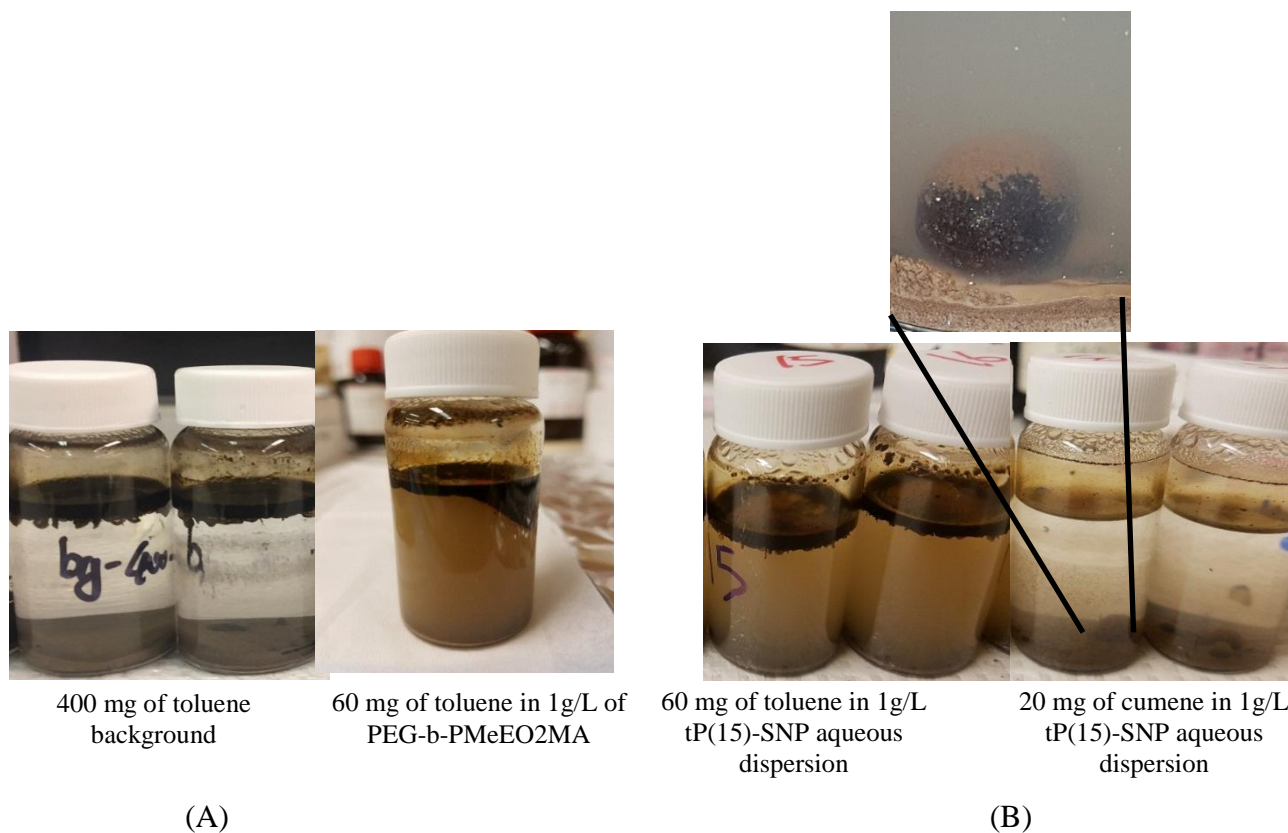


Figure 3.14. Pictures of (A) the clear three layers obtained for an ideal oil extraction and (B) the most common outcome from extractions showing large oil droplets stuck at the sand-water interface.

Figure 3.15 shows the oil extraction yields obtained after a second step was added to the extraction protocol. The oil from the oil sands was extracted as usual by shaking with a tSNP dispersion at 45 °C overnight and the layer of oil at the surface of the aqueous dispersion was collected with toluene. Then the aqueous dispersion was carefully pipetted out until the top of the large oil droplets sitting on the sand layer touched the surface of the aqueous layer. At that point, the oil droplets spread spontaneously on the surface of the water. The aqueous dispersion that had been pipetted out was pipetted back into the vial and the oil at the surface of the aqueous layer was collected with toluene. Figure 3.15 provides the oil extraction yield after the first

extraction step (black bar) and the second extraction step (white bar). It is obvious that all the oil had been separated from the oil sands, but the large droplets made denser by fines bound to their surface could not reach the surface of the aqueous layer. The second step enabled the oil droplets to contact the surface of the aqueous phase, resulting in a close to 100 wt% extraction yields.

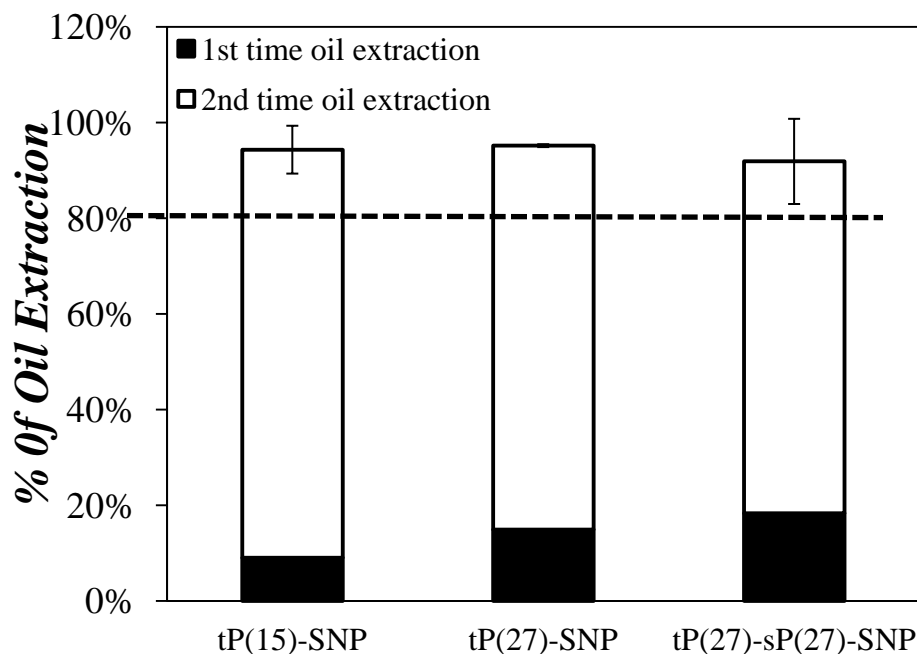


Figure 3.15. Yields for oil extractions conducted at 45 °C with 1 g of SBos, 15 mL of 1 g/L aqueous dispersions of tP(15)-SNP(0.06), and 60 mg toluene. The black portion represent the amount of oil collected after a normal oil extraction and the white bars refer to the oil portion that was collected in the second step of the oil extraction (see text for further explanations).

3.3 Characterization of tSNPs by Pyrene Fluorescence

3.3.1 SNPs modified with styrene and butene oxide

SO-BO-SNPs (Samples #1-3 in Table 2.2) were used to determine the influence of the order used for conducting the chemical modification on the SNPs. Pyrene (0.5 μ M) was dissolved in the

SO-BO-SNPs and its fluorescence spectrum was acquired as a function of the concentration of the SO-BO-SNPs. The I_1/I_3 ratio of the three samples was determined from the analysis of the fluorescence spectra (see Figure 2.8) and was plotted as a function of the SO-BO-SNP concentration in Figure 3.16. The ratio equaled 1.8 in water and decreased to a lower value with increasing SO-BO-SNP concentration. The I_1/I_3 ratio is a measure of the hydrophobicity of the local environment of pyrene. Since Sample #3 had a lower I_1/I_3 ratio compared with Samples #1 and #2, Sample #3 was more hydrophobic than the other samples despite their similar chemical composition. However, some insoluble small particles were found in the vial containing the aqueous dispersion of Sample #3 with 0.5 μM pyrene. By contrast, no particle precipitate was seen in aqueous dispersions of Samples #1 and #2. It seemed that the more hydrophobic Sample #3 promoted particle aggregation.

The 16 g/L aqueous dispersion of Sample #3 was centrifuged. The supernatant was collected and freeze-dried to determine the mass of Sample #3 present in the supernatant. The fraction of Sample #3 recovered in the supernatant would have represented a concentration of 11.7 g/L if re-suspended in the same volume of water as for the original 16 g/L aqueous dispersion of Sample #3. The I_1/I_3 ratios were determined at different concentrations of aqueous dispersion of centrifuged Sample #3 (referred to as Sample #3c) and were plotted in Figure 3.16. The I_1/I_3 ratio of Sample #3c was similar to that of Samples #1 and #2. Thus, the lower I_1/I_3 ratios obtained for Sample #3 were due to the more hydrophobic particles present in Sample #3, which were removed by centrifugation.

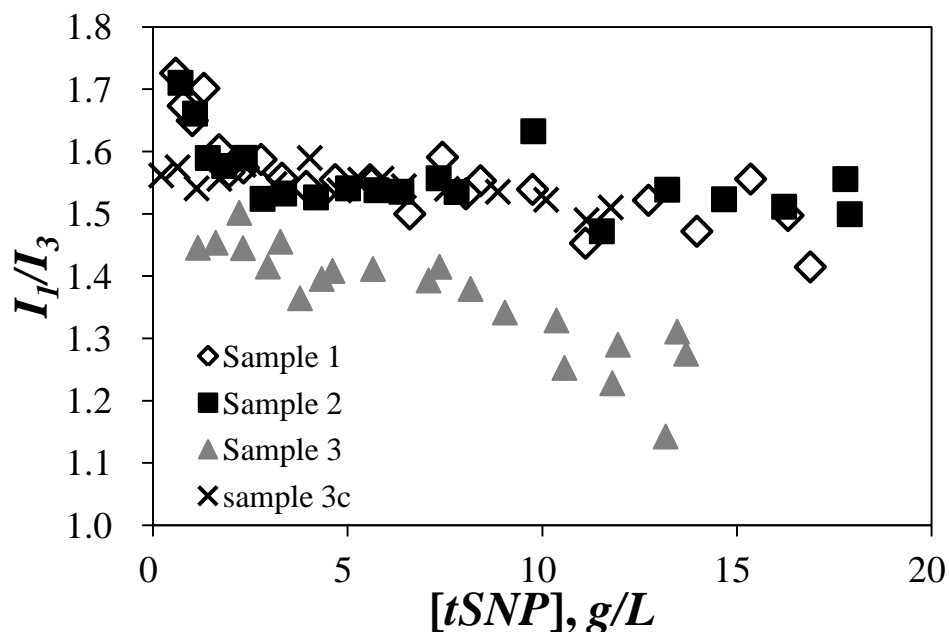


Figure 3.16. I_1/I_3 ratio as a function of [tSNP] determined by steady-state fluorescence for aqueous dispersions of tSNPs with [Py]=0.5 μM . (Sample #1 (\diamond), Sample #2 (\blacksquare), Sample #3 (\blacktriangle), and Sample #3c (\times)).

The fluorescence decays for 0.5 μM pyrene in aqueous dispersions of Samples #1, #2, #3, and #3c were acquired at different tSNP concentrations and were analyzed with a sum of four exponentials. The lifetime of one of the exponentials was fixed to 130 ns, the lifetime of pyrene in water, for the decay analysis. A long lifetime of more than 200 ns was attributed to pyrene bound to the SO-BO-SNPs. The ratio of the pre-exponential factors $a_{\text{Py}_b}/a_{\text{Py}_w}$ in Equation 4 yielded the ratio of the concentration of pyrene bound to SO-BO-SNP over the concentration of pyrene in water, namely the ratio $[P_{y_b}]/[P_{y_w}]$, which was plotted as a function of tSNP concentration in Figure 3.17. The ratio $[P_{y_b}]/[P_{y_w}]$ increased linearly with increasing tSNP concentration at low tSNP concentration, but the plots showed a clear break point at a tSNP concentration of around 6 g/L. The linear increase of $[P_{y_b}]/[P_{y_w}]$ with increasing tSNP

concentration reflected the equilibrium between pyrene free in water and bound to the tSNPs, with more pyrene being bound to the tSNPs as more tSNPs were added to the solution. The breakpoint observed at 6 g/L has been reported before when studying the binding of pyrene to other chemically modified SNP⁶¹ and has been attributed to SNP aggregation which prevented the access of pyrene to internal binding sites of the SNPs. Equation 5 was applied for tSNP concentrations below the break point, where the slope of the plots in Figure 3.17 yielded K , the equilibrium constant for the binding of pyrene to the tSNPs. The binding constants for the different samples were listed in Table 3.1. Pyrene bound more efficiently to Samples #1 and #2 than to Sample #3. This result might appear surprising at first glance since Sample #3 yielded I_1/I_3 ratios in Figure 3.16 that were much lower than for Samples #1 and #2, suggesting that Sample #3 was more hydrophobic, and thus should result in stronger pyrene binding. That this was not the case suggested that pyrene would bind to the surface of the tSNPs, a conclusion that had been drawn earlier.⁶¹ tSNP aggregation reduced the surface accessibility for pyrene binding resulting in the lower binding constant retrieved for Sample #3. Centrifuging the more hydrophobic fraction of Sample #3 yielded Sample #3c whose binding constant was on par with that of Samples #1 and #2 since Sample #3c was less hydrophobic, and thus less likely to aggregate.

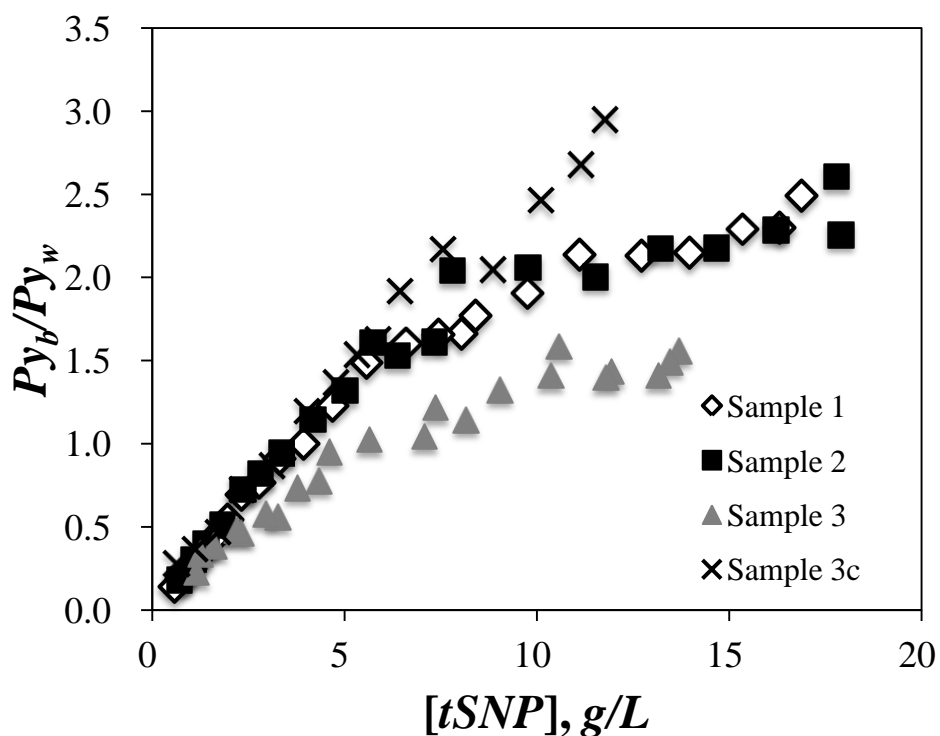


Figure 3.17. Ratio $[Py_b]/[Py_w]$ plotted as a function of $[tSNP]$ obtained from the analysis of the time-resolved decays acquired with $[Py]=0.5 \mu M$ in aqueous dispersion of tSNPs. (Sample #1 (\diamond), #2 (\blacksquare), #3 (\blacktriangle), and #3c (\times)).

Table 2.1. Binding Constant K in $L.g^{-1}$ for Samples #1, 2, 3 and 3c of SO-BO-SNP at $25^\circ C$.

tSNP	Binding Constant K ($L.g^{-1}$)
Sample 1	$0.27 (\pm 0.01)$
Sample 2	$0.27 (\pm 0.01)$
Sample 3	$0.13 (\pm 0.02)$
Sample 3c	$0.28 (\pm 0.01)$

The pyrene binding experiments suggested that tSNP aggregation occurred at tSNP

concentrations greater than 6 g/L. Since tSNP aggregation reflects poor colloidal stability, extractions with SO-BO-SNPs should be conducted at concentration lower than 6 g/L to minimize SNP aggregation and precipitation during oil extraction from oil sands. The selection of a 1 g/L tSNP concentration in all oil extraction experiments should thus ensure that little tSNP aggregation takes place during the oil extraction.

Another important aspect highlighted by the pyrene binding experiments is that the SO-BO-SNPs do not always have a homogeneous composition. As shown in Figures 3.16 and 3.17, Sample #3 appears to contain a substantial fraction of hydrophobic material that aggregates in solution. Such heterogeneities would be detrimental to the colloidal stability of the tSNPs and might be the reason why poor extraction yields were obtained with the SO-BO-SNPs (see Figure 3.3).

3.3.2 SNPs modified with PMeEO₂MA and PHEA

3.3.2.1 Hydrophobicity of the tP-sP-SNPs characterized from the I_1/I_3 ratio

The I_1/I_3 ratios of 0.5 μ M pyrene in aqueous dispersions of PEG-*b*-PMeEO₂MA prepared by Yang,²⁶ tP(15)-SNP(0.02) prepared by Dasgupta, SO(0.26)-BO(0.82)-SNP prepared by Zheng, and naked SNP were compared in Figure 3.18 as a function of polymer concentration and solution temperature at 25 and 50 °C for the two tSNPs. The I_1/I_3 ratio of all polymer aqueous dispersions was found to decrease from 1.73 (\pm 0.03) or 1.60 (\pm 0.09) for pyrene in water at 25 or 50 °C, respectively, to lower values with increasing polymer concentration. The addition of polymer to the aqueous dispersion promoted binding of pyrene to the polymer, which reduced the I_1/I_3 ratio as pyrene experienced the more hydrophobic environment generated by the polymer.

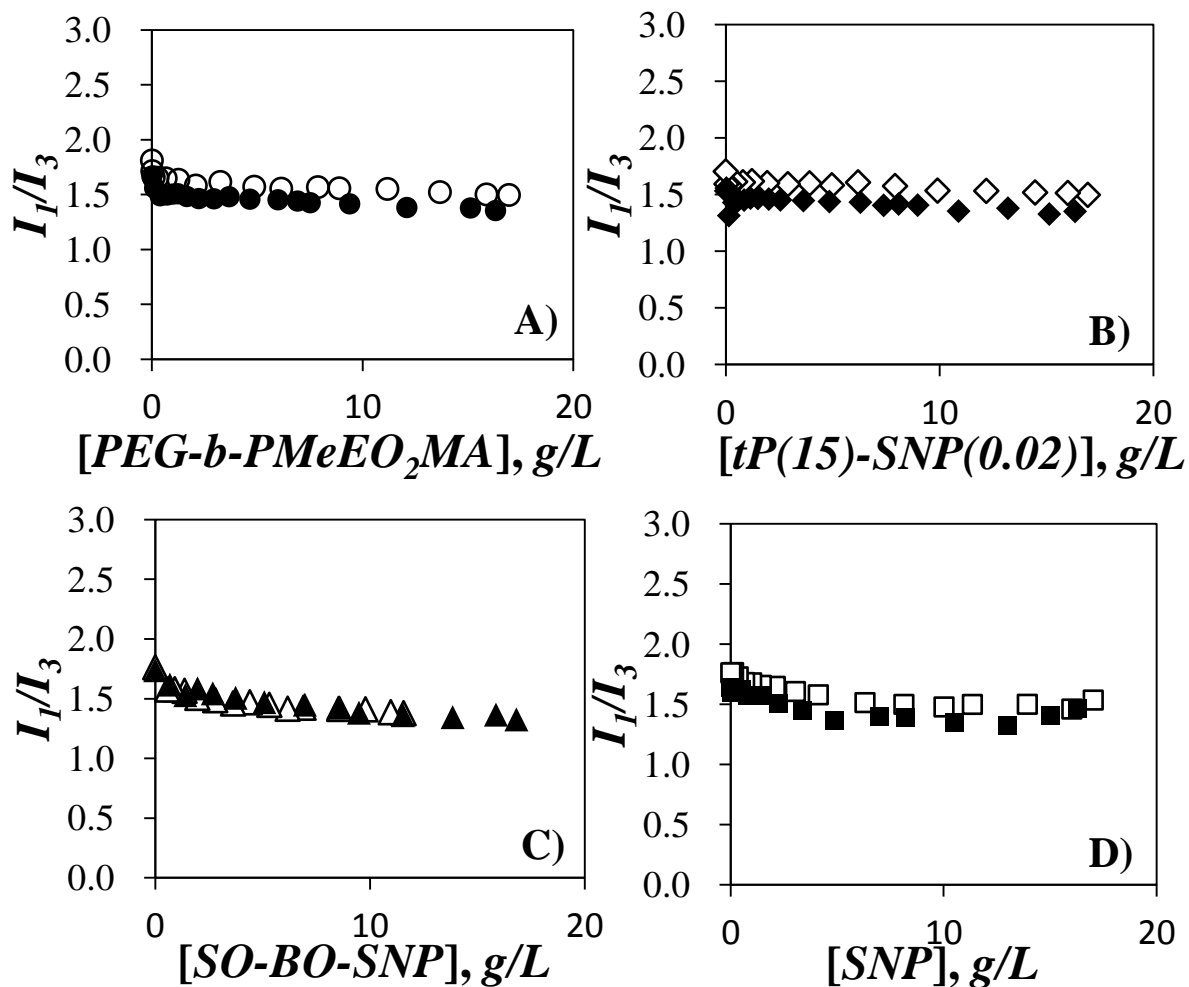


Figure 3.18. I_1/I_3 ratio plotted as a function of polymer concentration obtained from the analysis of the fluorescence spectra of 0.5 μM pyrene in a 1 g/L aqueous solution of (A) PEG-*b*-PMeEO₂MA and 1 g/L aqueous dispersions of (B) tP(15)-SNP(0.02), (C) SO(0.26)-BO(0.82)-SNP (Sample #4), and (D) naked SNP. Empty and filled symbols acquired at 25 and 50 °C, respectively.

The fluorescence decays of 0.5 μM pyrene in an aqueous solution of PEG-*b*-PMeEO₂MA and aqueous dispersions of tP(15)-SNP(0.02), SO(0.26)-BO(0.82)-SNP, and naked SNP were acquired at 25 and 50 °C with various polymer concentrations and they were analyzed with a sum of three or four exponentials (see Equation 4). The pre-exponential factors corresponding to pyrene in water and pyrene bound to the different polymers yielded the ratio $[P_{y_b}]/[P_{y_w}]$, which was plotted as a function of polymer concentration in Figure 3.19. A break point was observed for most samples. The only exception was the naked SNP (NSNP) sample which was too water-soluble to undergo some aggregation and showed no break point.

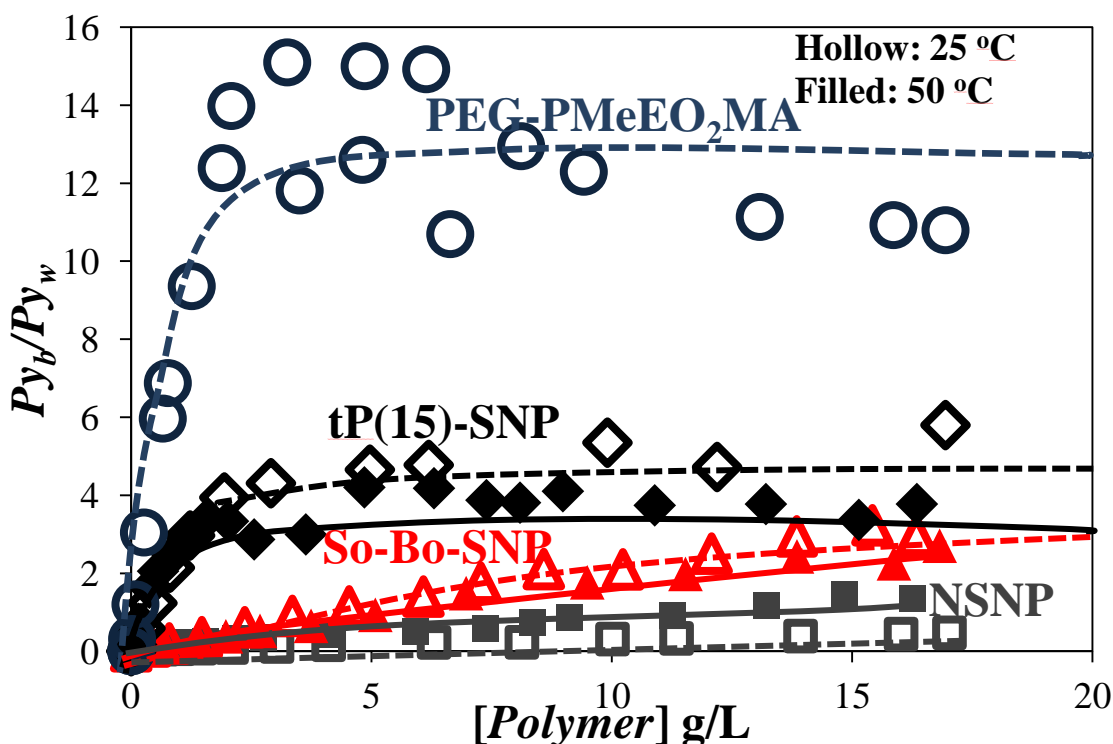


Figure 3.19. Ratio $[P_{y_b}]/[P_{y_w}]$ as a function of polymer concentration obtained from the analysis of the time-resolved fluorescence decays acquired for 0.5 μM pyrene in a 1 g/L aqueous solution of (\circ) PEG-*b*-PMeEO₂MA and 1 g/L aqueous dispersions of (\blacklozenge , \diamond) tP(15)-SNP(0.02), (\blacktriangle , \triangle) SO(0.26)-BO(0.82)-SNP (sample 4), and (\blacksquare , \square) naked SNP. Empty and filled symbols acquired at 25 and 50 °C, respectively.

Equation 6 was applied to the $[Py_w]/[Py_b]$ ratios shown in Figure 3.19 for polymer concentrations below the break point to obtain the binding constant K (L/g) of all samples. Table 3.2 lists the K values of each sample. Since pyrene is a hydrophobic molecule which binds more strongly to more hydrophobic polymers, the binding constant K directly reflects the relative hydrophobicity of each sample.

Table 3.2. Binding Constant K in $L.g^{-1}$ for PEG-*b*-PMeEO₂MA, two Modified SNPs, and the Naked SNPs at 25 °C and 50 °C

	25 °C	50 °C
NSNP	0.03 (± 0.00)	0.08 (± 0.00)
SO(0.26)-BO(0.82)-SNP	0.27 (± 0.01)	0.17 (± 0.01)
tP(15)-SNP(0.02)	2.4 (± 0.1)	2.1 (± 0.2)
PEG-<i>b</i>-PMeO₂MA	6.4 (± 1.0)	-

Based on the values listed in Table 3.2, it is clear that the binding of pyrene to the different polymers follows the sequence NSNP < SO(0.26)-BO(0.82)-SNP < tP(15)-SNP(0.02) < PEG-*b*-PMeEO₂MA. Interestingly, the yield of the oil extractions conducted with aqueous dispersions of these polymers in the presence of toluene was found to increase according to this sequence. Consequently, the determination of the equilibrium constant for the binding of pyrene to polymers through the analysis of fluorescence decays might provide an experimental means to predict whether a tSNP might work well in an oil extraction experiment.

The ratio of $[Py_b]/[Py_w]$ at 50 °C was always lower than at 25 °C in Figure 3.19. This was also reflected in the binding constants that were smaller for the tSNPs at 50 than at 25 °C. The

lower binding of pyrene to the tSNPs could have two causes. First, hydrogen bonds are known to weaken upon increasing the temperature. Weaker hydrogen bonding would reduce the drive for pyrene to bind to the polymers in order to reduce its exposure to the aqueous phase, resulting in a lower binding constant. Second, pyrene appears to bind to domains generated by the thermoresponsive polymer on the surface of the tSNPs. Since the tSNPs were selected so that 50 °C was above their LCST, particle aggregation took place at 50 °C resulting in some binding sites becoming inaccessible. Both effects contributed to reducing the pyrene to the tSNPs at 50 °C.

3.3.2.2 Binding of pyrene to the PMeEO₂MA block of the tP-SNPs

According to the equilibrium constants listed in Table 3.2, pyrene would hardly bind to the SNP substrate used to prepare the tSNPs. The fact that pyrene would bind much more strongly to tP(15)-SNP(0.02) suggested that pyrene would bind selectively to the PMeEO₂MA block. To confirm this assumption, the ratio $[Py_b]/[Py_w]$ was plotted as a function of the mass concentration of PMeEO₂MA for the aqueous dispersions of PEG-*b*-PMeEO₂MA and tP(15)-SNP(0.02) in Figure 3.20. The $[Py_b]/[Py_w]$ ratio increased linearly with increasing PMeEO₂MA concentration before plateauing at higher polymer concentrations. Before the break points, the trends obtained with the $[Py_b]/[Py_w]$ ratios overlapped perfectly for PEG-*b*-PMeEO₂MA and tP(15)-SNP(0.02), confirming that pyrene targeted the PMeEO₂MA block. The binding constants obtained for the binding of pyrene to PMeEO₂MA were similar, within experimental error, and equaled 0.06 (± 0.00) and 0.05 (± 0.02) L/g for tP(15)-SNP(0.02) and PEG-*b*-PMeEO₂MA, respectively. The main difference in the profiles shown in Figure 3.20 was the difference in the plateau value of the $[Py_b]/[Py_w]$ ratio which took a much larger value of 12.43 ± 1.80 for PEG-*b*-PMeEO₂MA compared to a value of 6.32 ± 1.02 for tP(15)-SNP(0.02). The plateau observed in

Figure 3.20 suggested that past the break point, all the pyrene was bound to PMeEO₂MA. However, this observation implies that the $[P_{yb}]/[P_{yw}]$ ratio should become infinite, which it was not. In turn, this suggests that not all pyrene bound to PMeEO₂MA might emit with a long lifetime, but that a non-zero fraction of the pyrene molecules bound to PMeEO₂MA might be exposed to water and emit with a lifetime of 130 ns, which is the lifetime of pyrene in water. Consequently, the plateau value of the $[P_{yb}]/[P_{yw}]$ ratio would then represent the ratio between those pyrene molecules that were protected from (P_{yb-P}^*) and exposed to (P_{yb-NP}^*) the solvent, a higher $[P_{yb}]/[P_{yw}]$ ratio reflecting an environment where pyrene would be more protected. Since $[P_{yb}]/[P_{yw}]$ is larger for PEG-*b*-PMeEO₂MA than tP(15)-SNP(0.02), it suggests that the PMeEO₂MA segments in the former polymer might be longer, and thus reduce more strongly exposure of pyrene to water, than in the tSNPs.

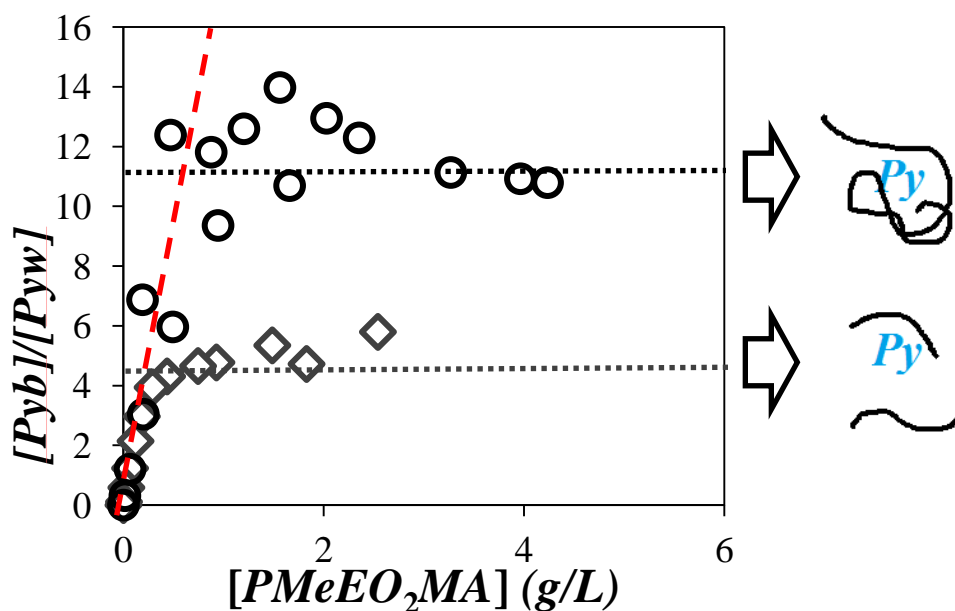


Figure 3.20. $[P_{yb}]/[P_{yw}]$ ratio as a function of the PMeEO₂MA massic concentration obtained from the analysis of the time-resolved fluorescence decays of 0.5 μ M pyrene in aqueous dispersions of (○) PEG-*b*-PMeEO₂MA and (◇) tP(15)-SNP(0.02) at 25 °C.

Chapter 4

Conclusions and Future Work

4.1 Conclusions

This project aimed to design a cheaper and more environmentally friendly procedure to extract oil from oil sands using thermoresponsive starch nanoparticles (tSNPs). This thesis described the characterization of the solution properties of these tSNPs (LCST, I_1/I_3 ratio, K) and their applicability to oil extraction based on their oil extraction efficiency. The sample tP(15)-SNP with a DS around 0.02 was selected to conduct the bulk of the oil extraction experiments conducted in this thesis.

Oil sands provided by Imperial Oil (IOOs) and the Alberta Innovate Technology Futures Sample Bank (SBos) were employed in the oil extraction experiments described in this project. Soxhlet extraction was used to determine the difference between the two types of oil sands. The oil content of the SBos and IOOs equaled 11.1 (± 0.1) wt% and 10.5 (± 0.2) wt%, respectively. Furthermore the SBos contained 2 wt% of fines, while the IOOs did not contain any. The presence of fines in the SBos appeared to make a difference, since the PEG-*b*-PMeEO₂MA block copolymer that had been reported earlier to quantitatively extract the oil from the IOOs was inefficient with the SBos. This result led to the conclusion that it was necessary to prepare a better thermoresponsive polymer to extract oil from oil sands.

Since PEG-*b*-PMeEO₂MA was able to achieve a more than 90% oil extraction yield with the IOOs, its main features were identified to design the tSNPs. First, it was recognized that aqueous dispersions of the tSNPs needed to be colloidally stable above the LCST to achieve good extractions. Since poor stability would induce the particles to precipitate out of the aqueous dispersions, it would prevent them from interacting with the oil sands and hinder their effectiveness for oil extraction. The stability of the tSNPs above their LCST could be assessed from the reduction of the $T\%$ of a tSNP aqueous dispersion as it passed through the LCST. Using

this criterion, a series of tSNPs were selected to conduct oil extraction experiments. It was found that an SNP grafted with 15 wt% of PMeEO₂MA was thermoresponsive, with an LCST around 30 °C. Lower PMeEO₂MA contents resulted in tSNPs having a much higher LCST, whereas higher PMeEO₂MA contents yielded tSNPs that were not colloidally stable at temperatures above the LCST. Consequently, tP(15)-SNPs with a DS around 0.02 were selected.

The SO-BO-SNPs that have been prepared so far showed a low *T*% at temperatures above their LCST, indicating that they would yield unstable aqueous dispersions in this temperature range. Even the SO-BO-SNPs that were stabilized with 20K PEG showed poor stability above the LCST. Not surprisingly, all SO-BO-SNPs that were used in this study to conduct oil extractions resulted in poor oil extraction yields.

Oil extraction experiments were conducted to assess the effectiveness of the different tSNPs. The oil extraction protocol was based on the protocols established by Yang³¹ with slight modifications, including the scale up of the extractions to minimize variations due to sample heterogeneities, and the implementation of two calculation methods to determine the oil extraction yield. For comparison, oil extraction was carried out with either pure water or an aqueous polymer dispersion to assess the effectiveness of a given tSNPs for oil extraction.

All SO-BO-SNPs resulted in low oil extraction yields that were below 15 wt%, as expected based on their poor colloidal stability above the LCST. Similarly, aqueous dispersions of tP(15)-SNP(0.06) resulted in poor oil extraction. This result might have been caused by the relatively high DS of this tSNP sample, which implied that the PMeEO₂MA segments grafted onto the SNP were too short to induce sufficient interactions with the oil sands. When oil extractions were conducted with tP(15)-SNP(0.016), tP(15)-sP(7.5)-SNP(0.016), and tP(15)-SNP(0.06) in the presence of 60 mg of toluene, the tP(15)-SNP(0.016) showed an oil extraction yield was close to

32 wt%, as compared to 9 wt% for tP(15)-SNP(0.06) and 5 wt% for tP(15)-sP(7.5)-SNP(0.016). The PMeEO₂MA segments of tP(15)-SNP(0.06) might have been too short and tP(15)-sP(7.5)-SNP(0.016) might have been too water-soluble for these tSNPs to enable good oil extraction. The substantial improvement in oil extraction yield achieved with tP(15)-SNP(0.016) led to the selection of tP(15)-SNP with a DS around 0.02 to examine the influence of the organic co-solvent during oil extraction. Several organic solvents were investigated, but since cumene and octanol were found to achieve better oil extractions on their own without polymer, these two solvents were selected to conduct further oil extraction experiments with various amounts of these organic co-solvents with or without tP(15)-SNP(DS~0.02). Within experimental error, aqueous dispersions of the tP(15)-SNP(DS~0.02) samples resulted in extraction yields that were never better than those achieved with pure water. These experiments led to the conclusion that the tP(15)-SNP(DS~0.02) samples did not improve the oil extraction yield for all the organic solvents other than toluene, tried in this thesis. Although the oil extraction yields were poor, this did not mean that the dispersions had not interacted with the oil sands. In fact, visual inspection of the vials showed that the oil had already been separated from the sand, generating large oil droplets at the surface of the sand layer. Interactions between the oil droplets and clay particles apparently increased the density of the oil droplets, which prevented them from rising to the surface of the aqueous dispersion and resulted in poor oil extraction. Interestingly, extractions conducted with tP(15)-SNP(DS~0.02) and different amounts of toluene showed substantially improved extraction yields as compared to extractions conducted with pure water alone. It appeared that the PMeEO₂MA block needed to be long enough, and the DS of the xanthate derivative low enough, to ensure good interactions between toluene and the PMeEO₂MA block. As was noted earlier, interactions between toluene and the PMeEO₂MA block appear to be

critical for obtaining good extraction yields.³¹

While the colloidal stability of the tSNPs above their LCST could be assessed by conducting turbidimetry measurements with a UV-Vis spectrophotometer, fluorescence experiments with the dye pyrene were also carried out to determine the relative hydrophobicity of the tSNPs. These experiments assessed whether the tSNPs would be able to interact with the organic co-solvents and the oil of the oil sands. The fluorescence spectra acquired with 0.5 μM pyrene in aqueous dispersions of tSNPs yielded the I_1/I_3 ratio, which provided a measure of the hydrophobicity of the local environment experienced by pyrene. Furthermore, analysis of the time-resolved fluorescence decays yielded the ratio $[P_{y_b}]/[P_{y_w}]$ of the molar fractions of pyrene either bound to the tSNPs or free in water. The $[P_{y_b}]/[P_{y_w}]$ ratio was plotted against the tSNP concentration to yield the equilibrium constant for the binding of pyrene to the tSNPs.

All tSNPs yielded similar I_1/I_3 ratios, which suggested that they exhibited similar hydrophobicity. However, the binding constant was found to increase according to the sequence NSNP < SO(0.26)-BO(0.82)-SNP < tP(15)-SNP(0.02) < PEG-*b*-PMeEO₂MA. Interestingly, the samples yielding a larger binding constant worked best in the oil extraction experiments. All tSNPs also yielded a lower binding constant when the dispersion temperature was increased from 25 to 50 °C, probably due to the weaker drive experienced by pyrene to bind to the SNPs at higher temperatures. Break points were observed in almost all plots of $[P_{y_b}]/[P_{y_w}]$ as a function of polymer concentration. The break points were attributed to tSNP aggregation that reduced the surface area of the tSNPs available for pyrene binding. Since pyrene hardly bound to the naked SNPs, the large binding constant obtained for the tP(15)-SNP(0.02) sample suggested that pyrene would selectively bind to the PMeEO₂MA block of the tSNP. To confirm this deduction, the ratios $[P_{y_b}]/[P_{y_w}]$ were plotted as a function of the PMeEO₂MA concentration for the aqueous

dispersions of PEG-*b*-PMeEO₂MA and tP(15)-SNP(0.02) at 25 °C. The two samples gave a same binding constant of 0.05 (±0.02) L/g, demonstrating that pyrene was binding to the PMeEO₂MA block. The main difference in behaviour between the PEG-*b*-PMeEO₂MA and tP(15)-SNP(0.02) samples was the plateau value reached by the ratio $[P_{y_b}]/[P_{y_w}]$ at polymer concentrations above the break point. Since the plateau region indicated that all pyrene was bound to the polymer above the breakpoint, the difference in the $[P_{y_b}]/[P_{y_w}]$ ratios indicated that some pyrene molecules were more exposed to water for the tP(15)-SNP(0.02) sample than for the PEG-*b*-PMeEO₂MA block copolymer. This effect was attributed to the difference in chain length of the PMeEO₂MA segments, the PEG-*b*-PMeEO₂MA having much longer PMeEO₂MA segments than tP(15)-SNP.

4.2 Future Work

So far, only tP(15)-SNP(0.02) achieved decent oil extraction at 45 °C with the SBos sample using minute amounts of toluene. Obviously, a wider range of tSNP samples with different chemical compositions need to be generated to achieve better oil extraction yield. tSNPs that are within a range of hydrophobic at temperatures above the LCST, possibly with longer PMeEO₂MA segments, and that are more stable, need to be designed. The clay content of the SBos and IOos must be determined, perhaps by applying the methylene blue adsorption test.⁶² The binding constant for the tSNPs onto clay and sand particles also needs to be determined. To this end, a procedure is being implemented in the Duhamel lab that uses pyrene-labeled SNPs. Chemical substituents other than styrene oxide, butene oxide, or PMeEO₂MA should also be investigated to generate more efficient tSNPs.

References

1. S. Walker. Future Oil Sands Development Involves Big Decisions-and Big Dollars. *Eng. Min. J.* **2014**, 28-34.
2. OPP-Wet: Slurry preparation plants, *Oil Sand Mag.* **2018**.
3. Cottrell J. H. Development of an Anhydrous Process for Oil-Sand Extraction. Garrigy, M. A. (ed) *The K. A. Clark Volume* **1963**, pp193-206.
4. Gosselin, P.; Hrudey, S. E.; Naeth, M. A.; Plourde, A.; Terrien, R.; Kraak, G. V. D.; Xu, Z. Environmental and Health Impacts of Canada's Oil Sands Industry. *R. Soc. Can.* **2010**, Ottawa, Canada, 33-50.
5. Boyd, M. L.; Montgomery D. S. Composition of Athabasca Bitumen Fractions as Determined by Structural-Group Analysis Methods. Garrigy, M. A. (ed) *The K. A. Clark Volume.* **1963**, pp101-108.
6. Miroshnichenko, N. Control and Assessment of the Hydrocarbon Contamination of Ukrainian Soils. *Eurasian Soil Sci.* **2008**, *41*, 542-549.
7. Hart, A. The Catalytic Upgrading of Heavy Crude Oil In-Situ:-The Role of Hydrogen: A Review. *Int. J. Pet. Sci. Technol.* **2012**, *6*, 79-96.
8. Li, S.; Wang, J.; Qian, J. The Investment and Application of Oil Sand Reserves in the World. Petroleum University of China. *SINO-Global Energy.* **2011**, *16*, 10-24.
9. Pow, J. R.; Fairbanks, G. H.; Zamora, W. J. Description and Reserve Estimates of the Oil Sands of Alberta. *Res. Counc. Alberta Inf.* **1963**, *45*, 1-14.
10. Stewart, G. A. Geological Controls on the Distribution of Athabasca Oil Sands Reserves. Garrigy, M. A. (ed) *The K. A. Clark Volume.* **1963**, pp15-25.
11. Clark, K. A., Pasternack, D. S. Hot Water Separation of Bitumen from Alberta Bitumen

- Sand. Res. Counc. Alberta, *Ind. Eng. Chem.* **1932**, *24*, 1410-1416.
12. Hydrotransport Explained-Mining, *Oil Sand Mag.* **2018**.
 13. Bitumen Extraction Explained-Mining, *Oil Sand Mag.* **2018**.
 14. Parkinson, G. A Cleaner, More-Efficient Way to Recover Oil from Tar Sands. *Chem. Eng.* **2001**, *108*, p17.
 15. Long, J.; Xu, Z.; Masliyah, J. H. On the Role of Temperature in Oil Sands Processing, *Energy & Fuels*, **2005**, *19*, 1440-1446.
 16. Romanova, U. G.; Valinasab, E. N.; Stasiuk, E. N.; Yarranton, H. W. The Effect of Oil Sands Bitumen Extraction Conditions on Forth Treatment Process. *J. Can. Pet. Technol.* **2006**, *25*, 36-45.
 17. Schramm, L. L.; Stasiuk, E. H.; Yarranton, H.; Maini, B.B.; Shelfantook, B. Temperature Effects from the Conditioning and Flotation of Bitumen from Oil Sands in Terms of Oil Recovery and Physical Properties. *J. Can. Pet. Technol.* **2003**, *42*, 55-61.
 18. Yuan, H.; Han, D. Pressure and Temperature Effect on Heavy Oil Sands Properties. *SEG Houston Annu. Meet.* **2013**, 2984-2988.
 19. Sury, K. N. Low Temperature Bitumen Recovery Process. *US Patent* 4 946 597, **1990**.
 20. Jun, L.; Drelich, J.; Xu, Z.; Masliyah, J. H. Effect of Operating Temperature on Water-Based Oil Sands Processing. *Can. J. Chem. Eng.* **2007**, *85*, 726-738.
 21. Flury, C.;† Afacan, A.; Bakhtiari, M. T.; Sjoblom, J.; Xu, Z. Effect of Causic type on Bitumen Extraction from Canadian Oil Sand. *Energy & Fuels*. **2014**, *28*, 431-438.
 22. Sakin Omer, O.; Hussein, M. A.; Hussein, B. H. M.; Mgaidi, A. Adsorption Thermodynamics of Cationic Dyed (Methylene Blue and Crystal Violet) to Nature Clay Mineral from Aqueous Solution between 293.5 and 323.15 K. *Arabian J. Chem.* **2017**,

- 1-9. (in press)
23. Kastner, M.; Asaro, F.; Michel, H. V.; Alvarez, W.; Alvarez, L. W. The Precursor of Cretaceous-Tertiary Boundary Clays at Stevns Klint, Denmark and DSDP hole 465A. *Science* **1984**, *226*, 137-143.
24. Tan, S. Y.; Tabor, R. F.; Ong, L.; Stevens, G. W.; Dagastine, R. R. Nano-mechanical Properties of Clay-Armoured Emulsion Droplets. *Nat. Commun.* **2012**, *8*, 3112-3121.
25. Liu, J.; Xu, Z.; Masliyah, J. Interaction Between Bitumen and Fines in Oil Sands Extraction System: Implication to Bitumen Recovery. *Can. J. Chem. Eng.* **2004**, *82*, 655-666.
26. Yang, H.; Wang, Y.; Ding, M.; Hu, B.; Ren, S. Water-Assisted Solvent Extraction of Bitumen from Oil Sands. *Ind. Eng. Chem. Res.* **2012**, *51*, 3020-3038.
27. Hong, P. K.; Cha, Z.; Zhao, X.; Cheng, C. J. Duyvesteyn, W. Extraction of Bitumen from Oil Sands with Hot Water and Pressure Cycles. *Fuel Process. Technol.* **2013**, *106*, 460-467.
28. Schramm, L. L.; Isaacs, E.; Singhal, A. K.; Hawkins, B.; Schulmeister, B.; Wassmuth, F.; Randall, L.; Turta, A.; Zhou, J.; Tremblay, B.; Lillico, D. Technology Development for Conventional Petroleum Reservoirs. *J. Can. Pet. Technol.* **2000**, *Canadian advantage 2000 Special Issue*. 31-36.
29. Wang, T.; Zhang, C.; Zhao, C.; Yang, C.; Liu, C. Solvent Extraction of Bitumen from Oil Sands. *Energy & Fuels* **2014**, *28*, 2297-2304.
30. Dai, Q.; Chung, K. H. Hot Water Extraction Process Mechanism Using Model Oil Sands. *Fuel* **1966**, *75*, 220-226.
31. Yang, B.; Duhamel, J. Extraction of Oil from Oil Sands Using Thermoresponsive

- Polymeric Surfactants. *Appl. Mater. Interfaces* **2015**, 7, 5879-5889.
32. Karski, M. Thermoresponsive starch nanoparticles. M. Sc. Thesis, **2015**.
33. Zheng, B. Synthesis and Characterization of Thermoresponsive Starch Nanoparticles. M. Sc. Thesis, **2016**.
34. Sun, K.; Xu, M.; Zhou, K.; Nie, H. Quan, J. Zhu, L. Thermoresponsive Deblock Glycopolymer by RAFT Polymerization for Lectin Recognition. *Mater. Sci. Eng. C*, **2016**, 68, 172-176.
35. Hooshiar, A.; Uhilik, P.; Ivey, D. G.; Liu, Q.; Etsell, T. H. Clay Minerals in Nonaqueous Extraction of Bitumen from Alberta Oil Sands: Part 2 Characterization of Clay Minerals. *Fuel* **2012**, 96, 183-194.
36. Luque, C. M. D.; Priego-Capote, F. Soxhlet Extraction: Past and Present Panacea. *J Chrom. A* **2010**, 1217, 2383–2389.
37. Rumble, J. R. CRC Handbook of Chemistry and Physics 98th Ed. *CRC*. **2017-2018**, 42.
38. Smith, R. L. Review of Glycol Ether and Glycol Ether Ester Solvent Used in The Coating Industry. *Environ. Health Perspect.* **1984**, 57, 1-4.
39. Carpenter, C. P.; Kinkead, E. R.; Geary, D. L.; Sullivan, L. J.; King, J. M. Petroleum Hydrocarbon Toxicity Studies. *Toxico. Appl. Pharmacol.* **1975**, 32, 263-281.
40. Patidar, P.; Bahadur, A. Modulating Effect of Different Biomolecules and other Additives on Cloud Point and Aggregation of Amphiphilic Linear and Starblock Copolymer. *J. Mol. Liq.* **2018**, 249, 219-226
41. De Oliveira, T. E.; Mukherji, D.; Kremer, K.; Netz, P. A. Effect of Stereochemistry and Copolymerization on the LCST of PNIPAm. *J. Chem. Phys.* **2017**, 146, 1-10.
42. Boutris, C.; Chatzi, E. G.; Kiparissides, C. Characterization of the LCST Behaviour of

- Aqueous Poly(N-isopropylacrylamide) Solutions by Thermal and Cloud Point Techniques. *Polymer*. **1997**, 38, 2567-2570.
43. Pineiro, L.; Novo, M.; Al-Soufi, W. Fluorescence Emission of Pyrene in Surfactant Solutions. *Adv. Colloid Interface Sci.* **2015**, 215, 1-12.
44. Huang, C.; Yuan, X. Zhao, J.; Bryant, D. A. Kinetic Analyses of State Transitions of the Cyanobacterium *Synechococcus* sp. PCC 7002 and Its Mutant Strains Impaired in Electron Transport. *Biochim. Biophys. Acta.* **2003**, 1607, 121-130.
45. Yip, J.; Duhamel, J.; Qiu, X. P.; Winnik, F. M. Fluorescence Studies of a Series of Monodisperse Telechelic α , ω -dispyrenyl poly(N-isopropylacrylamide)s in Ethanol and in Water. *Can. J. Chem.* **2011**, 89, 163-172.
46. Kacheff, A.; Prouzet, E. Stability and Dynamics of Silicate/Organic Hybrid Micelles. *C. R. Chim.* **2017**, 20, 526-533.
47. Teertstra, S. J.; Lin, W. Y.; Gauthier, M.; Ingratta, M., Duhamel, J. Comparison of the Long Range Polymer Chain Dynamic of Polystyrene and Cis-polyisoprene Using Polymers Randomly Labeled with Pyrene. *Polymer*. **2009**, 50, 5456-5466.
48. Wang, M.; Law, M.; Duhamel, J. Interaction of a Self-Assembling Peptide with Oligonucleotides: Complexation and Aggregation. *Biophys. J.* **2007**, 93, 2477-2490.
49. Berlman, I. B. Handbook of Fluorescence Spectra of Aromatic Molecules. 2nd ed. N.Y: Academic Press, **1971**.
50. Lakowicz. J. R., Principle of Fluorescence Spectroscopy, 3rd Edition, Plenum, **2006**, Maryland, USA, 19-48.
51. Thomas, J. K.; Kalyanasundaram, K. Environment Effects on Vibronic Band Intensities in Pyrene Monomer Fluorescence and Their Application in Studies of Micellar Systems.

- J. Am. Chem. Soc.* **1977**, *99*, 2039-2044.
52. Pineiro, L.; Novo, M.; Soufi, W. A. Fluorescence Emission of Pyrene in Surfactant Solutions, *Adv. Colloid Interface Sci.* **2015**, *215*, 1-12
53. Anthony, O.; Zana, R. Fluorescence Investigation of the Binding of Pyrene to Hydrophobic Microdomains in Aqueous Solution of Polysoaps. *Macromolecule* **1994**, *27*, 3885-3891.
54. Pineiro, L.; Freire, S.; Bordello, J.; Novo, M.; Soufi, W. A. Dye Exchange in Micellar Solutions. Quantitative Analysis of Bulk and Single Molecule Fluorescence Titrations. *Soft Matter*. **2013**, *9*, 10779-10790.
55. Barros, T. C.; Adronov, A.; Winnik, F. M.; Bohne, C. Quenching Studies of Hydrophobically Modified Poly(N-isopropylacrylamides). *Langmuir*. **1997**, *13*, 6089-6094.
56. Duhamel, J. New Insights in the Study of Dendritic Molecules Probed by Pyrene Excimer Formation. *Polymers*. **2002**, *4*, 211-239.
57. Shi, M.; Liang, X.; Yan, Y.; Pan, H.; Liu, Y. Influence of Ethanol-Water Solvent and Ultra-high Pressure on the Stability of Amylose-n-octanol complex. *Food Hydrocolloids* **2018**, *74*, 315-323.
58. Torrens, F.; Castellano, G. (Co-)solvent Selection for Single-wall Carbon Nanotubes: Best Solvents, Acids, Superacides, and Guest-host Inclusion Complexes. *Nanoscale* **2011**, *3*, 2494-5100.
59. Hung, H. W.; Lin, T. F.; Chiou, C. T. Partition Coefficients of Organic Contaminants with Carbohydrates. *Environ. Sci. Technol.* **2010**, *44*, 5430-5436.
60. Richard, J. A. Hydrophobically Modified Starch-Nanoparticles for Oil Extraction from

Oil Sands. **2017**. (Unpublished results)

61. Kim, D. Characterization of Hydrophobically Modified Starch Nanoparticles by Pyrene Fluorescence. M. Sc. Thesis, **2017**.
62. Gurses, A.; Dogar, C. Yaicin, M.; Acikyildiz, M.; Bayrak, R.; Karaca, S. The Adsorption Kinetics of the Cationic Dye, Methylene Blue, onto Clay. *J. Hazard. Mater. B.* **2005**, *131*, 217-228.
63. Abayazeed, S. D.; El-Hinnawi, E. Characterization of Egyptian Smectitic Clay Deposits by Methylene Blue Adsorption. *Am. J. Appl. Sci.* **2011**, *8*, 1282-1286.
64. Recovering the Oil, *Canada's Oil Sands*. <https://www.vistaprojects.com/blog/solvent-technology-promises-oil-sands-benefits/>. (access Mar 10, 2018)
65. Breakthrough Solvent Tech Promises Benefits for Oil Sands, *Technol. & Innovation* <https://www.canadasoilsands.ca/en/what-are-the-oil-sands/recovering-the-oil>. (access Mar 10, 2018)

Appendices

Determination of binding constant K

Table S.1. Parameters retrieved from the analysis of the fluorescence spectra and decays with Equation 6 acquired with 0.5 μM pyrene in aqueous dispersions of SO(0.28)-BO(0.34)-SNP (Sample #1) at 25 $^{\circ}\text{C}$.

[Sample 1], (g/L)	I_1	I_3	I_1/I_3	τ_{Pyb} (ns)	τ_{Pyw} (ns)	τ_{SNP} (ns)	α_{Pyb}	α_{Pyw}	α_{SNP}	$\alpha_{Pyb}/\alpha_{Pyw}$	χ^2
16.89	35.42	25.04	1.41	288	130	4.89	0.011	0.005	0.984	2.49	1.00
16.32	31.87	21.28	1.50	289	130	4.82	0.012	0.005	0.983	2.30	1.06
15.36	35.90	23.08	1.56	285	130	1.90	0.013	0.006	0.982	2.29	1.03
13.98	44.22	30.04	1.47	286	130	0.56	0.014	0.006	0.980	2.15	0.96
12.73	45.71	30.04	1.52	284	130	1.27	0.015	0.007	0.978	2.13	1.07
11.11	70.93	48.83	1.45	282	130	2.90	0.017	0.008	0.975	2.14	1.09
9.75	59.84	38.88	1.54	284	130	1.31	0.019	0.010	0.971	1.91	1.01
8.42	83.48	53.76	1.55	284	130	2.50	0.017	0.010	0.973	1.77	1.00
8.04	89.29	58.28	1.53	284	130	1.35	0.020	0.012	0.968	1.66	1.06
7.44	92.78	58.33	1.59	283	130	1.94	0.020	0.012	0.968	1.66	1.04
6.60	113.54	75.70	1.50	280	130	3.15	0.019	0.012	0.969	1.60	1.08
5.58	131.44	84.55	1.55	279	130	6.16	0.021	0.014	0.965	1.49	1.04
4.68	171.43	110.25	1.55	283	130	0.00	0.021	0.017	0.961	1.23	1.15
3.94	256.30	165.99	1.54	282	130	0.55	0.023	0.023	0.953	1.01	1.06
3.31	218.09	140.06	1.56	280	130	0.00	0.021	0.023	0.955	0.91	1.16
2.78	301.78	190.13	1.59	282	130	0.24	0.023	0.030	0.948	0.77	1.07
2.33	358.90	228.08	1.57	277	130	0.06	0.019	0.028	0.953	0.70	1.10
1.96	532.70	339.90	1.57	277	130	0.57	0.019	0.035	0.946	0.55	0.99
1.70	498.89	311.25	1.60	281	130	0.00	0.011	0.025	0.964	0.45	1.09
1.31	460.00	270.37	1.70	279	130	0.00	0.011	0.031	0.959	0.35	1.01
1.01	1143.49	693.20	1.65	280	130	1.05	0.012	0.047	0.941	0.25	1.15
0.78	2030.82	1213.68	1.67	284	130	0.00	0.010	0.053	0.937	0.19	1.05

0.58	1453.34	842.19	1.73	277	130	0.00	0.009	0.063	0.928	0.14	1.02
------	---------	--------	------	-----	-----	------	-------	-------	-------	------	------

Table S.2. Parameters retrieved from the analysis of the fluorescence spectra and decays with Equation 6 acquired with 0.5 μM pyrene in aqueous dispersions of SO(0.24)-BO(0.38)-SNP (Sample #2) at 25 $^{\circ}\text{C}$.

[Sample 2], (g/L)	I_1	I_3	I_1/I_3	τ_{Pyb} (ns)	τ_{Pyw} (ns)	τ_{SNP1} (ns)	τ_{SNP2} (ns)	α_{Pyb}	α_{Pyw}	α_{SNP1}	α_{SNP2}	$\alpha_{Pyb}/\alpha_{Pyw}$	χ^2
17.90	0.70	0.47	1.50	280	130	23.3	4.57	0.095	0.042	0.098	0.735	2.26	0.99
17.79	0.62	0.40	1.56	276	130	30.0	5.69	0.126	0.048	0.086	0.740	2.61	1.07
16.22	0.72	0.48	1.51	277	130	24.8	5.08	0.117	0.051	0.100	0.732	2.29	1.08
14.67	0.90	0.59	1.52	276	130	25.8	5.27	0.129	0.059	0.104	0.708	2.18	1.07
13.21	0.97	0.63	1.54	272	130	25.0	4.96	0.135	0.062	0.107	0.695	2.18	1.14
11.53	1.35	0.92	1.47	273	130	24.5	4.98	0.145	0.072	0.105	0.678	2.01	1.11
9.77	1.31	0.80	1.63	272	130	25.5	4.47	0.141	0.069	0.103	0.687	2.06	1.07
7.80	1.55	1.01	1.53	270	130	24.3	4.29	0.158	0.077	0.113	0.651	2.04	1.03
7.34	1.71	1.10	1.56	273	130	22.6	4.20	0.172	0.107	0.117	0.603	1.61	1.07
6.38	2.31	1.51	1.54	271	130	21.4	3.63	0.166	0.108	0.146	0.580	1.53	1.08
5.75	2.63	1.71	1.54	267	130	28.9	5.35	0.222	0.138	0.127	0.512	1.61	1.00
5.01	2.49	1.62	1.54	269	130	28.1	5.19	0.220	0.166	0.125	0.489	1.32	1.07
4.19	3.55	2.32	1.53	269	130	27.0	4.94	0.220	0.192	0.133	0.454	1.15	1.15
3.37	4.24	2.77	1.53	268	130	27.9	5.68	0.231	0.244	0.138	0.386	0.95	1.02
2.82	4.91	3.22	1.52	267	130	25.1	4.31	0.218	0.264	0.165	0.353	0.82	1.05
2.36	5.87	3.69	1.59	263	130	30.9	5.68	0.222	0.305	0.146	0.327	0.73	1.04
1.83	7.03	4.46	1.58	267	130	27.6	7.19	0.183	0.357	0.210	0.250	0.51	0.99
1.41	16.54	10.41	1.59	263	130	31.6	7.60	0.185	0.463	0.144	0.208	0.40	1.07
1.08	14.56	8.76	1.66	262	130	35.3	9.31	0.149	0.490	0.145	0.216	0.30	0.99
0.71	18.58	10.86	1.71	261	130	28.3	17.24	0.117	0.650	0.091	0.142	0.18	1.05

Table S.3. Parameters retrieved from the analysis of the fluorescence spectra and decays with Equation 6 acquired with 0.5 μM pyrene in aqueous dispersions of SO(0.24)-BO(0.40)-SNP (Sample #3) at 25 $^{\circ}\text{C}$.

[Sample 3], (g/L)	I_1	I_3	I_1/I_3	τ_{Pyb} (ns)	τ_{Pyw} (ns)	τ_{SNP1} (ns)	τ_{SNP2} (ns)	α_{Pyb}	α_{Pyw}	α_{SNP1}	α_{SNP2}	$\alpha_{Pyb}/\alpha_{Pyw}$	χ^2
13.70	233.70	183.25	1.28	262	130	36.0	5.24	0.116	0.075	0.124	0.684	1.56	1.14
13.47	264.05	201.42	1.31	263	130	41.0	6.46	0.142	0.095	0.138	0.624	1.49	0.92
13.17	95.13	83.27	1.14	268	130	34.5	5.90	0.117	0.083	0.088	0.711	1.41	1.02
11.95	288.76	223.89	1.29	262	130	40.1	6.44	0.154	0.107	0.171	0.568	1.44	1.01
11.80	220.88	179.89	1.23	266	130	36.4	5.94	0.120	0.086	0.090	0.705	1.40	1.00
10.57	209.43	167.20	1.25	262	130	41.0	6.36	0.139	0.088	0.098	0.675	1.59	1.03
10.37	351.59	264.59	1.33	261	130	40.3	7.14	0.165	0.117	0.195	0.524	1.41	0.98
9.04	274.23	204.42	1.34	262	130	36.2	5.77	0.139	0.105	0.099	0.657	1.32	1.13
8.16	517.95	375.52	1.38	263	130	39.9	6.56	0.174	0.152	0.192	0.483	1.15	0.97
7.36	284.27	200.91	1.41	260	130	39.0	5.77	0.152	0.125	0.113	0.610	1.22	1.07
7.08	582.96	418.52	1.39	262	130	35.3	5.77	0.167	0.160	0.233	0.440	1.05	1.06
5.65	708.18	501.74	1.41	258	130	39.4	10.04	0.185	0.181	0.248	0.386	1.03	1.04
5.35	373.90	364.41	1.03	261	130	38.3	6.98	0.190	0.206	0.148	0.456	0.92	1.12
4.61	872.61	619.67	1.41	257	130	50.3	12.34	0.217	0.228	0.202	0.353	0.95	1.07
4.34	518.59	371.63	1.40	259	130	35.8	6.32	0.184	0.237	0.153	0.426	0.78	0.97
3.78	994.18	728.64	1.36	257	130	37.4	7.79	0.185	0.251	0.241	0.323	0.74	1.09
3.28	631.81	434.18	1.46	263	130	32.6	5.67	0.165	0.295	0.154	0.386	0.56	1.09
2.95	1211.38	856.00	1.42	256	130	38.7	10.60	0.179	0.309	0.253	0.259	0.58	1.01
2.31	1513.59	1047.64	1.44	254	130	34.5	9.31	0.147	0.318	0.273	0.261	0.46	1.07
2.22	866.55	577.13	1.50	255	130	43.3	7.32	0.179	0.373	0.134	0.314	0.48	1.03
1.61	2045.49	1407.33	1.45	251	130	43.7	15.68	0.124	0.324	0.175	0.377	0.38	1.10
1.26	1480.00	746.77	1.98	246	130	44.1	8.88	0.167	0.492	0.134	0.207	0.34	1.18
1.16	2523.16	1745.66	1.45	263	130	29.6	5.51	0.071	0.316	0.236	0.376	0.23	1.05

Table S.4. Parameters retrieved from the analysis of the fluorescence spectra and decays with Equation 6 acquired with 0.5 μM pyrene in aqueous dispersions of centrifuged SO(0.24)-BO(0.40)-SNP (Sample #3c) at 25 $^{\circ}\text{C}$.

[Sample 3c], (g/L)	I_1	I_3	I_1/I_3	τ_{Pyb} (ns)	τ_{Pyw} (ns)	τ_{SNP1} (ns)	τ_{SNP2} (ns)	α_{Pyb}	α_{Pyw}	α_{SNP1}	α_{SNP2}	$\alpha_{Pyb}/\alpha_{Pyw}$	χ^2
11.76	481.98	319.17	1.51	266	130	27.1	4.65	0.268	0.091	0.080	0.560	2.95	1.06
11.14	677.55	454.82	1.49	257	130	26.8	4.60	0.273	0.102	0.087	0.537	2.68	1.07
10.10	741.01	486.70	1.52	259	130	23.8	4.93	0.283	0.115	0.092	0.510	2.46	1.11
8.86	551.19	359.02	1.54	259	130	20.7	3.90	0.239	0.117	0.101	0.543	2.05	1.00
7.55	843.24	547.57	1.54	255	130	34.7	7.94	0.398	0.183	0.087	0.333	2.17	1.20
6.45	683.66	442.73	1.54	255	130	30.5	7.27	0.408	0.213	0.095	0.284	1.92	0.99
5.87	706.67	454.01	1.56	258	130	29.5	6.08	0.333	0.205	0.097	0.365	1.63	1.05
5.33	772.49	496.84	1.55	257	130	30.9	8.56	0.366	0.238	0.084	0.311	1.54	1.07
4.79	658.18	428.05	1.54	257	130	24.0	4.86	0.279	0.204	0.109	0.408	1.37	1.00
4.03	781.41	491.60	1.59	257	130	27.8	5.87	0.294	0.246	0.100	0.360	1.20	1.03
3.12	1478.59	955.40	1.55	260	130	26.6	6.87	0.284	0.327	0.109	0.280	0.87	0.97
2.33	1289.70	816.93	1.58	255	130	35.1	6.92	0.286	0.395	0.089	0.230	0.72	0.92
1.71	1805.54	1160.34	1.56	261	130	17.0	16.95	0.254	0.541	0.013	0.191	0.47	1.05
1.12	7121.03	4622.12	1.54	261	130	47.5	10.14	0.201	0.547	0.057	0.195	0.37	1.02
0.63	3490.96	2216.86	1.57	240	130	19.5		0.148	0.666	0.185		0.22	1.13
0.21	3179.51	2036.09	1.56	240	130	20.3		0.053	0.818	0.129		0.06	1.12

Table S.5. Parameters retrieved from the analysis of the fluorescence spectra and decays with Equation 6 acquired with 0.5 μM pyrene in aqueous dispersions of NSNP at 25 $^{\circ}\text{C}$.

[NSNP], (g/L)	I_1	I_3	I_1/I_3	τ_{Pyb} (ns)	τ_{Pyw} (ns)	τ_{SNP1} (ns)	τ_{SNP2} (ns)	α_{Pyb}	α_{Pyw}	α_{SNP1}	α_{SNP2}	$\alpha_{\text{Pyb}}/\alpha_{\text{Pyw}}$	χ^2
17.02	366504	238869	1.53	212	132	35.7	6.05	0.176	0.374	0.149	0.301	0.47	1.01
16.02	311355	213319	1.46	212	132	26.1	6.60	0.138	0.315	0.300	0.247	0.44	1.03
13.92	303545	202464	1.50	212	132	24.8	4.63	0.142	0.364	0.275	0.220	0.39	0.99
11.35	283808	189443	1.50	212	132	25.5	5.84	0.129	0.392	0.285	0.194	0.33	0.97
10.01	274450	185807	1.48	212	132	36.8	12.64	0.121	0.388	0.176	0.314	0.31	1.11
8.13	267750	178697	1.50	212	132	23.7	4.90	0.086	0.375	0.397	0.143	0.28	1.00
6.30	260321	172048	1.51	212	132	43.8	14.19	0.104	0.460	0.128	0.307	0.23	1.04
4.11	257359	163105	1.58	212	132	44.5	13.17	0.088	0.533	0.128	0.251	0.17	0.98
3.03	251514	156667	1.61	212	132	40.3	15.75	0.073	0.596	0.116	0.215	0.12	1.03
2.09	246316	149407	1.65	212	132	30.8	7.73	0.061	0.638	0.178	0.123	0.10	1.01
1.43	246327	148674	1.66	212	132	63.0	19.06	0.055	0.697	0.045	0.204	0.08	0.99
0.98	238036	141893	1.68	212	132	38.1	12.93	0.047	0.731	0.111	0.111	0.06	1.06
0.65	235295	140035	1.68	212	132	59.4	15.27	0.036	0.659	0.079	0.226	0.05	1.11
0.35	232377	134546	1.73	212	132	48.8	14.37	0.033	0.745	0.072	0.151	0.04	1.13
0.13	234733	133133	1.76	212	132	22.21		0.027	0.849	0.124		0.03	1.17
0.02	234419	133615	1.75	212	132	27.13		0.029	0.890	0.081		0.03	1.04
0.00	240343	136474	1.76										

Table S.6. Parameters retrieved from the analysis of the fluorescence spectra and decays with Equation 6 acquired with 0.5 μM pyrene in aqueous dispersions of NSNP at 50 $^{\circ}\text{C}$.

[NSNP], (g/L)	I_1	I_3	I_1/I_3	τ_{Pyb} (ns)	τ_{Pyw} (ns)	τ_{SNP1} (ns)	τ_{SNP2} (ns)	α_{Pyb}	α_{Pyw}	α_{SNP1}	α_{SNP2}	$\alpha_{\text{Pyb}}/\alpha_{\text{Pyw}}$	χ^2
16.26	267568	176227	1.52	134	110	30.7	4.14	0.368	0.177	0.186	0.268	2.08	1.05
14.84	215310	155682	1.38	134	110	29.2	6.30	0.356	0.160	0.265	0.219	2.23	1.07
13.23	203084	147725	1.37	134	110	27.0	5.48	0.268	0.169	0.349	0.214	1.58	1.03
11.27	195552	141668	1.38	134	110	27.0	5.80	0.243	0.214	0.359	0.184	1.13	1.05
9.11	188937	137160	1.38	134	110	28.5	6.44	0.248	0.238	0.351	0.163	1.04	1.00
8.35	177910	129829	1.37	134	110	28.9	7.82	0.213	0.235	0.358	0.194	0.91	1.11
7.37	126051	109728	1.15	134	110	28.2	8.89	0.116	0.187	0.481	0.215	0.62	1.02
5.90	127769	109348	1.17	134	110	28.5	9.48	0.091	0.196	0.485	0.229	0.47	1.10
4.12	172658	134214	1.29	134	110	26.2	7.92	0.115	0.307	0.447	0.132	0.37	1.03
2.76	153477	111019	1.38	134	110	25.0	4.17	0.103	0.367	0.390	0.141	0.28	1.02
2.17	154428	106695	1.45	134	110	26.8	9.32	0.092	0.369	0.386	0.153	0.25	1.03
1.55	149946	103982	1.44	134	110	25.6	9.22	0.068	0.526	0.311	0.096	0.13	1.06
1.16	144528	100715	1.44	134	110	23.5	2.73	0.054	0.489	0.348	0.108	0.11	0.98
0.77	147273	101284	1.45	134	110	23.6	5.32	0.038	0.613	0.282	0.067	0.06	1.06
0.50	145259	96896	1.50	134	110	23.1	7.53	0.061	0.543	0.310	0.087	0.11	1.08
0.21	142603	90778	1.57	134	110	21.2	1.79	0.029	0.599	0.227	0.145	0.05	1.03
0.08	136453	87177	1.57	134	110	20.0	1.58	0.041	0.652	0.180	0.127	0.06	1.10
0.00	244917	150400	1.63										

Table S.7. Parameters retrieved from the analysis of the fluorescence spectra and decays with Equation 6 acquired with 0.5 μM pyrene in aqueous dispersions of SO(0.26)BO(0.82)-SNP (sample 4) at 25 $^{\circ}\text{C}$.

[SOBO-SNP], (g/L)	I_1	I_3	I_1/I_3	τ_{Pyb} (ns)	τ_{Pyw} (ns)	τ_{SNP1} (ns)	τ_{SNP2} (ns)	α_{Pyb}	α_{Pyw}	α_{SNP1}	α_{SNP2}	$\alpha_{Pyb}/\alpha_{Pyw}$	χ^2
11.56	251378	182474	1.38	276	133	19.3	3.67	0.155	0.052	0.079	0.714	2.96	1.16
10.97	240568	173629	1.39	272	133	24.6	4.03	0.164	0.051	0.081	0.704	3.23	1.11
9.79	237654	168594	1.41	272	133	19.7	3.59	0.157	0.053	0.111	0.679	2.94	1.12
8.57	233308	165082	1.41	274	133	24.2	4.25	0.179	0.072	0.010	0.652	2.50	1.04
6.91	223101	156753	1.42	275	133	24.0	4.36	0.183	0.087	0.109	0.620	2.10	1.16
6.17	219408	155098	1.41	272	133	25.3	3.93	0.177	0.084	0.110	0.630	2.11	1.03
5.31	216378	149515	1.45	274	133	25.6	4.32	0.204	0.116	0.108	0.573	1.76	1.10
4.41	206139	140357	1.47	275	133	22.9	4.30	0.212	0.151	0.131	0.507	1.40	0.98
3.63	196677	134824	1.46	273	133	30.5	5.23	0.228	0.198	0.134	0.461	1.15	1.16
2.79	193734	130342	1.49	272	133	32.9	5.93	0.224	0.248	0.156	0.373	0.91	1.10
1.96	188739	125326	1.51	274	133	31.0	7.59	0.189	0.308	0.176	0.237	0.62	1.08
1.36	181817	116212	1.56	280	133	32.4	5.26	0.160	0.445	0.153	0.243	0.36	1.01
0.91	182233	115512	1.58	276	133	38.8	6.61	0.109	0.544	0.113	0.233	0.20	1.15
0.56	185577	117783	1.58	268	133	31.09		0.063	0.776	0.160		0.08	1.06
0.00	204423	115989	1.76										

Table S.8. Parameters retrieved from the analysis of the fluorescence spectra and decays with Equation 6 acquired with 0.5 μM pyrene in aqueous dispersions of SO(0.26)BO(0.82)-SNP (sample 4) at 50 $^{\circ}\text{C}$.

[SOBO-SNP], (g/L)	I_1	I_3	I_1/I_3	τ_{Pyb} (ns)	τ_{Pyw} (ns)	τ_{SNP1} (ns)	τ_{SNP2} (ns)	α_{Pyb}	α_{Pyw}	α_{SNP1}	α_{SNP2}	$\alpha_{Pyb}/\alpha_{Pyw}$	χ^2
16.82	124847	94208	1.33	229	110	9.5	2.36	0.081	0.030	0.103	0.786	2.71	1.07
15.87	122408	89657	1.37	228	110	8.5	1.95	0.070	0.031	0.116	0.784	2.25	1.14
13.85	123675	92005	1.34	225	110	12.4	2.77	0.117	0.048	0.083	0.752	2.43	1.05
11.53	129819	95426	1.36	226	110	10.2	2.33	0.114	0.058	0.105	0.724	1.98	1.05
9.49	133005	96287	1.38	225	110	23.0	3.03	0.128	0.072	0.035	0.765	1.77	1.11
6.97	137224	94701	1.45	225	110	17.0	3.67	0.223	0.150	0.085	0.541	1.49	1.07
5.08	137224	93347	1.47	225	110	13.6	3.25	0.204	0.219	0.104	0.473	0.93	1.00
3.74	136345	90516	1.51	225	110	11.6	2.32	0.157	0.242	0.108	0.493	0.65	1.16
2.68	130695	84689	1.54	225	110	14.7	2.32	0.152	0.291	0.092	0.464	0.52	0.96
1.97	129135	81495	1.58	225	110	13.5	3.06	0.169	0.442	0.111	0.278	0.38	0.97
1.40	119738	78348	1.53	225	110	12.3	2.08	0.115	0.450	0.087	0.347	0.26	0.98
0.68	125380	775566	0.16	225	110	11.05		0.122	0.747	0.131		0.16	1.14
0.00	167300	96308	1.74										

Table S.9. Parameters retrieved from the analysis of the fluorescence spectra and decays with Equation 6 acquired with 0.5 μM pyrene in aqueous dispersions of tP(15)-SNP(0.016) at 25 $^{\circ}\text{C}$.

[tP(15)-SNP], (g/L)	I_1	I_3	I_1/I_3	τ_{Pyb} (ns)	τ_{Pyw} (ns)	τ_{SNP1} (ns)	τ_{SNP2} (ns)	α_{Pyb}	α_{Pyw}	α_{SNP1}	α_{SNP2}	$\alpha_{Pyb}/\alpha_{Pyw}$	χ^2
16.94	239139	159710	1.50	265	133	21.7	2.90	0.332	0.057	0.066	0.545	5.80	1.06
12.19	290026	189267	1.53	265	133	15.3	2.19	0.328	0.069	0.094	0.509	4.72	1.08
9.91	315259	205408	1.53	265	133	33.5	3.96	0.454	0.085	0.063	0.398	5.35	1.08
6.19	366980	228310	1.61	265	133	28.1	2.56	0.419	0.088	0.072	0.421	4.77	1.07
4.97	369457	233611	1.58	265	133	33.8	3.54	0.526	0.113	0.075	0.286	4.65	1.02
3.92	386799	241953	1.60	265	133	62.8	5.42	0.583	0.095	0.085	0.237	6.13	1.15
2.91	387963	243789	1.59	265	133	39.4	4.77	0.576	0.134	0.080	0.210	4.31	1.16
1.94	390848	244173	1.60	265	133	65.0	10.72	0.634	0.161	0.075	0.129	3.94	1.06
1.23	385131	238025	1.62	265	133	55.0	7.14	0.591	0.199	0.086	0.129	2.97	1.12
0.80	370876	230640	1.61	265	133	76.3	15.96	0.563	0.263	0.062	0.113	2.14	1.05
0.44	339045	210175	1.61	265	133	43.3	5.57	0.441	0.357	0.091	0.111	1.23	1.06
0.19	297128	188091	1.58	265	133	57.9	10.70	0.308	0.527	0.073	0.092	0.59	1.12
0.04	258289	162107	1.59	265	133	38.7	7.64	0.085	0.767	0.090	0.058	0.11	1.13
0.00	279302	163898	1.70										

Table S.10. Parameters retrieved from the analysis of the fluorescence spectra and decays with Equation 6 acquired with 0.5 μM pyrene in aqueous dispersions of tP(15)-SNP(0.016) at 50 $^{\circ}\text{C}$.

[tP(15)-SNP], (g/L)	I_1	I_3	I_1/I_3	τ_{Pyb} (ns)	τ_{Pyw} (ns)	τ_{SNP1} (ns)	τ_{SNP2} (ns)	α_{Pyb}	α_{Pyw}	α_{SNP1}	α_{SNP2}	$\alpha_{Pyb}/\alpha_{Pyw}$	χ^2
16.34	406180	300502	1.35	200	103	12.3	1.22	0.158	0.042	0.046	0.754	3.77	1.11
15.14	490729	369505	1.33	204	103	10.1	1.20	0.177	0.053	0.063	0.707	3.37	1.05
13.20	689633	499929	1.38	204	103	15.8	1.66	0.256	0.068	0.060	0.616	3.77	1.10
10.89	812604	600173	1.35	204	103	12.0	1.27	0.228	0.061	0.072	0.639	3.74	1.06
8.98	925675	658153	1.41	205	103	14.3	1.44	0.273	0.067	0.073	0.587	4.10	0.89
8.09	969458	684352	1.42	206	103	20.8	2.36	0.407	0.107	0.084	0.402	3.81	0.95
7.39	1012240	720563	1.40	207	103	28.0	4.52	0.500	0.129	0.069	0.301	3.87	1.06
6.30	1033930	721643	1.43	205	103	18.7	2.03	0.409	0.098	0.103	0.390	4.18	1.09
4.85	999559	695005	1.44	205	103	19.5	1.36	0.278	0.066	0.069	0.587	4.20	0.99
3.63	960019	663504	1.45	208	103	13.6	1.42	0.331	0.111	0.095	0.464	2.99	1.08
2.01	848517	581139	1.46	207	103	23.4	4.55	0.573	0.172	0.097	0.157	3.33	1.20
1.50	788118	537632	1.47	206	103	19.6	2.02	0.490	0.148	0.105	0.257	3.31	1.06
1.16	755992	514811	1.47	207	103	26.7	8.64	0.587	0.199	0.077	0.137	2.95	0.98
0.86	660198	454932	1.45	204	103	17.1	0.96	0.324	0.132	0.095	0.450	2.46	1.13
0.56	609263	422000	1.44	204	103	17.8	3.56	0.508	0.248	0.198	0.046	2.05	1.05
0.38	529094	370137	1.43	198	103	22.1	6.98	0.443	0.272	0.164	0.121	1.63	1.05
0.15	371198	282431	1.31	178	103	23.8	7.52	0.234	0.333	0.306	0.127	0.70	1.09
0.03	343507	220612	1.56	139	103	22.5	6.15	0.261	0.478	0.199	0.063	0.55	1.04
0.00	277458	181094	1.53										

Table S.11. Parameters retrieved from the analysis of the fluorescence spectra and decays with Equation 6 acquired with 0.5 μM pyrene in aqueous dispersions of PEG-*b*-PMeEO₂MA at 25 °C.

[PEG-PMeEO ₂ MA], (g/L)	I_1	I_3	I_1/I_3	τ_{Pyb} (ns)	τ_{Pyw} (ns)	τ_{SNP1} (ns)	τ_{SNP2} (ns)	α_{Pyb}	α_{Pyw}	α_{SNP1}	α_{SNP2}	$\alpha_{Pyb}/\alpha_{Pyw}$	χ^2
16.94	1635290	1050440	1.56	279	139	28.6	6.40	0.407	0.028	0.030	0.527	14.75	1.20
15.86	1586380	1009230	1.57	279	140	22.5	6.43	0.388	0.031	0.059	0.522	12.65	1.10
13.08	1149630	729807	1.58	279	140	22.1	6.06	0.388	0.027	0.051	0.534	14.52	1.11
9.42	968059	605330	1.60	279	140	46.1	7.10	0.449	0.028	0.023	0.501	15.84	1.05
8.11	931977	587559	1.59	279	140	18.4	5.71	0.451	0.033	0.083	0.434	13.70	1.11
6.64	874543	551197	1.59	279	140	19.4	7.15	0.533	0.046	0.081	0.339	11.52	1.12
6.14	424865	273547	1.55	279	139	23.7	6.81	0.366	0.025	0.056	0.552	14.92	1.10
4.86	407148	259117	1.57	279	139	19.3	5.80	0.391	0.026	0.103	0.480	15.00	0.98
4.81	785053	491217	1.60	279	140	31.4	8.53	0.598	0.051	0.031	0.320	11.71	1.15
3.50	756338	472815	1.60	279	140	16.4	5.47	0.589	0.057	0.097	0.258	10.42	1.06
3.25	379524	235082	1.61	279	139	23.4	5.85	0.471	0.031	0.092	0.405	15.09	1.11
2.08	346431	219040	1.58	279	139	38.5	7.65	0.587	0.042	0.043	0.328	13.98	1.06
1.26	324543	198608	1.63	279	139	21.0	4.81	0.625	0.067	0.084	0.224	9.36	1.05
0.76	527810	327806	1.61	279	140	17.5	1.00	0.186	0.031	0.023	0.761	6.06	1.16
0.66	304020	184557	1.65	279	139	15.1	0.42	0.010	0.002	0.002	0.987	5.96	0.99
0.26	271537	164387	1.65	279	139	25.6	8.01	0.665	0.219	0.049	0.067	3.04	1.08
0.09	225179	135992	1.66	279	139	21.6	0.70	0.101	0.084	0.019	0.796	1.20	1.13
0.02	186839	109073	1.71	279	139	55.2	11.69	0.205	0.652	0.074	0.068	0.31	1.10
0.00	198641	109760	1.81										

Table S.12. LCST values of tP-sP-SNPs determined by UV-Vis spectrophotometry.

	DS = Degree of Substitution	LCST(°C)
PEG-PMeEO ₂ MA		32
tP(5.9)-SNP	0.020	ND
tP(7.5)-SNP	0.016	38
	0.068	35
tP(15)-SNP	0.016	30
	0.020	30
	0.022	31
	0.038	34
	0.060	-
tP(27)-SNP	0.020	29
tP(30)-SNP	0.016	19
	0.022	21
	0.031	26
	0.038	20
tP(15)-sP(15)-SNP	0.060	27
tP(15)-sP(27)-SNP	0.020	-
tP(27)-sP(27)-SNP	0.020	-
tP(15)-sP(7.5)-SNP	0.016	29
	0.038	35
	0.060	-
tP(30)-sP(15)-SNP	0.031	26
	0.022	25
	0.060	-
tP(15)-sP(30)-SNP	0.038	30